1993-06

The effect of oil on the onset of nucleate pool boiling of R-124 from a single horizontal tube

Perry, George D.

Monterey, California. Naval Postgraduate School

(2)

NAVAL POSTGRADUATE SCHOOL
Monterey, California

THESIS

EFFECT OF OIL ON THE ONSET OF NUCLEATE POOL BOILING OF R-124 FROM A SINGLE HORIZONTAL TUBE

by

George D. Perry

June 1993

Thesis Advisor: Paul J. Marto
Thesis Co-Advisor: Stephen B. Memory

Approved for public release; distribution is unlimited.

164 pgs

REPORT DOCUMENTATION PAGE

1a Report Security Classification: Unclassified			1b Restrictive Markings
2a Security Classification Authority			3 Distribution/Availability of Report
2b Declassification/Downgrading Schedule			Approved for public release; distribution is unlimited.
4 Performing Organization Report Number(s)			5 Monitoring Organization Report Number(s)
6a Name of Performing Organization Naval Postgraduate School	6b Office Symbol 34		7a Name of Monitoring Organization Naval Postgraduate School
6c Address *(city, state, and ZIP code)* Monterey CA 93943-5000			7b Address *(city, state, and ZIP code)* Monterey CA 93943-5000
8a Name of Funding/Sponsoring Organization Naval Surface Warfare Center	6b Office Symbol 2722		9 Procurement Instrument Identification Number
Address *(city, state, and ZIP code)* Annapolis, MD 21402-5067			10 Source of Funding Numbers
		Program Element No	Project No / Task No / Work Unit Accession No

11 Title *(include security classification)* EFFECT OF OIL ON THE ONSET OF NUCLEATE POOL BOILING OF R-124 FROM A SINGLE HORIZONTAL TUBE (UNCLASS)

12 Personal Author(s) George D. Perry

13a Type of Report	13b Time Covered	14 Date of Report *(year, month, day)*	15 Page Count
Master's Thesis	From To	June 1993	164

16 Supplementary Notation The views expressed in this thesis are those of the author and do not reflect the official policy or position of the Department of Defense or the U.S. Government.

17 Cosati Codes			18 Subject Terms *(continue on reverse if necessary and identify by block number)*
Field	Group	Subgroup	HEAT TRANSFER, OIL EFFECT ON THE ONSET OF NUCLEATE POOL BOILING, R-124 REFRIGERANT

19 Abstract *(continue on reverse if necessary and identify by block number)*

An investigation on the effect of oil on the onset of nucleate pool boiling of R-124 from a single horizontal tube was conducted at saturation temperature of 2.2 °C. Pure R-124 and R-124/oil mixtures of 3% and 10% (by weight) miscible alkylbenzene oil were used. The tubes tested were: (1) smooth tube, (2) 19 fins per inch and (3) 26 fins per inch low-integral finned (GEWA-K) tubes, and (4) porous-coated (HIGH FLUX) tube. The effect of dissolved gases, subcooling and pressure on the onset of nucleate boiling were also investigated.

An oil concentration of 3% tends to delay the onset of nucleate pool boiling (compared to pure R-124) on the smooth tube and GEWA-K 19 fins per inch tube, but not on the GEWA-K 26 fins per inch and HIGH FLUX tubes. The reason for this is not known precisely but is very repeatable. A 10% oil concentration tends to delay the onset of nucleate pool boiling on all tubes tested. This is due mainly to the increase of surface tension, and saturation temperature with increase in oil concentration. The presence of dissolved gases in the pool tends to lower the onset of nucleate pool boiling by increasing the number of entrapped vapor nuclei. Pressurization and subcooling tend to increase the onset of nucleate pool boiling by deactivating potential nucleation sites.

20 Distribution/Availability of Abstract	21 Abstract Security Classification	
_x_ unclassified/unlimited __ same as report __ DTIC users	Unclassified	
22a Name of Responsible Individual P. J. MARTO	22b Telephone *(include Area Code)* 1-408-656-2098	22c Office Symbol ME/Mx

DD FORM 1473,84 MAR 83 APR edition may be used until exhausted security classification of this page
All other editions are obsolete Unclassified

Approved for public release; distribution is unlimited.

The Effect of Oil on the Onset of Nucleate Pool Boiling
of R-124 from a Single Horizontal Tube

by

George D. Perry
Lieutenant, United States Navy
B.S.C.E., University of Washington, 1984

Submitted in partial fulfillment
of the requirements for the degree of

MASTER OF SCIENCE IN MECHANICAL ENGINEERING

from the

NAVAL POSTGRADUATE SCHOOL
June 1993

Author: [redacted]
George D. Perry

Approved by: [redacted]
Paul J. Marto, Thesis Advisor

[redacted]
Stephen B. Memory, Thesis Co-Advisor

[redacted]
Matthew D. Kelleher, Chairman
Department of Mechanical Engineering

ABSTRACT

An investigation on the effect of oil on the onset of nucleate pool boiling of R-124 from a single horizontal tube was conducted at saturation temperature of 2.2 °C. Pure R-124 and R-124/oil mixtures of 3% and 10% (by weight) miscible alkylbenzene oil were used. The tubes tested were: (1) smooth tube, (2) 19 fins per inch and (3) 26 fins per inch low-integral finned (GEWA-K) tubes, and (4) porous-coated (HIGH FLUX) tube. The effect of dissolved gases, subcooling and pressure on the onset of nucleate boiling were also investigated.

An oil concentration of 3% tends to delay the onset of nucleate pool boiling (compared to pure R-124) on the smooth tube and GEWA-K 19 fins per inch tube, but not on the GEWA-K 26 fins per inch and HIGH FLUX tubes. The reason for this is not known precisely but is very repeatable. A 10% oil concentration tends to delay the onset of nucleate pool boiling on all tubes tested. This is due mainly to the increase of surface tension, and saturation temperature with increase in oil concentration. The presence of dissolved gases in the pool tends to lower the onset of nucleate pool boiling by increasing the number of entrapped vapor nuclei. Pressurization and subcooling tend to increase the onset of nucleate pool boiling by deactivating potential nucleation sites.

TABLE OF CONTENTS

LIST OF FIGURES

LIST OF TABLES

NOMENCLATURE

SYMBOL	UNITS	NAME/DESCRIPTION
A_b	m^2	Outside surface area of tube's boiling section
A_c	m^2	Cross-sectional area of tube
C_p	J/Kg K	Specific heat
D_o	m	Tube outside diameter
D_1	m	Tube diameter at thermocouple position
D_2	m	Outer diameter of boiling tube
g	m/s^2	Gravitational acceleration
h	W/m^2 K	Heat-transfer coefficient
h_{fg}	W/m^2 K	Latent heat of vaporization
I	amps	Current
I_s	amps	Current reading by AC Current Sensor
k	W/m K	Thermal conductivity of refrigerant
k_c	W/m K	Thermal conductivity of copper
L	m	Active boiling tube length
L_u	m	Non-boiling length of the test tube
Nu		Nusselt number
p	m	Tube outside wall perimeter
Pr		Prandtl Number
p_g	Pa	Gas pressure
p_v	Pa	Vapor pressure
Q	W	Heat-transfer rate from boiling surface

Q_f	W	Heat-transfer rate through one non-boiling end
Q_h	W	Heat-transfer rate from cartridge heater
q"	W/m^2	Heat flux
Ra		Rayleigh number
T_{avg}	C	Average wall temperature
T_c	C	Critical temperature
T_f	C	Film temperature
T_{sat}	C	Pool saturation temperature
T_{wo}	C	Tube outer wall temperature
V	volts	Voltage across the cartridge heater
v_{fg}	m^3/kg	Specific volume of mixture
V_s	volts	AC-DC true RMS converter voltage reading
α	m^2/s	Thermal diffusivity
β	1/K	Volumetric thermal expansion coefficient
δ		Uncertainty in measurement
γ	degree	Half of cavity angle
θ_a	degree	Advancing contact angle
θ_b	degree	Receding contact angle
ΔT	K	Wall superheat (T_{wo}-T_{sat})
μ	Kg/m s	Dynamic viscosity
υ	m^2/s	Kinematic viscosity
ρ	kg/m^3	Density of pure refrigerant
ρ_m	kg/m^3	Density of mixture
σ	N/m	Surface tension

ACKNOWLEDGMENTS

I would like to express my most sincere gratitude and appreciation to Professor Marto for his continuing guidance, understanding and encouragement throughout this research. I am also very grateful to Professor Memory for his assistance and advice during this endeavor.

Special thanks and appreciation to Mr. Tom McCord, Mr. Mardo Blanco, and Mr. Charles Crow of the Mechanical Engineering Machine Shop for their quick response, expertise, support and patience.

Most especially, I would like to thank my wife, Virginia, my daughters, Jenny and Anne and my son, Michael for their understanding, patience, encouragement and undying support throughout my tour at the Naval Postgraduate School.

I. INTRODUCTION

A. BACKGROUND

CFCs are manmade chemicals of chlorine, fluorine and carbon. They are used today in numerous applications, such as refrigerants for air-conditioning systems, aerosol propellants, fire retardants, foam blowing agents, degreasing solvents and for defluxing printed circuit boards [Ref. 1].

These fluids are generally inert, very stable and do not react with other elements in the lower atmosphere. However, their stability allows them to reach the stratosphere where the earth's protective ozone layer is located. Here the CFC molecules are broken apart by intense ultraviolet radiation, producing free chlorine atoms that react with ozone molecules, converting them to ordinary oxygen atoms. Since a chlorine atom survives the ozone-destroying reaction, it is therefore free to repeat the process which can last for a long time - one CFC molecule being capable of destroying up to 100,000 ozone molecules [Ref. 1].

Recent studies indicate a continuous reduction of the ozone layer worldwide over the last 17 years causing an increase of ultraviolet radiation with very short wavelengths (called UV-B). A long-term increase in UV-B radiation will increase the risks to human health, reduce plant growth, cause

damage to the marine environment and increase atmospheric abundance of chemically reactive compounds, thus aggravating environmental pollution problems [Ref. 2].

With the global concern of the depletion of the ozone layer, an international agreement (called the "Montreal Protocol" [Ref. 2]) was reached in Sept 1987. The Protocol calls for the freeze in production and consumption of ozone-depleting CFCs (to 1986 levels starting in July 1989; this is followed by further cutbacks in production and consumption to a 20% reduction by 1993, and a further 50% reduction in 1998). All CFCs will be completely phased out in 2000 as agreed upon by UNEP (United Nations Environment Program) members in a 1990 progress meeting held in London [Ref. 3].

These phase-out dates were revised in November 1992, when the Protocol signatories met again in Copenhagen. This latest meeting called for 75% reduction of CFCs by 1994 and complete phaseout by 1996 (except for essential uses) [Ref. 4].

The phaseout of CFCs and particularly CFC-114 (R-114) is a major concern of the United States Navy because of the commitment the Navy has made to its use on existing ships and submarines [Ref. 5]. In compliance with the Montreal Protocol, and U. S. Legislation, the Naval Surface Warfare Center (NSWC) is currently pursuing research on alternative refrigerants. There are two principal alternatives currently developed that the Navy is considering to replace existing refrigerants: (1) hydrofluorocarbons (HFCs) like R-134a is the

planned replacement for R-12, since R-134a has zero ozone depletion potential (ODP), and (2) hydrochlorofluorocarbons (HCFCs) and in particular, HCFC-124 (R-124) which has been identified as an intermediate "drop-in" replacement for R-114.

The Naval Postgraduate School in support of NSWC started investigating the nucleate pool boiling characteristics of HCFC-124 (R-124) in 1992, Bertsch [Ref. 6] evaluated and compared the heat transfer performance of R-124 to R-114 using various refrigerant/oil mixtures on a smooth tube and four enhanced tubes. He reported that: (a) significant heat transfer improvement (>50%) was obtained in pure R-124 compared to pure R-114, (b) the largest enhancement over all heat flux ranges was obtained with the HIGH FLUX tube for pure R-124, (c) enhancement in heat transfer performance was realized from the smooth and finned tubes with increasing oil concentration in R-124 up to 6%. He also investigated the effect of oil on the onset of nucleate boiling from a smooth tube and a HIGH FLUX tube and found that addition of oil delays the point of incipience for the smooth tube, but no measurable effect was observed for the HIGH FLUX tube.

The onset of nucleate pool boiling is a very unstable process as pointed out by You et al. [Ref. 7], Memory and Marto [Ref. 8], and Bertsch [Ref. 6]. The purpose of this thesis is to continue the work with R-124 and to study the onset of nucleate boiling under various conditions.

B. OBJECTIVES

The objectives of this thesis are as follows:

1. Investigate in greater detail the effect of oil on the onset of nucleate pool boiling of R-124 from a smooth and enhanced single horizontal tube.

2. Investigate the effect of dissolved gases, subcooling and pressure on the onset of nucleate pool boiling of R-124 from a single smooth and enhanced horizontal tube.

II. LITERATURE SURVEY

A. POOL BOILING CURVE

Pool boiling occurs when boiling takes place from a heated surface immersed in a large pool of quiescent liquid. It is used in a variety of applications such as metallurgical quenching, flooded shell-and-tube evaporators, and immersion cooling of electronic components just to name a few. Figure 2.1 from Bar-Cohen [Ref. 9] shows the well-known pool boiling curve, and defines the various heat transfer regimes.

1. Single Phase Natural Convection

This regime (a-b) is in effect as wall superheat is increased from an initial low value until just before nucleation occurs and the first bubbles form on the heated surface. It should be noted that no bubbles are formed during natural convection, and that heat is transferred due to the buoyancy-driven convection of the liquid.

2. Boiling Incipience

Once nucleate boiling starts (point b) and bubbles begin to grow and depart from various nucleation sites on the heated surface (as depicted in Figure 2.2 from Thome [Ref. 10]), onset of nucleate boiling (ONB) or incipient boiling has been reached. According to Bar-Cohen [Ref. 9], shortly after incipience, nucleation frequently propagates rapidly across

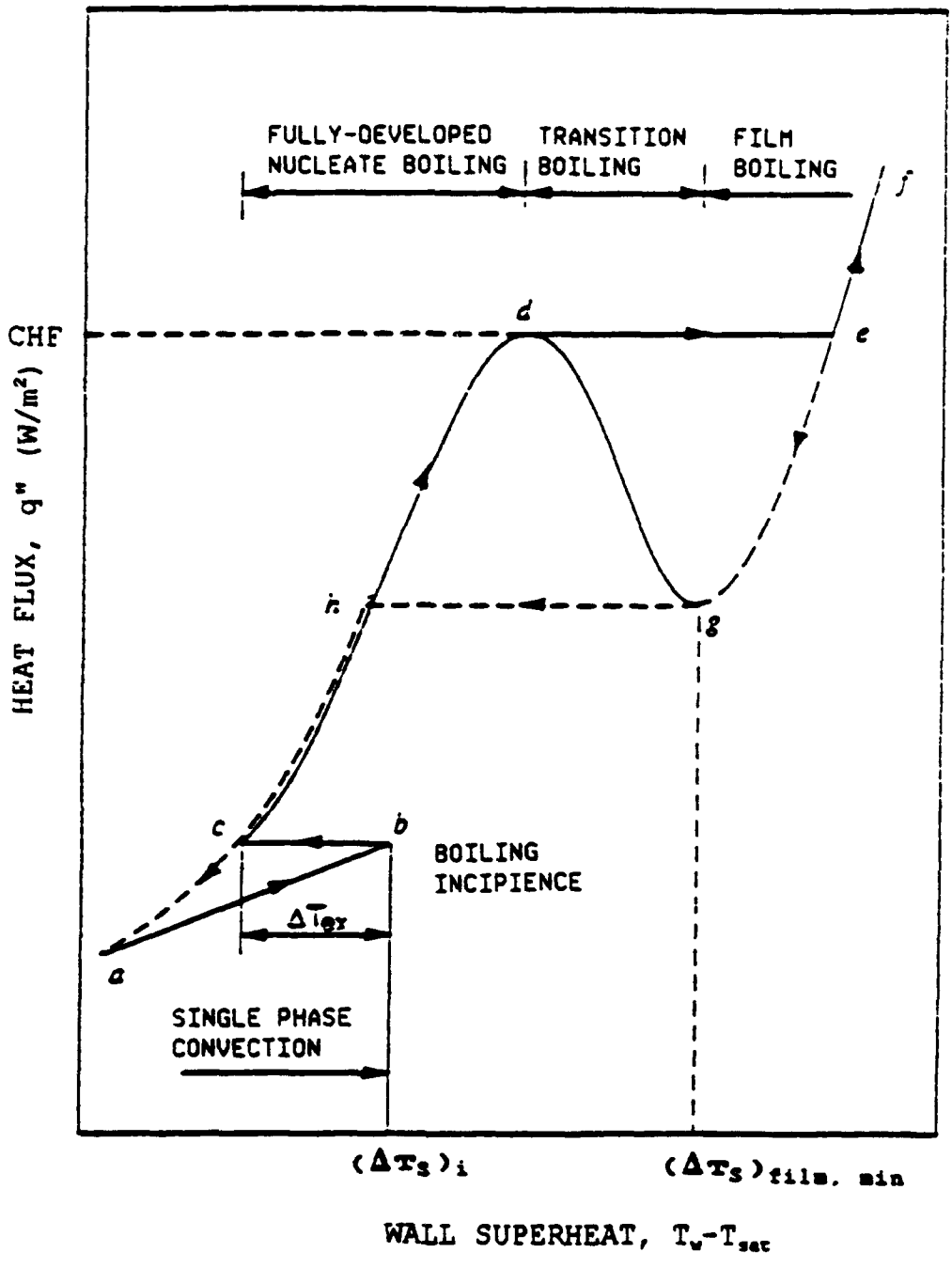

Figure 2.1 Pool Boiling Curve

the heated surface and reduces the wall superheat to the value associated with established nucleate boiling (point c). This rapid decrease in wall superheat has been described as thermal overshoot, or superheat excursion.

Incipient superheat excursion was first reported by Corty and Foust [Ref. 11], and Bankoff et al. [Ref. 12], in the boiling of organic fluids. Bergles and Chyu [Ref. 13] compared the nucleate pool boiling characteristics of a HIGH FLUX tube and a smooth tube in distilled water and R-113. Their results showed that both the HIGH FLUX and smooth tube displayed a significant temperature overshoot at ONB. Marto and Lepere [Ref. 14] in their investigation of the pool boiling of R-113 and FC-72 from smooth and enhanced tubes reported that the temperature overshoot was less severe in FC-72 than in R-113. Memory and Marto [Ref. 8] investigated the effect of oil on the incipience of nucleate boiling for a smooth tube and six enhanced tubes (low finned and modified integral-fin) and found that in the natural convection region, all seven tubes exhibited similar behavior with and without oil. They also found that oil concentration seemed to have no systematic effect on ONB for the smooth and low-integral fin tubes, and that the ONB occurred at lower heat fluxes for the structured surfaces. Bertsch [Ref. 6] investigated the effect of oil on the onset of nucleate boiling of R-124 from a smooth tube and a HIGH FLUX tube and found that addition of oil delays the point of incipience for the smooth tube, but found

no measurable effect for the HIGH FLUX tube. Several other researchers have investigated ONB (see Bar-Cohen and Simon [Ref.15]). Onset of nucleate boiling is a very random process (You et al. [Ref. 7]). It is affected by many factors including surface roughness, pressure-temperature history, contact angle, dissolved gases, subcooling, fluid properties (summarized by Brauer and Mayinger [Ref. 16]), and oil addition. All these factors will be discussed in more detail later in this chapter.

3. Nucleate Boiling Region

As heat flux is further increased from point c, larger patches and slugs of vapor depart from the heated surface (see Figure 2.2). This region (curve c-d) is commonly called the fully developed nucleate pool boiling region. Heat can leave the surface as sensible heat in a superheated liquid or as latent heat in vapor bubbles. Sustained improvement in heat transfer is realized throughout this region. As heat flux is further increased, a maximum value of heat flux called the Critical Heat Flux (CHF) or Departure from Nucleate Boiling (DNB) is attained (point d).

4. Transition Boiling

Increase in wall superheat beyond the critical heat flux results in a decrease in heat flux. The resulting region (curve d-g) is called the transition boiling region. According to Thome [Ref. 10], this regime is characterized by

partial and intermittent contact of the liquid with the heated surface, which sign ficantly reduces the heat transfer from the heated surface to the fluid. Point g is called the minimum heat flux, and at this wall superheat, the liquid is no longer in contact with the heated surface because of the rapid rate of vapor generation in the region next to the surface.

5. Film Boiling

As wall superheat is increased further from the minimum heat flux (point g), the film boiling region is attained. This region is characterized by a stable vapor film according to Thome [Ref. 10] that blankets the heated surface and separates the liquid from the wall. This region is

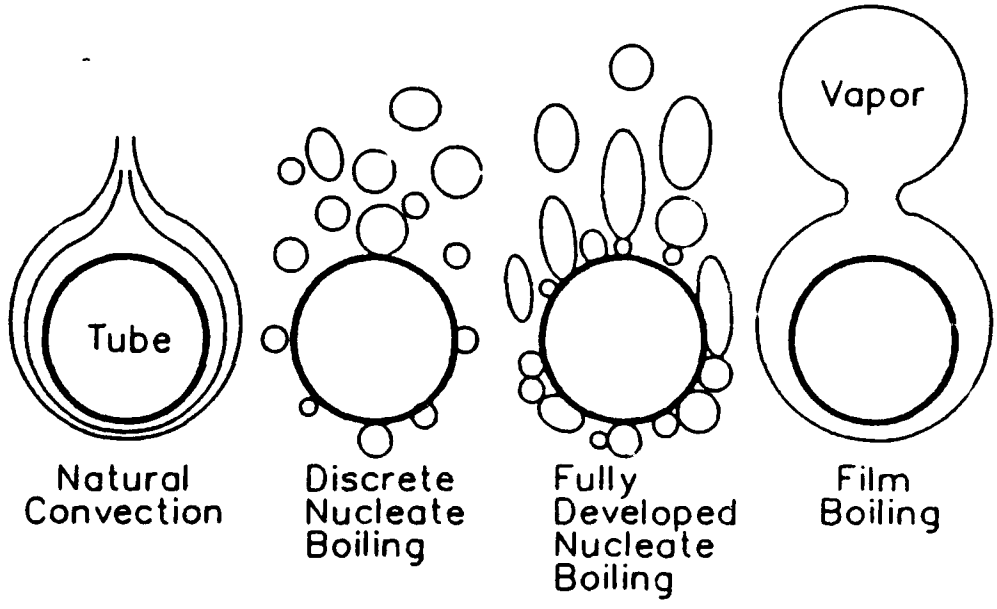

Figure 2.2 Nucleate Pool Boiling Regimes

normally avoided since the melting temperature of the heat source can be attained quickly.

B. BOILING NUCLEATION THEORY

Corty and Foust [Ref. 11], and Bankoff [Ref. 12] were the first to relate the presence of vapor bubbles with microcavities on the heated surface. They postulated that boiling is initiated from these pre-existing trapped vapor embryos. Bankoff [Ref. 12] showed that the free energy, or work of formation required to create a vapor nucleus at a planar solid surface in a liquid (heterogeneous nucleation) was less than that required for homogeneous nucleation in the liquid phase alone.

C. VAPOR TRAPPING MECHANISM

The process of trapping vapor or gas was first considered by Bankoff [Ref. 12]. He hypothesized that during the flow of liquid over a surface with scratches and cavities, air and/or vapor could be trapped in the wedge-shaped grooves if the contact angle of the flowing liquid on the solid surface was greater than the wedge angle as illustrated in Figure 2.3 provided by Carey [Ref. 17]. Referring to Figure 2.3(a), Carey [Ref. 17] stated:

> When a liquid film flows over a gas-filled cavity, the contact angle with the downslope tends to be maintained as the liquid begins to fill the cavity. Since the liquid front is convex, the "nose" of the liquid front will reach the opposite wall before the

contact line reaches the bottom of the cavity if the contact angle is greater than the groove angle 2γ.

The condition for entrapment of gas by the advancing liquid front can therefore be stated as:

$$\theta_a > 2\gamma \qquad (2.1)$$

where θ_a is the advancing contact angle that may be significantly greater than the static or equilibrium contact angle.

Now, considering Figure 2.3(b) for a receding liquid front, liquid entrapment in the cavity may be stated as

$$\theta_r < 180^\circ - 2\gamma \qquad (2.2)$$

where θ_r is the receding contact angle. The difference between the advancing contact angle and receding contact

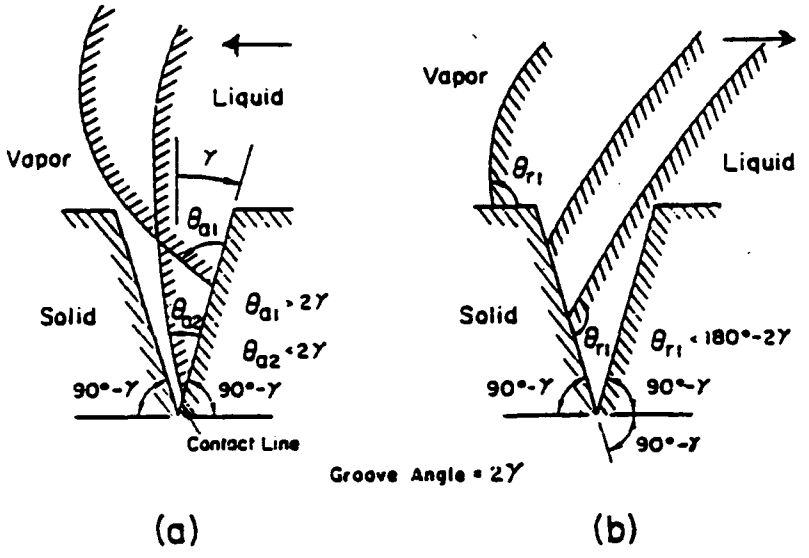

Figure 2.3 Vapor and Liquid Entrapment Schematic in a Cavity of (a) an advancing and (b) receding liquid film

angle during repeated wetting of the cavity due to an advancing and receding liquid film is called "contact angle hysteresis". Carey [Ref. 17] stated that this hysteresis effect may result in θ_r being much lower than the static or advancing contact angles, and may therefore serve to increase the tendency to trap vapor in surface cavities.

Bankoff [Ref. 12] noted that cavities can be classified into one of four categories: (1) cavities that trap vapor/gas only, (2) cavities that trap liquid only, (3) cavities that trap both liquid and vapor/gas, and (4) cavities that do not trap liquid, vapor or gas. Carey [Ref. 17] said that category of a cavity can be based on whether equations 2.1 and 2.2 are satisfied, and that contact-angle hysteresis enhances the probability that cavities that trap gas (category 1 or 3) will be present on the solid surface.

D. NUCLEATE BOILING HEAT TRANSFER MECHANISM

According to Chongrungreong and Sauer [Ref. 18], nucleate boiling starts when the temperature of the heated surface exceeds the saturation temperature of the liquid by a few degrees. Adjacent to the surface, a thin layer of superheated liquid is formed in which bubbles nucleate and grow.

1. Boiling On Plain Surfaces

Hsu and Graham [Ref. 19] investigated extensively the physical processes involved in nucleate pool boiling from plain surfaces and identified the following principal heat

transfer mechanisms as depicted in Figure 2.4 from Thome [Ref. 20]:

a. Bubble Agitation

As displayed in Figure 2.4, the motion imparted to the liquid from the growth and departure of bubbles improves the liquid-phase convection. Thome [Ref. 20] stated that a forced convection process is created in which the velocity of the liquid near the heated wall is the same or close to the velocity of the growing bubble, and that heat is transported as sensible heat in the superheated liquid.

b. Thermal Boundary-Layer Stripping

Thome [Ref. 20] said that hydrodynamic drag of the departing bubbles periodically scrubs the thermal boundary layer formed by transient heat conduction into the surrounding liquid. The sensible heat transport rate is controlled by the quantity of superheated liquid removed from the thermal boundary layer.

c. Evaporation

A vapor bubble growing on the heated wall at a nucleation site is formed by the vaporization of superheated liquid surrounding the bubble and by thin film evaporation in the microlayer trapped beneath the bubble. Heat is removed away as latent heat.

The actual boiling process is a combination of these three heat transfer mechanisms. According to Thome

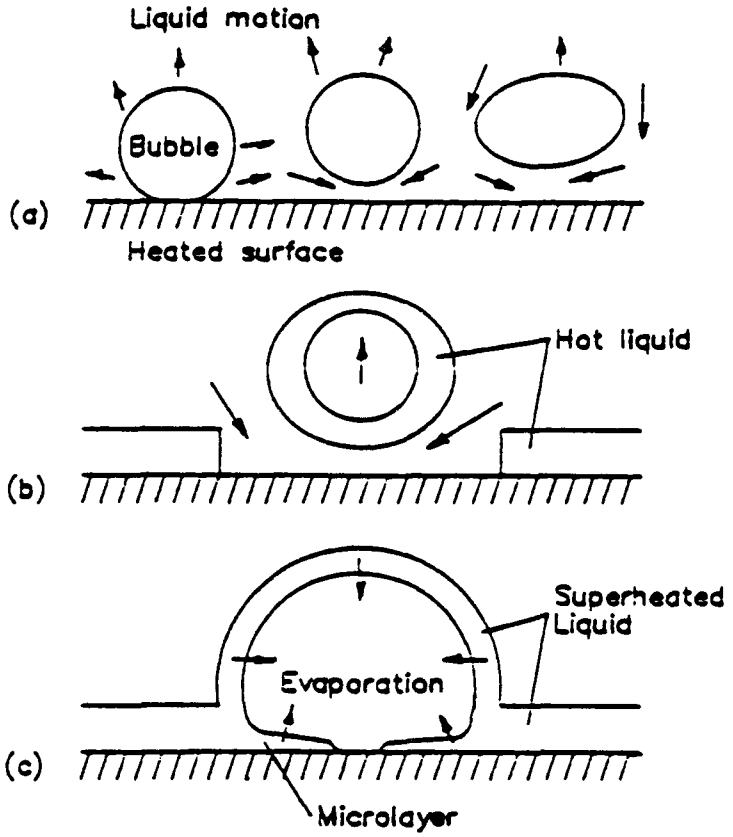

Figure 2.4 Nucleate Boiling Mechanisms

[Ref. 20], the heat removed, however, is not a simple summation of these three individual contributions since they interact and "overlap" in the heat carried away.

2. Boiling on Enhanced Surfaces

Surface geometry can affect significantly the heat transfer mechanisms. As before, heat can leave the surface as latent heat in vapor/bubbles or as sensible heat in superheated liquid. With enhanced surfaces, Thome [Ref. 21] said that latent heat can be transferred both inside reentrant

channels and by further growth of the vapor bubbles on the outside surface. Sensible heat can be removed by the liquid flowing into and out of the reentrant channels as well as on the external surfaces of the enhancement.

a. Evaporation

According to Thome [Ref. 20], this process is composed of three parts as depicted in Figure 2.5: (1) thin film evaporation resulting from the conduction and/or convection of heat across the thin liquid film, (2) capillary evaporation which results from the vaporization of liquid at menisci in the reentrant cavities, and (3) external evaporation in which the bubble continues to grow in the thermal boundary layer at the outer edge of the enhancement.

b. Convection

This process is influenced by: (1) the two-phase flow boiling process (first proposed by Stephan and Mitrovic [Ref. 22]) inside the reentrant channels where bubbles grow, circulate and eventually squeeze out to the surface and liquid fills in, (2) the external convection process which is controlled by bubble agitation and the vapor-liquid exchange mechanism as with plain surfaces (D.1) of Thome [Ref. 21]. Much analysis remains to be done on the mechanisms affecting overall heat transfer when boiling from enhanced surfaces.

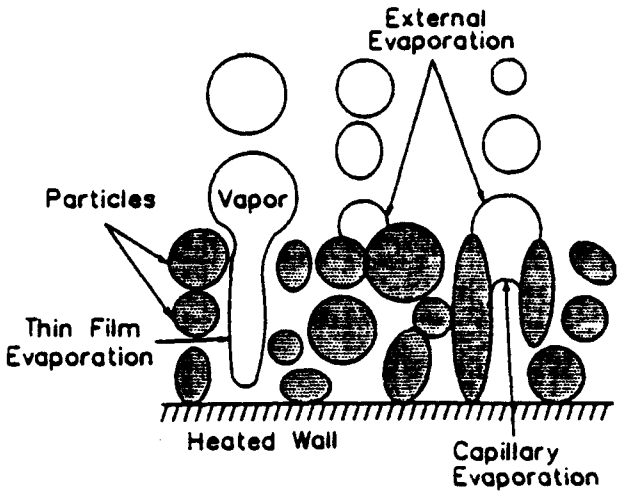

Figure 2.5 Evaporation Process on an Enhanced Surface

E. FACTORS AFFECTING INCIPIENT BOILING SUPERHEAT

1. Dissolved gases

Bar-Cohen [Ref. 9] noted that the formation of a vapor/gas embryo in a surface cavity creates a void into which superheated liquid can evaporate and into which dissolved gases can flow. Volume of the gaseous mixture increases until pressure equilibrium with the surrounding liquid is attained by each bubble.

Assuming the bubble to be hemispherical and recognizing the possible presence of dissolved gases, a force balance at the bubble interface for steady or quasi-steady-state conditions can be stated ([Roshenow [Ref. 23]) as:

$$p_v - P = \frac{2\sigma}{r} - p_g \qquad (2.3)$$

Using the Clausius-Clapeyron relation, Roshenow [Ref. 23] further derived an approximate relation for the incipient superheat for small pressure differences, ($2\sigma/r << p$) as:

$$(T_w - T_{sat})_i = \frac{T_{sat} v_{fg}}{h_{fg}} \left(\frac{2\sigma}{r} \frac{\rho}{\rho - \rho_m} - p_g \right) \qquad (2.4)$$

Murphy and Bergles [Ref. 24] observed that the presence of gas in an embryonic bubble trapped in a surface cavity or floating in the liquid can substantially reduce the vapor pressure needed to preserve the integrity of the bubble thus lowering the incipient superheat. They found that for R-113, which was well-mixed with air at room temperature and 1 bar absolute pressure, the saturation temperature was only 27 °C versus the normal 48 °C for the pure substance.

According to You et al. [Ref. 7], however, the presence of dissolved gases does not necessarily guarantee a reduction in the incipient superheat for nucleate pool boiling. In their experiments using FC-72 boiling from a cylindrical, sputtered-silicon heater, the incipient superheat for degassed liquid varied from 18 °C to 38 °C.

2. Surface Wettability

The incipience mechanism of a highly wetting liquid was investigated by Bar-Cohen and Simon [Ref. 15], Marsh and Mudawar [Ref. 25], and Tong et al. [Ref. 26]. They found the

following significant differences between highly-wetting liquids (such as refrigerants and dielectrics) and a poorly-wetting liquid (such as water). With highly-wetting liquids there will be fewer active embryos (gas retained in cavities) on a given surface than with poorly-wetting liquids. This is due to the increased ability of fluids with small wetting angle to effectively flood the cavities. Another difference is that the residual bubble in highly wetting liquids is small and therefore requires a larger superheat for its initial growth.

According to Tong et al. [Ref. 26], parameters such as volume of trapped vapor/air in a cavity, critical bubble radius, incipient superheat, and the superheat excursion at the onset of nucleate boiling are strongly affected by surface wettability. Brauer and Mayinger [Ref. 16] state that increase in surface wettability results in a decrease in the vapor trapping capability of the cavities on a surface, which in turn delays the onset of nucleate boiling.

Highly-wetting liquids like chorofluorocarbons have been observed by several investigators to have high wall superheats at the onset of nucleate boiling. Marto and Lepere [Ref. 14] reported that due to the high wettability of R-113 on copper, large cavities are flooded with liquid and higher wall superheats are therefore required to nucleate the smaller cavities.

You et al [Ref. 7] investigated the onset of nucleate boiling of R-113 under atmospheric conditions using an electrically heated 0.13 mm diameter chromel wire and a 0.51 mm platinum thin-film heater. Results of their repeated runs showed that the onset of nucleate boiling was very unstable and a probabilistic plot was utilized to display their results. They attributed the unstable behavior to the excellent wetting characteristics of R-113 and the poor reproducibility of contact angle.

3. Contact Angle

Contact angle between a liquid and a solid surface is one of the most important factors in phase change heat transfer. Griffith and Wallis [Ref. 27] concluded that contact angle is important in bubble nucleation primarily due to its effect on the stability of the bubble within the cavity. This importance was restated by Tong et al. [Ref. 26] and Cornwell [Ref. 28], since contact angle characterizes the wettability of a certain liquid on a specific surface.

4. Surface Roughness

Significant advances have been achieved in the development of enhanced boiling surfaces during the past 20 years. Some of the commonly-used enhanced surfaces are shown in Figure 2.6 from Thome [Ref. 20]. Commercially available porous coatings and grooved/finned surfaces are capable of providing significant increases in heat transfer for various

surface/fluid combinations. Bar-Cohen [Ref. 9] states that porous coating provide a significant increase in the number of active nucleation sites per unit area and shift the active nucleation site population toward a larger mean radii by forming reentrant cavities, thus resulting in a lower incipient wall superheat.

Numerous investigations have been conducted on enhanced surfaces and some are presented here. Chowdhury and Winterton [Ref. 29] report that an increased number of nucleation sites results in lower wall superheats, moving the nucleate boiling curve toward the left. Venart et al. [Ref. 30] did a comparison using R-11 between a non-porous and two porous surfaces and found that the porous surfaces showed a significant decrease in wall superheat. Memory and Marto [Ref. 8], and Wanniarachi et al. [Ref. 31 & 32] from their investigations using R-114 on smooth and enhanced tubes, concluded that the onset of nucleate boiling for an enhanced tube occurred at lower heat fluxes and wall superheats when compared to a smooth tube.

5. Subcooling

Surface subcooling is defined by Bergles and Chyu [Ref. 13] as the temperature difference between saturation temperature at the surface and the temperature of the bulk pool before the test. They found that the onset of nucleate boiling wall superheat for a smooth surface in R-113 increased

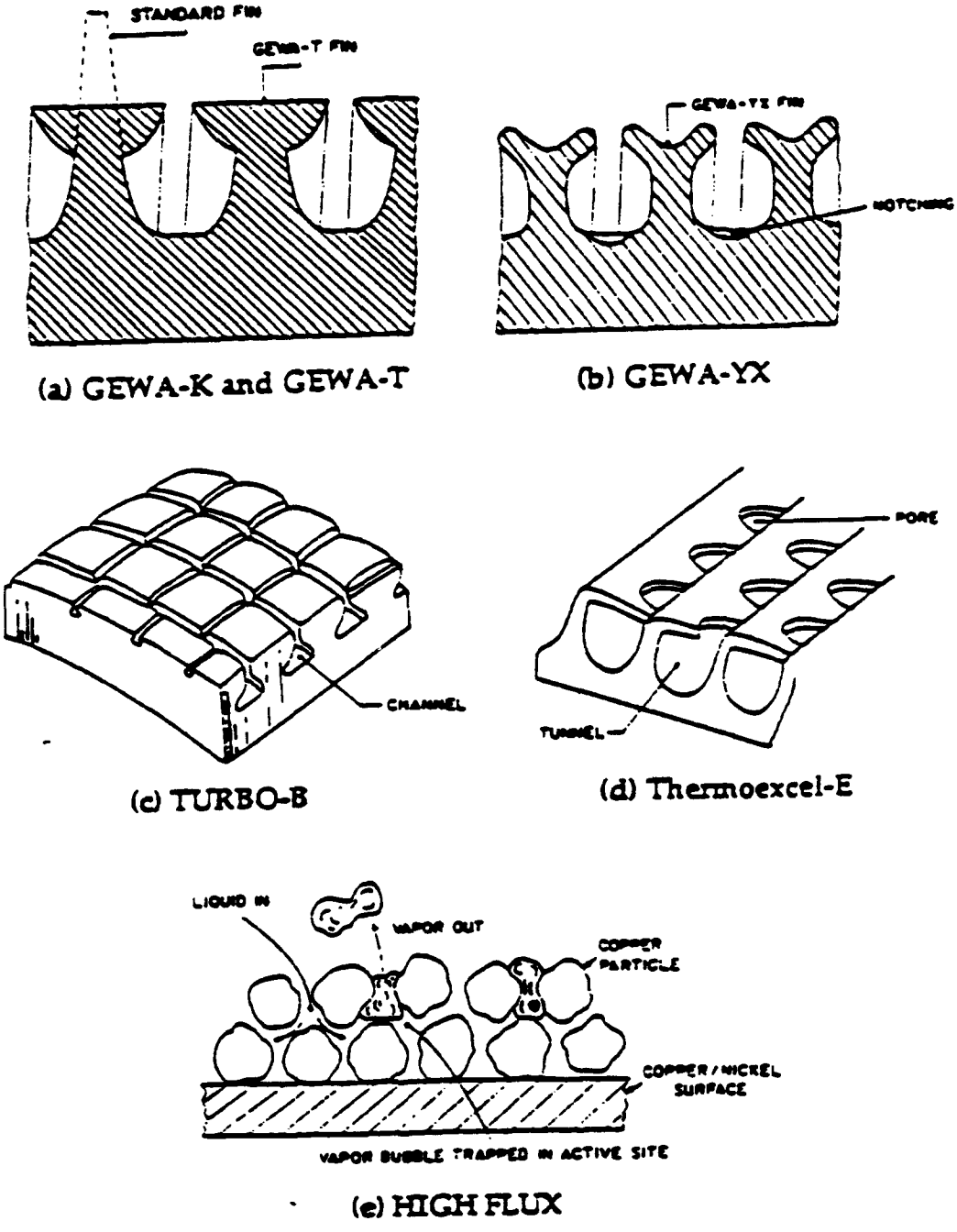

Figure 2.6 Commercially available enhanced surfaces

with an increase in subcooling. Marto and Lepere [Ref. 14] tested three different tubes using different surface preparations and found that the ONB wall superheat increased with increasing subcooling. Furthermore, they found that pre-boiling followed by 30 minutes of subcooling has almost the same effect on the incipient wall superheat as subcooling the specimen overnight. Faw et al. [Ref. 33], using heating elements made of platinum wire, investigated the effects of pressure on the initiation of subcooled pool boiling in water. They used saturation temperatures of 100, 150, and 195 °C and subcoolings as much as 30 K. They observed that with increased subcooling, the ONB wall superheat also increased. This behavior was confirmed recently by Normington et al. [Ref. 34], using D80 and HT110. All of the above findings can be attributed to condensation of the vapor trapped in the cavities when subcooled, thus eliminating or reducing many potential active nucleation sites.

6. Pressure and Temperature

Pressure and temperature both play vital roles in the incipience of nucleate pool boiling. In 1964, Bergles and Roshenow [Ref. 35] developed the following equation for incipient wall superheats for liquids operating far from their thermodynamic critical point:

$$(T_w - T_{sat})_i = \frac{2}{r}\left[\sigma T_{sat}\frac{v_{fg}}{h_{fg}}\right] \qquad (2.5)$$

They proposed using the bracketed fluid property group as a nucleation parameter. As pointed out by Bar-Cohen [Ref. 9] it can be seen that at saturation conditions, increasing system pressure and temperature will decrease the value of the above property group. This is not readily obvious, but if we take R-114 for example, as saturation temperature increases the latent heat of vaporization (h_{fg}), the liquid-vapor specific volume (v_{fg}) and the surface tension all decrease, thereby decreasing the wall superheat. Just like all other parameters affecting incipience, several studies have been conducted on pressure-temperature effects. Eddington and Kenning [Ref. 36] found from their study that applying excess pressures of 1/3 bar to a system at 1 bar reduces the number of nucleation sites of a given size by about 50%.

Hooper and Abdelmessih [Ref. 37] investigated the effect of decompression on nucleate boiling and noted that boiling initiation took place at higher superheats. This finding was confirmed by Weisman et al. [Ref. 38], Lienhard et al. [Ref. 39], and Faw et al. [Ref. 33].

7. Oil addition

In most applications involving chillers, the mixing of the refrigerant with a miscible refrigeration oil is inevitable due to the use of hermetically sealed centrifugal compressors. Oil seals deteriorate with time and oil leaks into and mixes with the working fluid. Several studies have

been done on the effect of oil on nucleate pool boiling of refrigerant-oil mixtures. Stephan [Ref. 40] was probably one of the earliest investigators. He studied the effect of oil on the boiling heat transfer coefficient using R-12 and R-22 on a smooth horizontal plate. He reported up to a 50% reduction in the boiling coefficient with 9% oil by mass, while 50% oil caused a 90% reduction. Daugherty and Sauer [Ref. 41] investigated the effects of R-11/oil and R-113/oil mixtures on boiling hysteresis from smooth tubes and found that oil addition (up to 10%) caused a significant increase in the incipient wall superheat for both fluids under the same operating conditions. Sauer et al. [Ref. 42] investigated the effect of oil (up to 10%) carryover on the boiling performance of R-11 with commercial copper 19 fpi finned tube. They found that incipient wall superheat increased with increasing oil concentration and that the effect of oil on finned tubes was similar to smooth tubes. Wanniarachi et al. [Ref. 32] studied the effect of oil on the performance of R-114 from smooth and porous surfaces and concluded that the presence of oil significantly delayed the ONB for the porous coated tube, but only had a small effect for the smooth tube. Memory and Marto [Ref. 8] in their study of R-114/oil mixtures, found that oil concentration had no systematic effect on the incipient point for smooth and low integral-fin tubes, but delayed it for structured type surfaces. Additionally, they concluded that boiling incipience is highly unpredictable and can easily

be triggered by an external source. Bertsch [Ref. 6] during his study of R-124/oil mixtures where he conducted many repeated experiments, concluded that oil addition does delay the point of incipience for a smooth tube. However, there was little measurable effect for a HIGH FLUX tube. This contradictory evidence is probably due to the unpredictable and statistical nature of incipience.

III. EXPERIMENTAL APPARATUS

A. SYSTEM DESCRIPTION

A schematic diagram representing the single-tube apparatus is shown in Figure 3.1, and a photograph is shown in Figure 3.2. Detailed discussions on its design, construction and assembly were done by Karasabun [Ref.43], and Reilley [Ref. 44]. The apparatus was relocated to its existing location and calibrated by Sugiyama [Ref. 45]. Existing Pyrex glass Tees for the condenser and evaporator were replaced by Bertsch [Ref. 6] with fiberglass re-inforced Pyrex glass Tees to withstand the higher operating pressure of R-124.

The present system consists of the following components: (1) two identical re-inforced Pyrex-glass Tees, one used as the evaporator to boil the R-124, and the other used as the condenser to condense the refrigerant vapor; (2) a liquid refrigerant reservoir; (3) a refrigerant/oil subsystem; (4) an aluminum/plexiglass framework; (5) an ethylene-glycol/water mixture cooling system; (6) a vacuum pump; and (7) a data acquisition and instrumentation system.

R-124 was boiled in the evaporator and was condensed in the condenser on a copper coil cooled by a refrigerated water and ethylene glycol mixture. Condensation rate was controlled via valve VC (see Figure 3.1). The condensate then returned

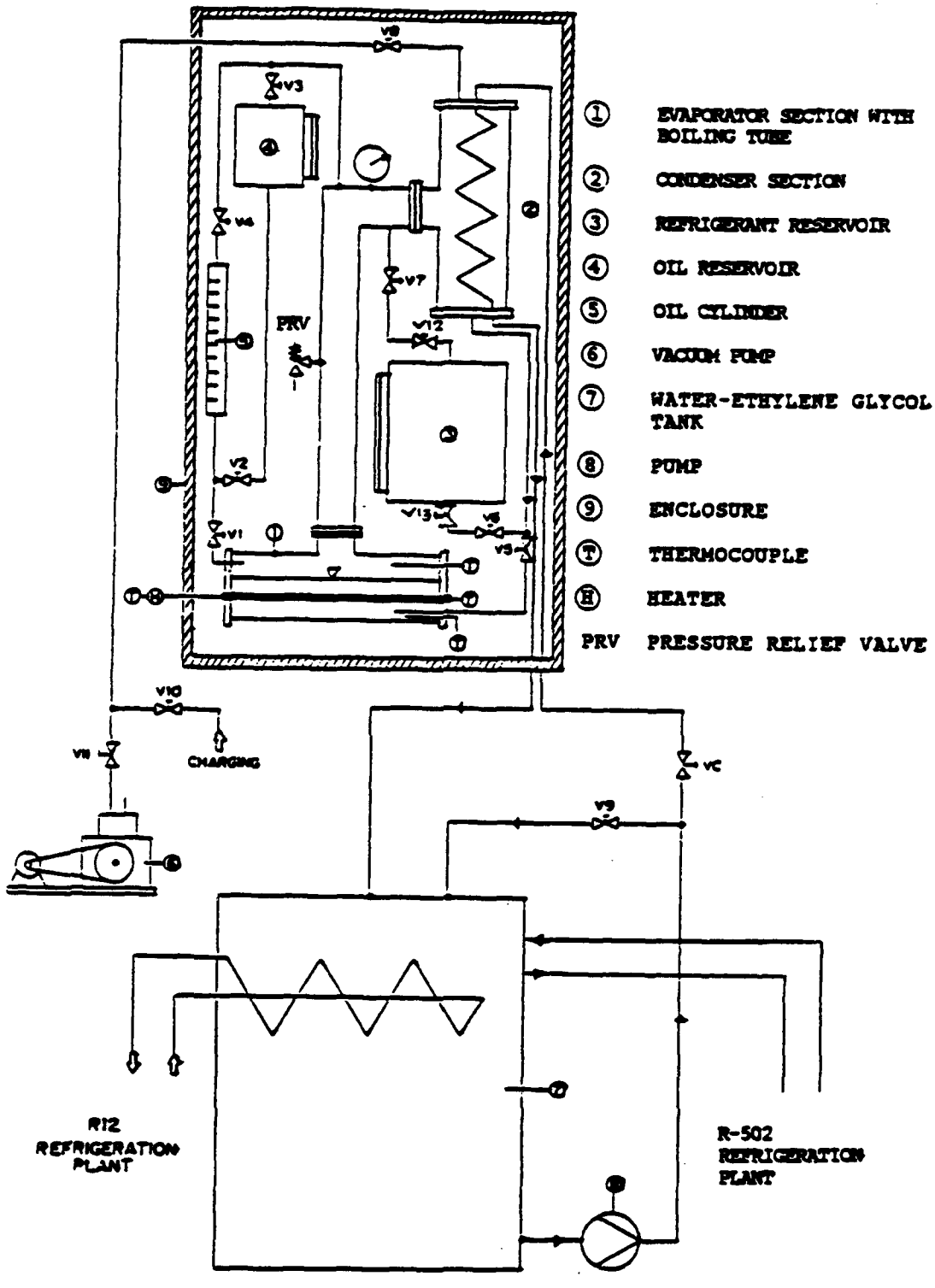

Figure 3.1 Schematic Diagram of Pool Boiling Apparatus

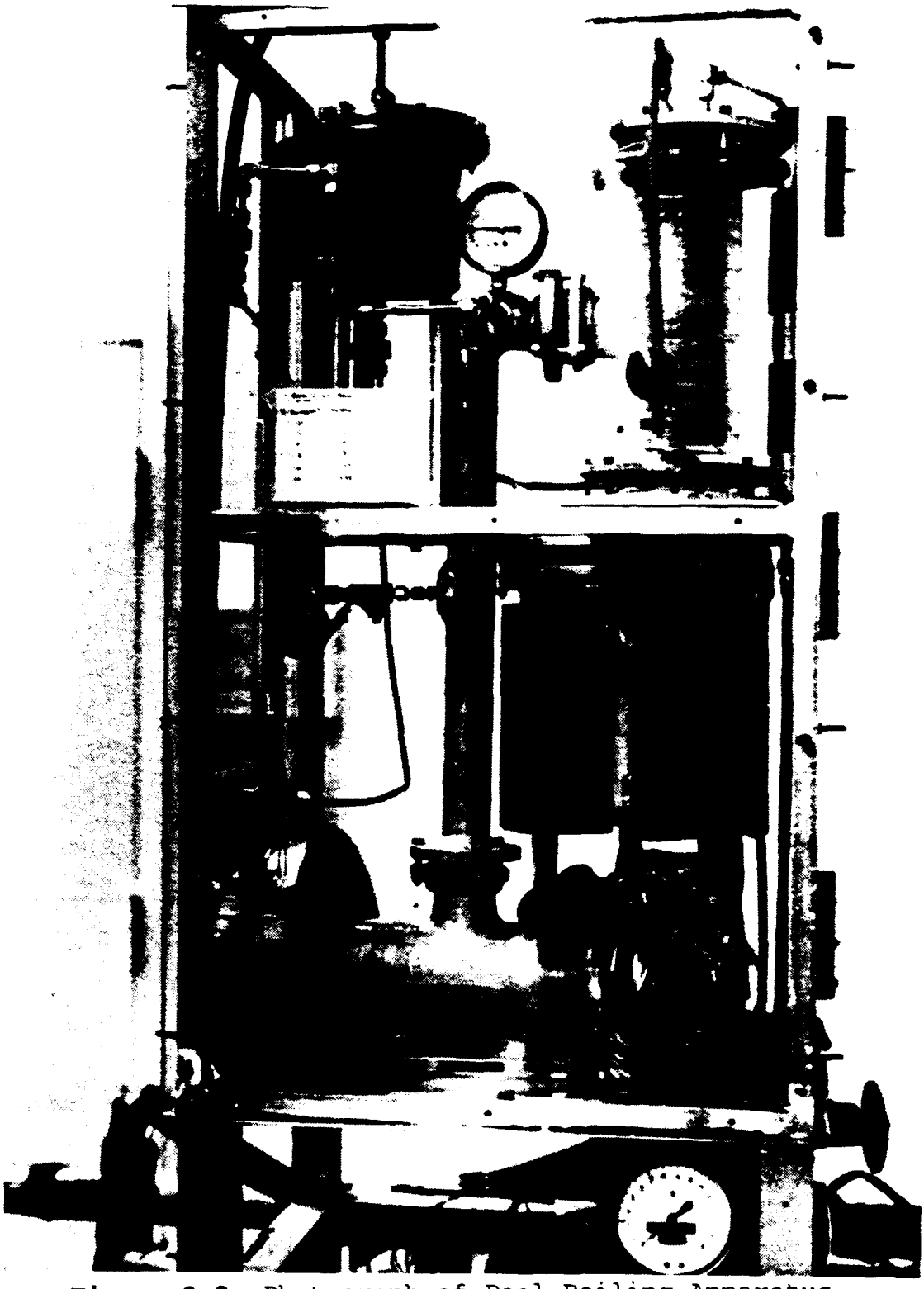

Figure 3.2 Photograph of Pool Boiling Apparatus

to the evaporator by gravity. A copper deflector (see Fig. 3.3) was fitted above the condensate discharge tube at the bottom of the evaporator to prevent any vapor bubbles that might come from the discharge tube from interfering with the boiling tube.

B. BOILING TEST SECTION

1. Evaporator

The evaporator was a Corning Pyrex fiberglass-reinforced glass Tees section designed to withstand a working pressure of 50 psig. Bertsch [Ref. 6] hydrostatically tested the system to 75 psig prior to the initial charging of R-124. Two aluminum endplates, 210 mm in diameter and 12.7 mm thick with thermocouple wells, oil entry fittings and Teflon inserts were bolted to the evaporator by means of cast-iron flanges and gasket assembly as shown in Figure 3.4 and Figure 3.5.

2. Evaporator tubes

Each evaporator tube tested was secured in place by two Teflon inserts and sealed by O-rings in the evaporator endplates. Strong-backs as shown in Figure 3.6 prevented the Teflon inserts from popping out due to internal pressure of the system. A schematic drawing of an evaporator tube is shown in Figure 3.7.

Each evaporator tube was 450 mm in length and 15.9 mm in diameter. The middle portion of the tube was heated by a

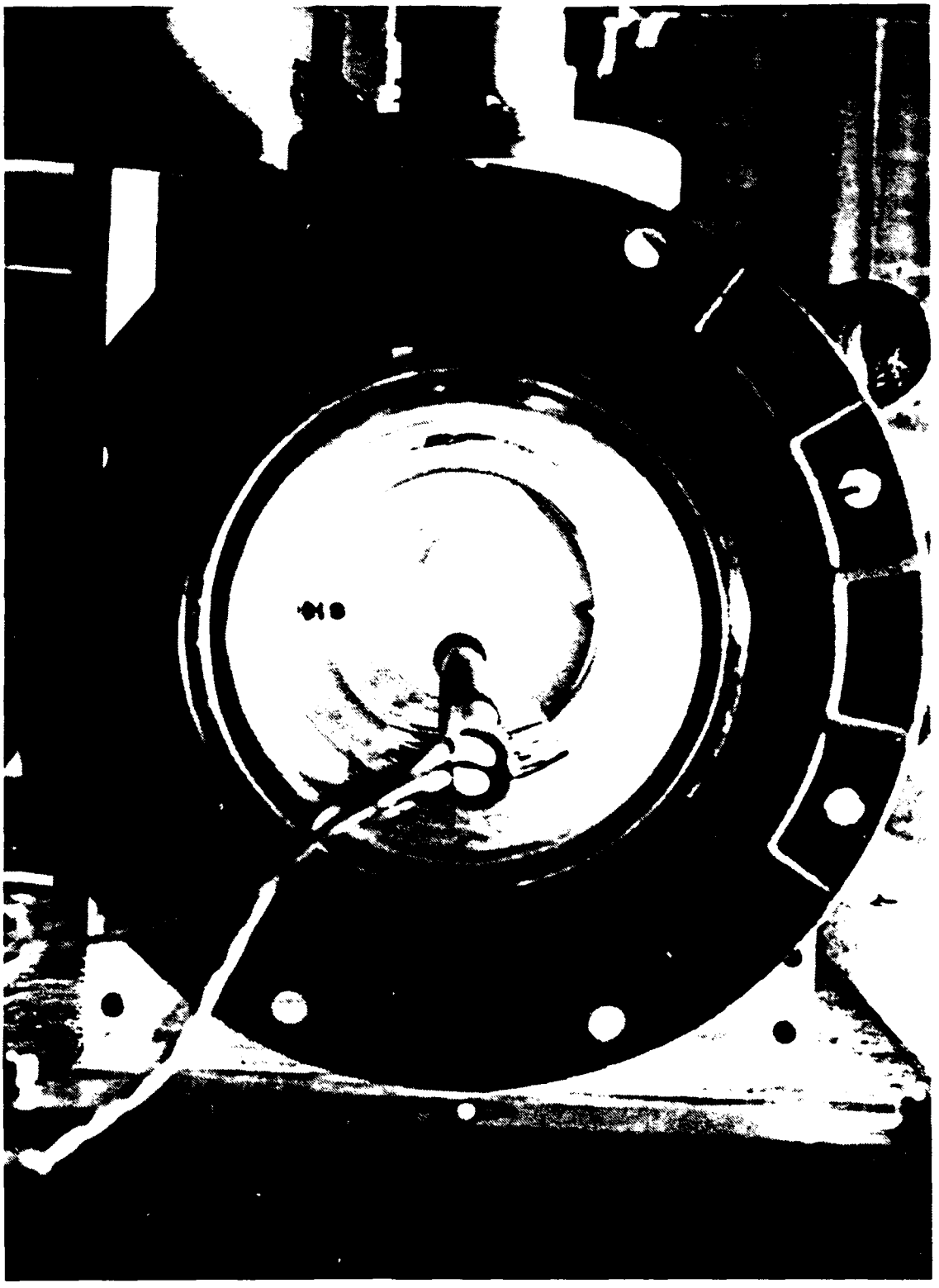

Figure 3.3 Photograph of Copper Deflector Plate

1 kW, 240-Volt stainless-steel-sheathed cartridge heater, 6.35 mm in outside diameter, 203.2 mm in actual length with a heated length of only 190 mm. Memory and Marto [Ref. 8], and Bertsch [Ref. 6] provide a detailed fabrication process of an instrumented tube.

Four tubes were tested in this study: (1) smooth tube, (2) GEWA-K 19 fin per inch (fpi) tube, (3) GEWA-K 26 fin per inch tube and (4) HIGH-FLUX porous tube. All the tubes were made of copper except the HIGH-FLUX tube that had copper particles on a copper-nickel substrate.

C. CONDENSER SECTION

The condenser was identical in size, shape and material to the evaporator shown in Figure 3.4. The refrigerant was condensed on a 3/8 inch outside diameter helical copper tube that was coiled inside the condenser. The condenser was mounted vertically as shown in Figure 3.1 with top and bottom plates bolted to the fitted cast-iron and gasket assembly. The top plate has both coolant entry and vacuum/charging fittings; the bottom plate was connected to the evaporator by a gravity feed return line via valve V5. The condenser was connected to the vapor outlet of the evaporator by a 2-inch diameter L-shaped aluminum piping. A relief valve (set at 50 psig) and a Bourdon pressure gage were mounted on the tube.

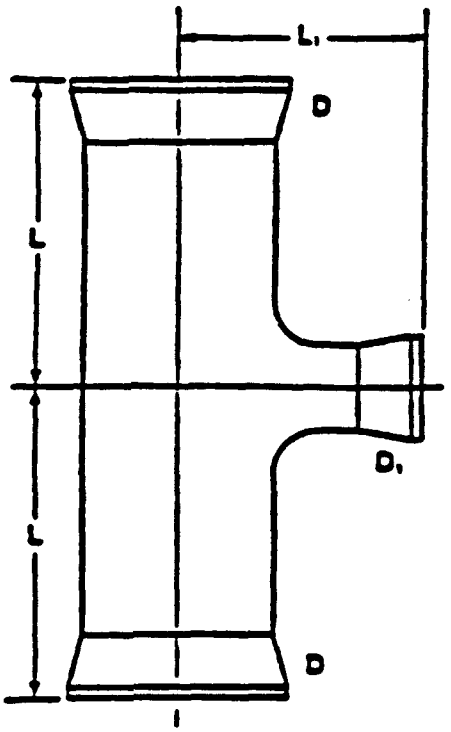

a) Corning Pyrex Glass Evaporator (D x D_1 = 402x51 mm, L = 178 mm, L_1 = 127 mm)

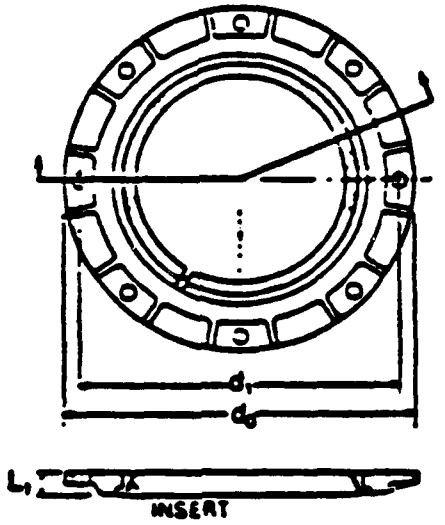

b) Cast Iron Flange and Gasket (d_1 = 190mm, d_0 = 210mm, L_1 = 14mm, A = 21°)

Figure 3.4 Sketch of Pyrex Glass Vessels and Flanges

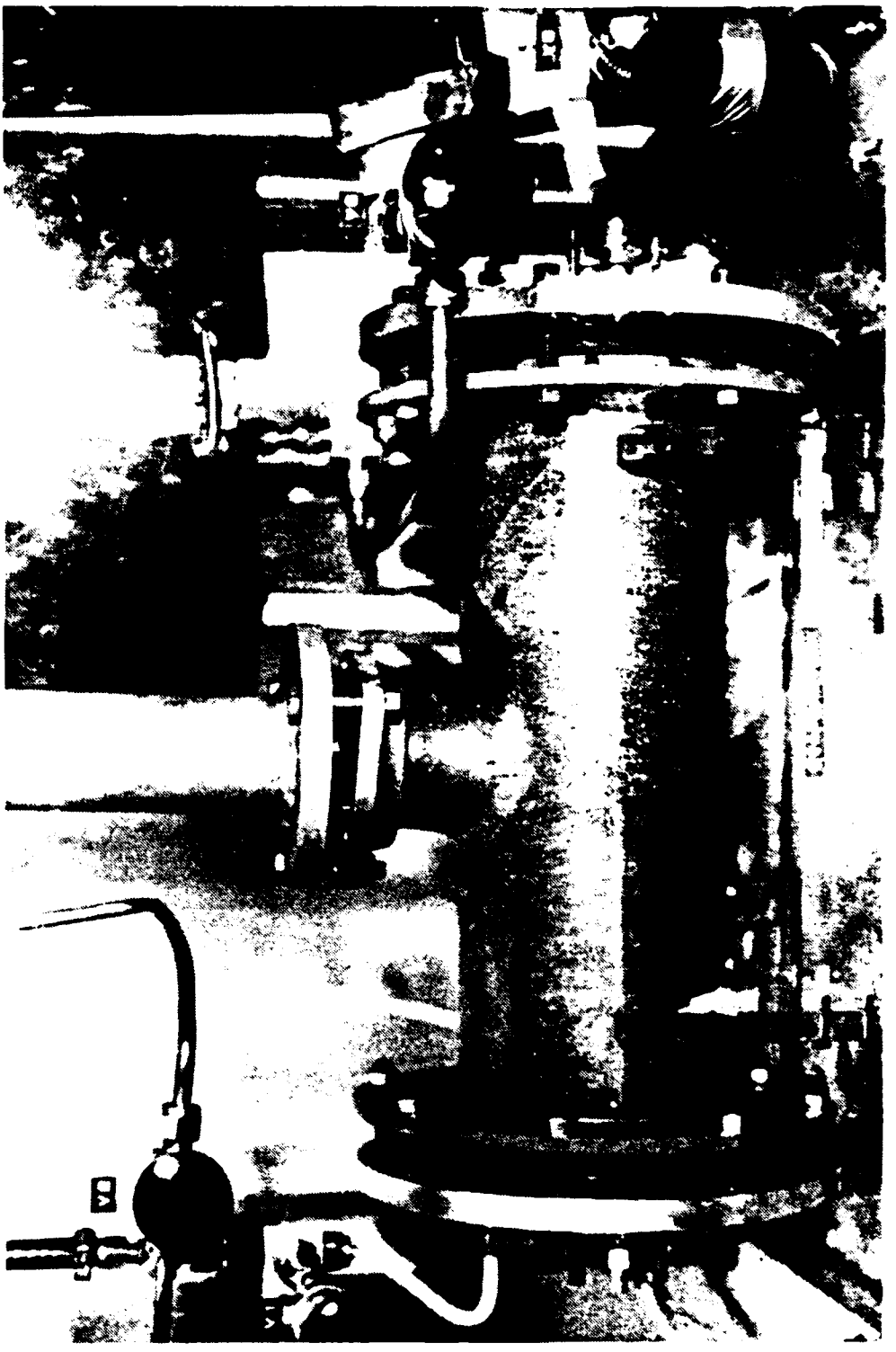

Figure 3.5 Photograph of Evaporator

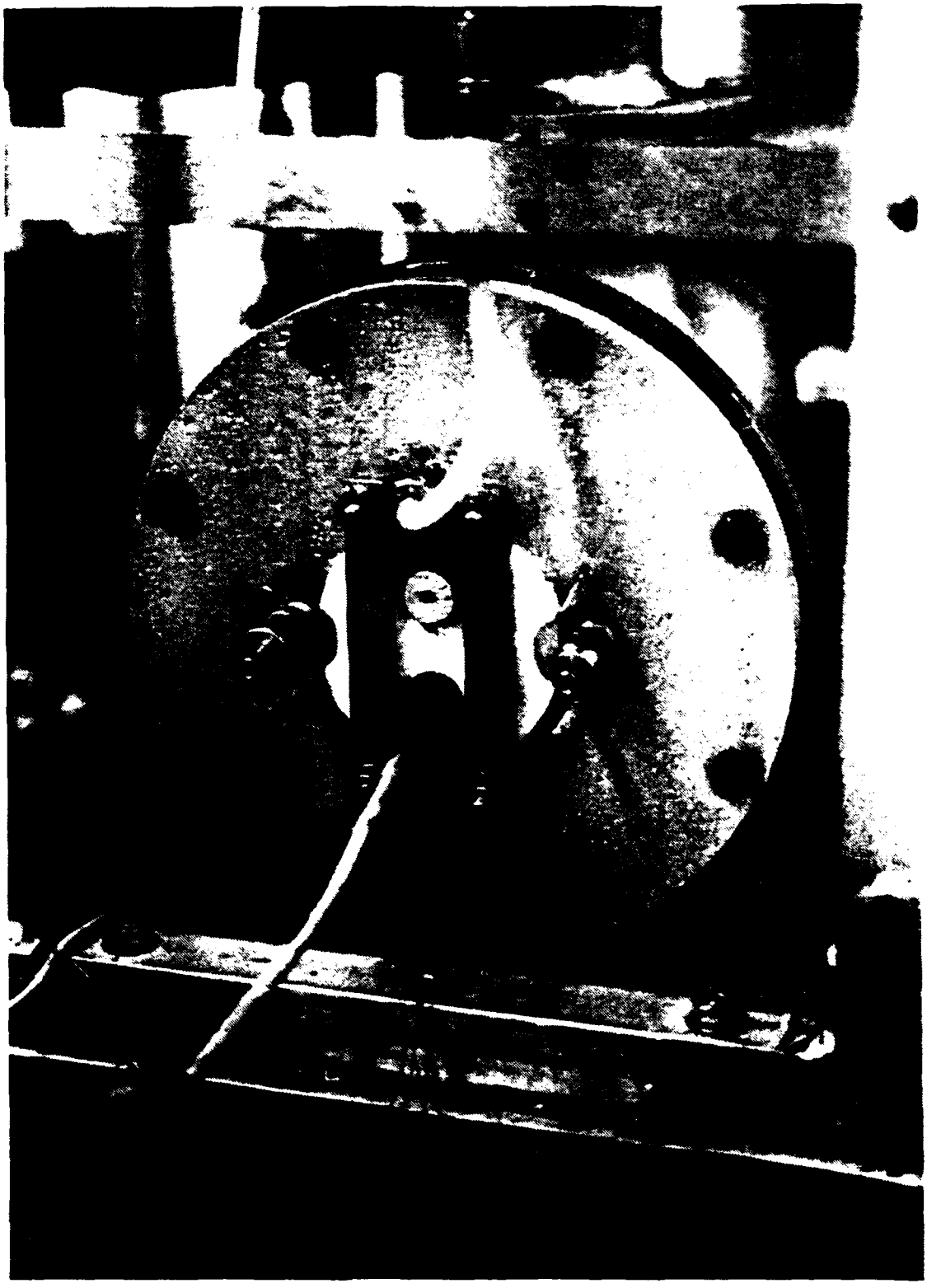

Figure 3.6 Endplate strongback to secure Teflon inserts

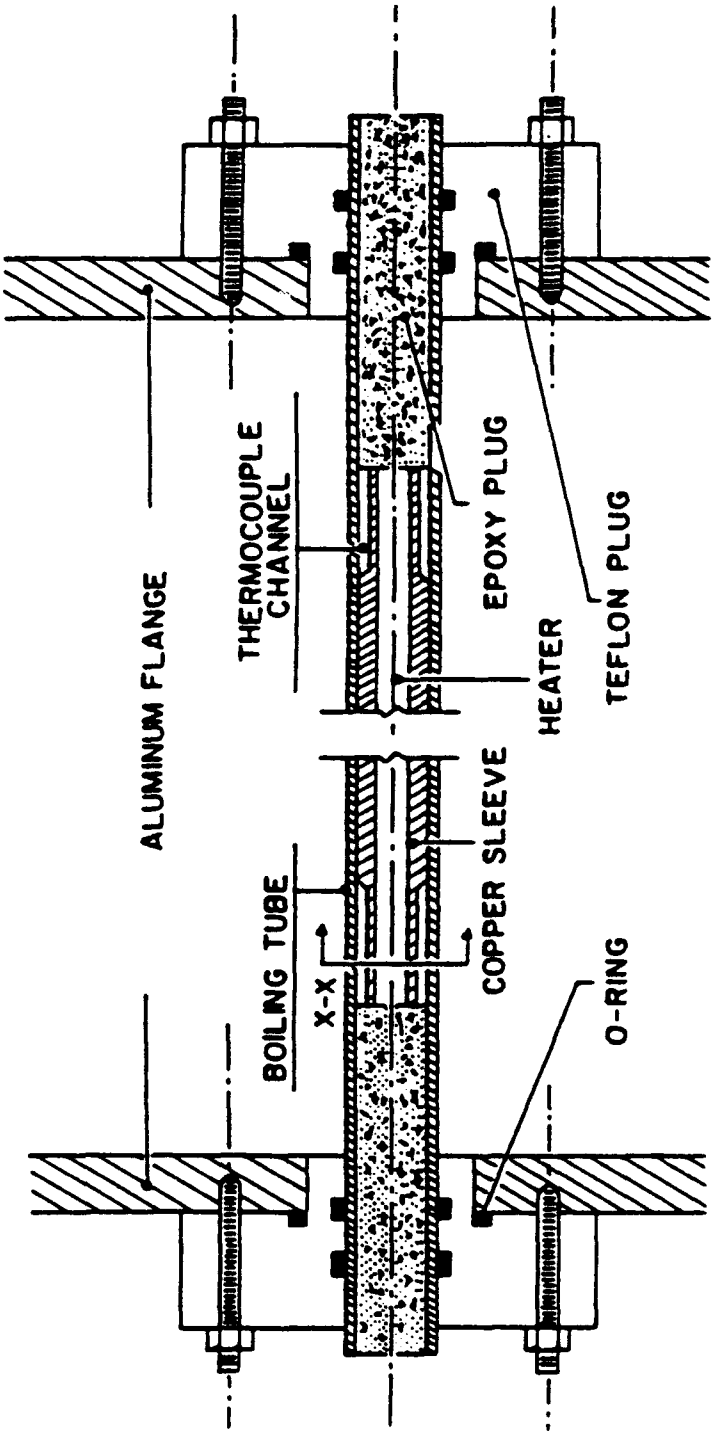

Figure 3.7 Schematic of boiling tube

D. OIL ADDITION SECTION

The oil addition section consisted of a 152.4 mm diameter by 152.4 mm high oil reservoir, and a 25.4 mm diameter by 355 mm high graduated glass cylinder mounted above the evaporator as shown in Figure 3.1. Replenishing oil in the reservoir was achieved by removing the filler cap, and pouring oil through a funnel. The graduated cylinder was connected to the oil reservoir through valves V4 and V2. A miscible alkylbenzene oil, *Zerol 300,* was used with R-124. Oil concentrations (by weight) of 0, 3, and 10% were used for each of the tubes. Addition of oil into the refrigerant was accomplished with the following procedure:

1. Ensure pneumatic hose is connected to the reservoir's filler tube and charged. Flow of oil into the graduated cylinder from the cylinder is controlled by means of valve V2.

2. Ensure refrigeration plants are on line and sump temperature is at least -10 °C. Start the condenser pump and lower the system pressure to about 5 psig by controlling condensate flow by means of valve VC.

3. Open valve V4 to equalize the pressure in the graduated cylinder and in the evaporator/condenser (indicated by no more pressure change with the installed pressure gage). Secure the condenser pump.

4. Pressurize the entire system by applying heat flux to the refrigerant pool by aligning the variac ring to approximately 90 KW. Secure heat flux when system pressure reaches approximately 30 psig. Then close valve V4 to contain the pressure in the tube.

4. Start condenser pump and open valve VC fully to lower pressure in the system to approximately 5 psig. Then open valve V1 to allow the measured oil in the graduated cylinder to flow into the pool.

The above procedure will expedite the oil addition process, the higher the pressure difference between the top and bottom of the cylinder, the quicker the flow of oil.

E. COOLING SYSTEM

1. Water/Ethylene-Glycol Coolant Sump

A plexiglass tank, 1.3 cm thick, 47.85 cm on its sides and 66.14 cm high contained a mixture of 13 gallons of ethylene-glycol and 25 gallons of distilled water. It was mounted at the base of the frame on a wooden platform, and was insulated with 22 mm thick rubber sheet. Supply and discharge ports were connected for the condenser and sump pumps. A thermocouple to measure sump temperature was installed through the condenser return line located on the top of the tank.

2. Refrigeration Plants

A 1/2 ton R-502 and 1/4 ton R-12 refrigeration system cooled the water/ethylene glycol mixture in the sump. Both systems consisted of the following components: (1) hermetically sealed compressor assembly, (2) air-cooled condenser, (3) receiver, (4) filter-dryer, (5) pressure regulator, (6) temperature control switch, and (7) thermostatic expansion valve. Each refrigeration plant was controlled by a temperature control switch and thermostatic expansion valve. The R-12 plant used a 9.5 mm coiled copper tubing installed in the sump tank as an evaporator as shown in Figure 3.1, while the R-502 plant used a counter-flow heat

exchanger as an evaporator as shown in Figure 3.8. The sump temperature was maintained at approximately -17 °C when both R-12 and R-502 plants were used. Figure 3.9 is a photograph of the R-12 and R-502 refrigeration plants.

3. Pump and Control Valve

A positive displacement, 8 gpm, 115V Burks turbine type pump was used to pump the ethylene glycol/water coolant mixture through cross-flow heat exchanger of the R-502 refrigeration plant. A similar pump was used to pump the coolant mixture to the condenser via valve VC as shown in Figure 3.1. Valve VC was used by the operator to control the refrigerant pool saturation temperature and condensation rate. A discharge bypass line with valve V9 was installed from the pump to prevent overloading the positive displacement pump during low heat flux application (i.e. low coolant flow through the condenser).

F. REFRIGERANT RESERVOIR

To facilitate tube removal without dumping the refrigerant into the atmosphere, an aluminum reservoir 228.6 mm in diameter by 254 mm high was mounted just above the evaporator (see Figure 3.1). The reservoir was equipped with a sight glass for liquid-level monitoring. The reservoir can be connected or isolated to or from the system by means of valves V6, V7, V12 and V13.

G. FRAME

An aluminum frame 107 cm X 51 cm X 61 cm contained all the components of the system with the exception of the R-502 and R-12 refrigeration plants. The top portion of the frame contained the evaporator, condenser, oil addition system, and the refrigerant reservoir. For safety considerations and to help maintain the evaporator and condenser in an isothermal condition, all sides of the frame were covered with 12.7 mm plexiglass. The left and right side covers were hinged to the frame to provide easy access to the assembly. The bottom and top portion of the frame were covered with an aluminum plate and plywood respectively. The coolant sump tank was mounted at the base of the frame.

H. INSTRUMENTATION

1. Power Measurement

A 240 volt AC source, adjustable from 0 to 220 volts and 0-5 amps by a variac controller, was used as the power source for the heater in the boiling tube. The AC current and voltage RMS sensors converted the AC input into DC voltages that were then used as input to the Data Acquisition and Control Unit as shown in Figure 3.10.

2. Temperature Measurement

Temperatures were measured using the thermal emf from 30 gage (0.25 mm diameter) copper-constantan (type T) thermocouples. Eight thermocouples were spaced both

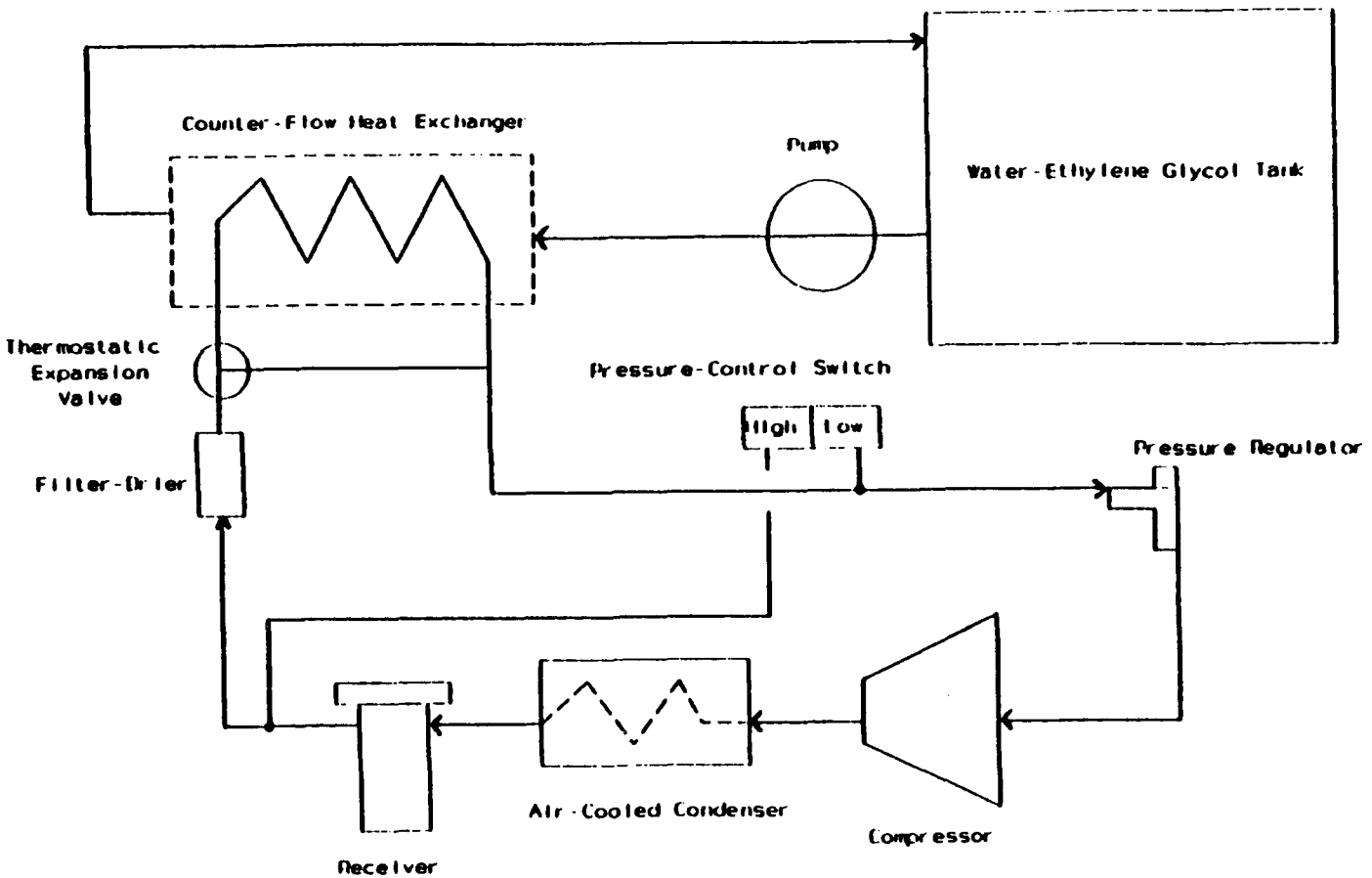

Figure 3.8 Schematic of R-502 refrigeration unit

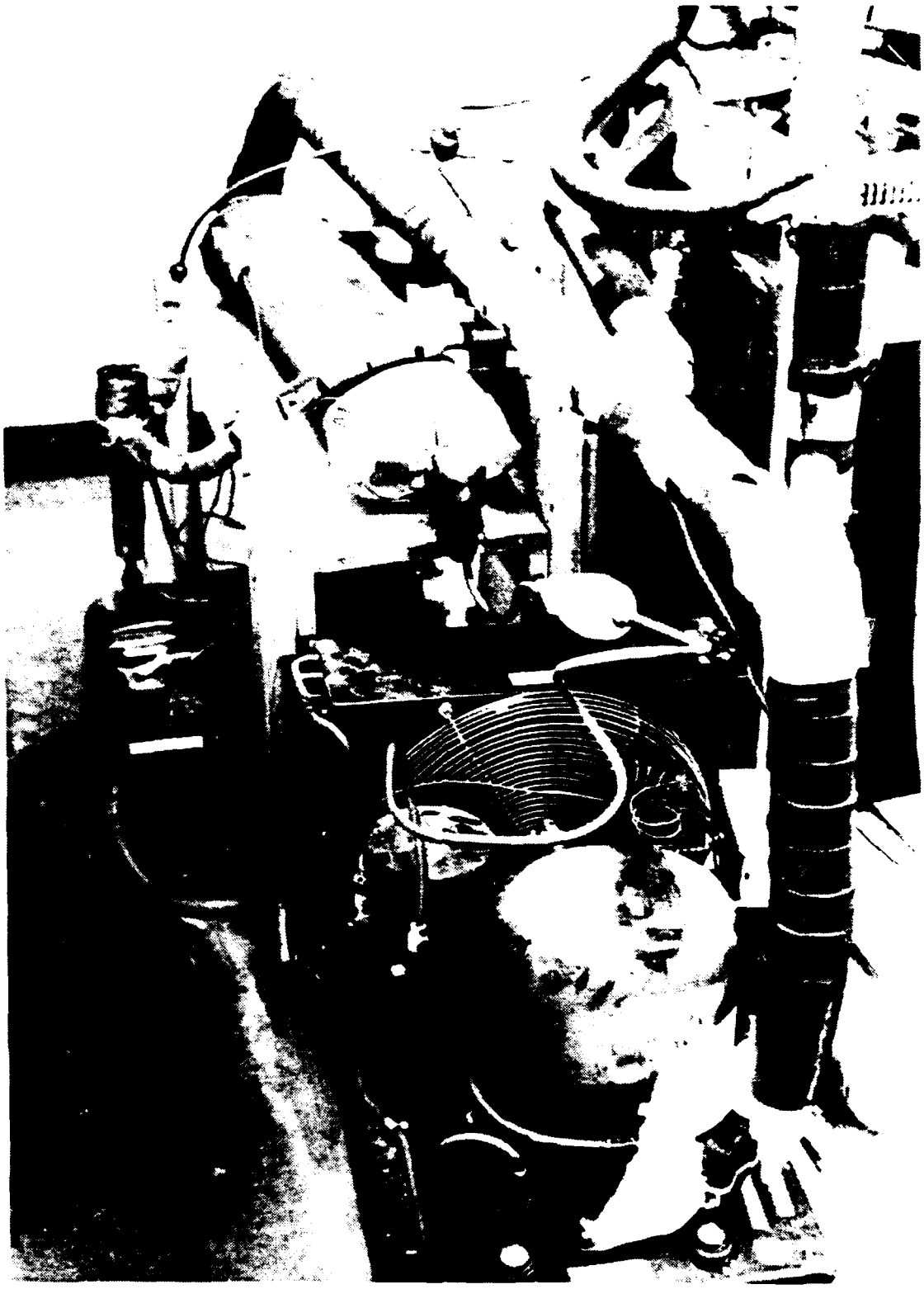

Figure 3.9 Photograph of refrigeration plants

circumferentially and axially over the heater sleeve, as shown in Figure 3.11, to measure the tube wall temperatures. Three thermocouples inserted into the evaporator thermocouple wells measured the evaporator pool temperatures. A single thermocouple inserted into the coolant sump tank measured the sump temperature.

I. DATA ACQUISITION AND REDUCTION PROGRAM

Bertsch's [Ref. 6] DRPGB data acquisition and reduction program was used in this study. The interactive data acquisition program directed the Hewlett-Packard 9826 computer and a Hewlett-Packard 3497a Data Acquisition Unit to read and process all thermocouples, current and R.M.S. voltage readings. Raw data were stored in the computer's hard drive, and a hardcopy printed on a Hewlett-Packard Inkjet printer. Channel assignments are listed in Table 3.1.

J. PROCEDURE FROM KEYBOARD

The following interactive procedure was used for data acquisition:

1. Load data acquisition/reprocessing program by pressing F5 (load button) then type in 'DRPGB'. Press F3 (run button) to run the program. Select '0' (TAKING DATA OR RE-PROCESSING PREVIOUS DATA OPTION).

2. After the prompt "GIVE A NAME FOR THE RAW DATA FILE", type filename of data to be processed and stored (see Appendix A for data file naming scheme used).

3. Enter any defective thermocouple locations that were previously identified by program SETUP71 (see Appendix E of Bertsch [Ref.6]).

4. Select test tube after the prompt "SELECT TUBE NUMBER" by typing the number corresponding tube type displayed on the screen. For example, type '5' for HIGH-FLUX tube, '7' for GEWA-K 26 fpi, '13' for GEWA-K 19 fpi.

5. Select option '1' (SET DESIRED HEAT FLUX), then adjust variac to the desired heat flux value.

6. Adjust coolant flow through the condenser with valve VC as required to obtain the desired pool and vapor temperatures (TL1, TL2, and TLV) close to saturation temperature (2.22 ± .01 °C).

7. When saturation temperature was reached, and after waiting 5 minutes for the temperature to stabilize, press F1 to display the select option, then press '0' to take data. This will direct the data acquisition computer to scan all the channels as listed in Table 3.1, do the required calculations, display them on the screen and print the results.

8. After the result is printed, press '1' after the prompt "OK TO STORE THIS DATA SET" to store data into the file name created in step 2.

9. After the prompt "WILL THERE BE ANOTHER RUN (1=Y,0=N)?", press '1'.

10. Repeat steps 5 to 9 for each change in heat flux. For the last heat flux entered, press '0' for step no. 9.

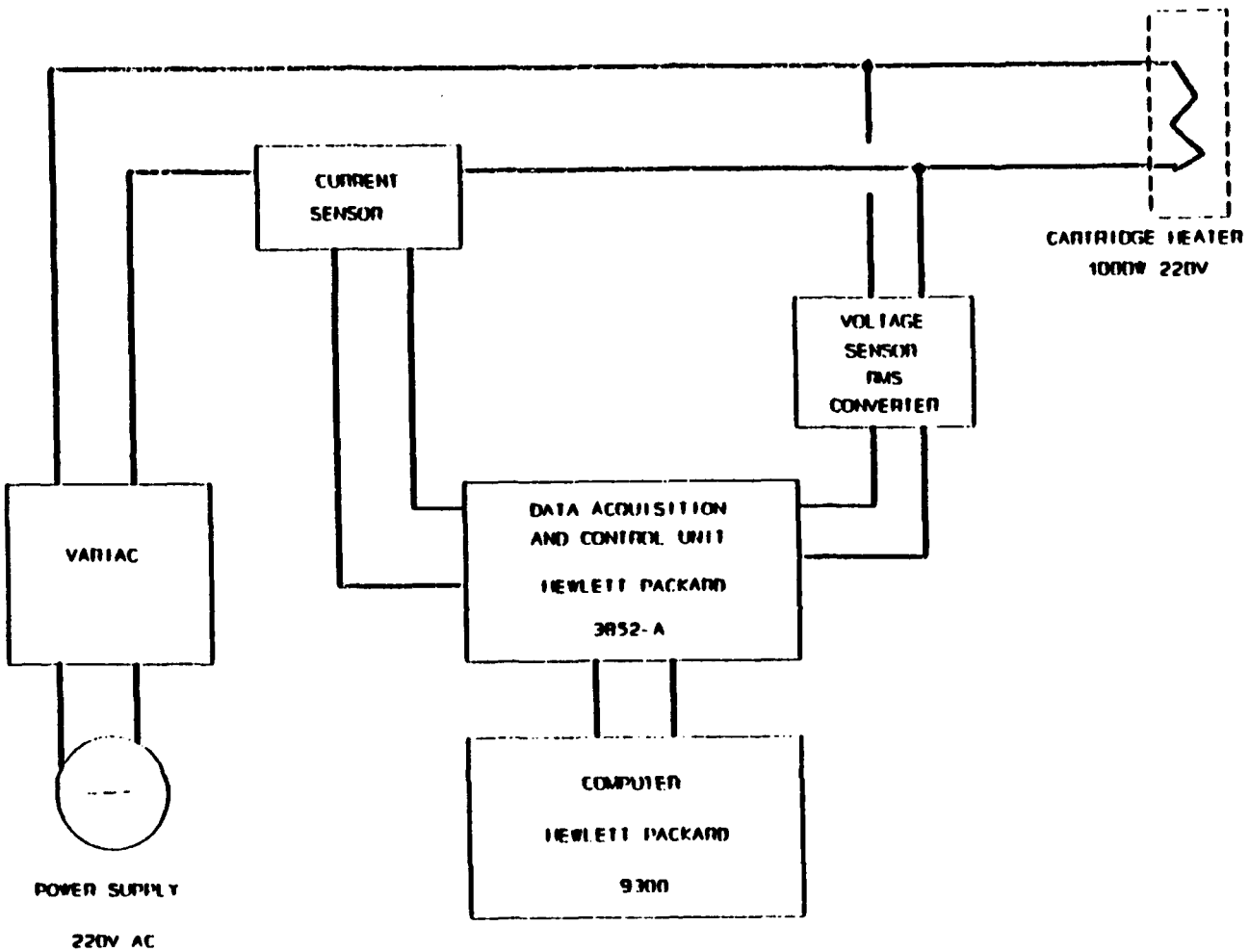

Figure 3.10 Data acquisition and control unit schematic diagram

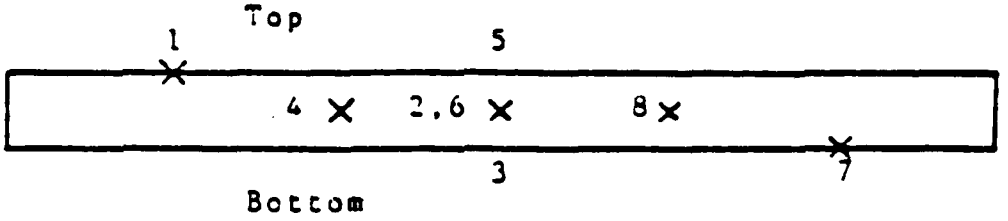

(a) View of the boiling tube thermocouple locations as seen from the front of the experimental apparatus.

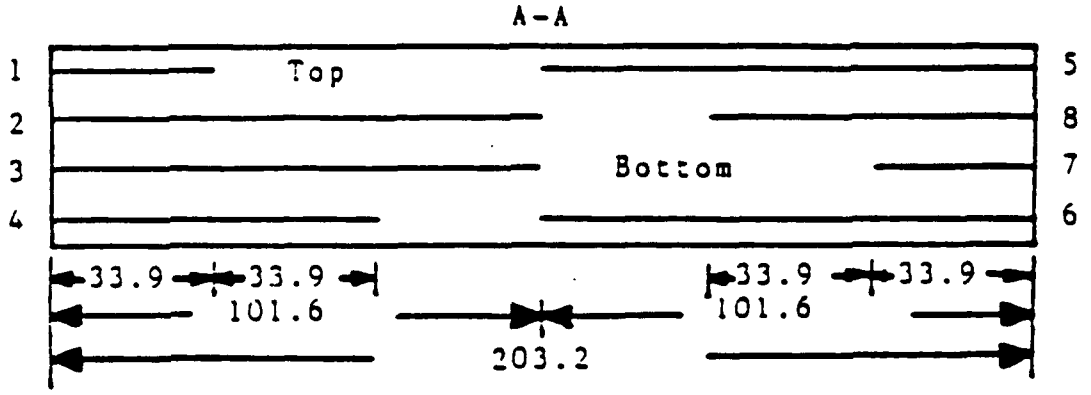

(b) Thermocouple sleeve unwrapped (at section A-A) to show the relative locations of the thermocouple channels (all dimensions in millimeters).

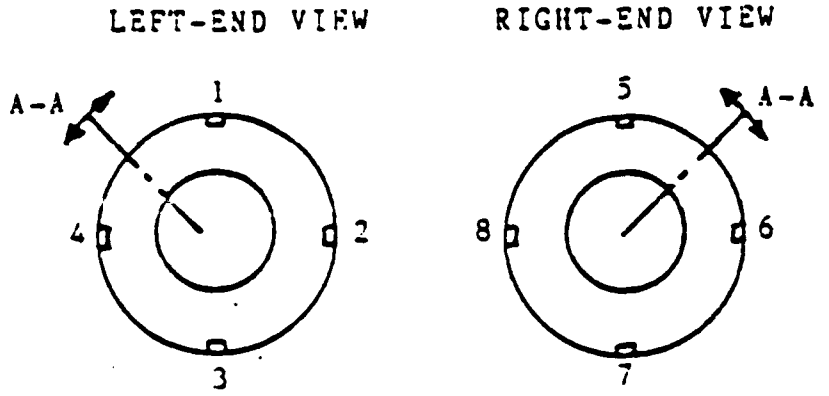

(c) End views of the boiling tube.

Figure 3.11 Thermocouple locations of instrumented tube

Table 3.1 HP 3497 CHANNEL ASSIGNMENTS

Channel	Channel Assignments
00-07	tube wall temperatures
08-10	pool liquid temperature
11	sump temperature
20	RMS voltage
21	current sensor

IV. EXPERIMENTAL PROCEDURE

A. SYSTEM PREPARATION

1. Vacuum Test

Once the evaporator tube was installed, and prior to charging with refrigerant, the system was evacuated by opening valves V11 and V8 and activating the vacuum pump (see Figure 3.1) to approximately 29 inch Hg. If no leak was detected within 30 minutes (i.e. no drop in vacuum), the system was charged with R-124.

2. Pressure Test

If there was a significant vacuum loss during the vacuum test, the system was pressurized with air to 20 psig via valves V10 and V8. Leaks were detected using soap/water solution. After identifying and correcting the leak source, the system was again evacuated and step 1 was repeated.

3. System Charging with R-124

After successful system integrity was accomplished, the evaporator was charged with refrigerant to a level of 20 mm above the top of the test tube using the following procedure:

a. Gravity Fill from the Reservoir

Valves V12 and V7 were opened to equalize pressure between the reservoir and the evaporator. Then valves V6 and

V13 were opened to allow the liquid refrigerant to drain into the evaporator. At the required liquid level in the evaporator, valves V6 and V7 were closed to isolate the reservoir.

b. From Refrigerant Cylinder

The cylinder was first connected to valve V10 by means of a charging hose. Valves V5, V8 and V10 were opened and refrigerant was released from the cylinder by opening the liquid valve. Slightly before the required liquid level was attained, the cylinder charging valve was closed, followed by the closure of valves V10 and V8.

4. Degassing Procedure

a. Degassing Procedure A

After charging the system with refrigerant, a leak test was conducted using the hand-held "Halogen Leak Detector", by energizing the detector and placing its probe near all flange connections and hose fittings. (If a leak is detected, the detector will emit a series of beeping sounds.) After correcting the leak (i.e. tightening flange bolts or hose fittings), the system was degassed by first boiling the refrigerant at a power setting of approximately 90 KW (on the variac ring) for 10 minutes with the condenser pump running to prevent overpressurizing the system. Any noncondensable gases produced by this process were collected in the top portion of the condenser. The heat flux and condenser pump were then

secured and the system allowed to sit for approximately 10-20 minutes; this allows the condensed refrigerant to drain back into the evaporator, leaving just the noncondensable gases. Finally, the vacuum pump was turned on and valves V11 and V8 were opened for approximately 10 seconds to suck out the non-condensable gases.

b. Degassing Procedure B

This degassing procedure came about as a result of consistently low incipient superheats after long settling time (time between runs of approximately 12 hours or more particularly on the HIGH FLUX tube). This procedure was very similar to degassing procedure A except for the following differences: (1) the pool was boiled for 30 minutes instead of 10 minutes, (2) the system was secured for approximately 30 minutes prior to activating the vacuum pump, (3) the vacuum was turned on for 20-30 seconds. Procedure B was also conducted after every oil addition due to the visible presence of entrapped air in the oil in the graduated cylinder prior to oil addition.

5. Data Acquisition Channel Check

After connecting all evaporator tube thermocouples, and inserting the three pool thermocouples into their respective wells, program SETUP71 (see Bertsch [Ref. 6]) was loaded and run to check the output of all thermocouples. Any inconsistent readings from the tube thermocouples were then

noted and excluded from the data acquisition portion. For any other erroneous readings, appropriate action was taken. In some cases, the apparatus was secured for at least 6 hours (usually overnight) to allow the tube surface to become fully wetted.

B. NORMAL OPERATING PROCEDURE

The following procedure was utilized to conduct test. This was closely followed from Bertsch [Ref. 6]:

1. Both R-502 and R-12 refrigeration systems were operated for approximately 2 hours to cool the sump to -17 °C.
2. The data acquisition unit, computer and variac control panel were energized.
3. Program SETUP71 was loaded and run. All data acquisition channels were checked, and the refrigerant pool temperature was slowly reduced to 2.2 °C by circulating coolant through the condenser via valve VC.
4. Data acquisition program DRPGB was loaded and run.
5. An initial heat flux (600-700 W/m^2) was entered in the program and the variac was adjusted to this preset value.
6. Coolant flow through the condenser was adjusted by opening slightly valve V10 until desired saturation temperature of 2.22 ± 0.1 °C was achieved.
7. Data were collected after the system had stabilized for 5 minutes.
8. Heat flux was increased logarithmically (i.e. in equal sized increments on a logarithmic plot) and steps 6 and 7 were repeated.

V. DISCUSSION OF RESULTS

A. REPRODUCIBILITY

Reproducibility/repeatability runs were initially conducted for familiarization with the equipment and operating/testing procedures. Figures 5.1 and 5.2 are plots of increasing heat flux runs for the two degassing procedures taken on four different days. Good agreement throughout, including the onset of nucleate boiling (indicated by arrows) is evident. Small amounts of scatter at lower heat fluxes (from 500 to 3000 W/m^2) which disappears at mid-range heat fluxes (3000 to 6000 W/m^2) can be seen in both figures. This scatter is probably due to thermal gradients within the pool in the convection region where the mixing is not very efficient. Large local variations in the wall and pool thermocouple readings tend to support this. For example, the run conducted on 29 Jan 93, at an initial heat flux of 430 W/m^2, three of six wall thermocouples (located close to both ends of the heated length of the tube) and one of the three pool thermocouples read about 5% lower than the other thermocouples. The same thermocouples read 2% lower at a heat flux of 1750 W/m^2. In the nucleate boiling regime (6000 to 90,000 W/m^2), excellent repeatability was achieved at all heat fluxes. The corresponding decreasing heat flux runs, shown in

Figure 5.3 for degas procedure A also displays a very repeatable behavior. In the boiling region, the pool and wall temperature are much more steady due to better mixing in the pool.

Figure 5.4 is a comparison of a representative increasing and decreasing heat flux run with the data of Bertsch [Ref. 6] for the smooth tube. As before, curves #1 (present data) and #3 (Bertsch) show slight scatter in the low heat flux natural convection region but merge at medium heat flux. Curve #1 nucleates at a wall superheat of 15.4 °C, while curve #3 nucleates at a lower wall superheat of 8.5 °C. The difference in incipient wall superheat results in a noticeable difference in the starting point of the nucleate boiling region. Curve #1 has a thermal overshoot (thermal overshoot is taken to be the horizontal jump between the incipient point and the decreasing heat flux curve (Memory and Marto [Ref. 8]) of about 11 °C while curve # 3 yielded only a 4 °C thermal overshoot. The reason for this difference is not clear since the tests were, in essence, identical. At higher heat fluxes in the nucleate boiling region, good agreement was obtained. In the decreasing heat flux runs, curves #2 and #4 were almost identical.

Other comparisons and repeatabilities are shown in Figures 5.5 to 5.15 for various tubes and various oil concentrations. In Figure 5.5, with 3% oil, the present data show a much higher heat transfer coefficient (lower wall superheat

throughout the natural convection region) and a lower ONB compared to Bertsch [Ref. 6]. Good repeatability was again shown in the nucleate boiling region. In the decreasing runs, both data are very repeatable at heat fluxes between 90,000 W/m^2 to 30,000 W/m^2; but separation occurred at lower heat fluxes. As mentioned earlier, reasons for the differences are not clear. Figure 5.6 with 10% oil, show the same trend in the natural convection and nucleate boiling regions between Bertsch [Ref. 6] and the present data, except that a relatively higher ONB was obtained. The decreasing runs display good level of repeatability.

Figures 5.7, 5.8, and 5.9 are GEWA-K 19 fpi finned tube comparison plots of pure R-124, 3% oil and 10% oil data of Bertsch [Ref. 6] and the present study respectively. All plots display good repeatabilities throughout the natural convection and nucleate boiling regions, with consistently higher ONB points obtained from the present study. This may be attributed to the difference in degassing procedures used.

Figures 5.10, 5.11, and 5.12 are GEWA-K 26 fpi finned tube comparison plots for pure, 3% and 10% oil respectively of Bertsch [Ref. 6] and the present study. All plots show significant differences throughout in the natural convection region and most notably in the nucleate boiling region where a consistent difference of about 10 K can be seen at 100,000 W/m^2. This can probably be due to a better cleaning procedure used in the present study (cleaning procedure B as discussed

in Chap IV) in which the fin gaps were brushed with alcohol then with acetone before installation, vice just spraying with acetone (cleaning procedure A) used by Bertsch [Ref. 6].

Figures 5.13, 5.14 and 5.15 are HIGH FLUX tube comparison plots. Consistently higher ONB points from the present study (due to better degassing procedure) and good agreement in the nucleate boiling region are evident.

B. EFFECT OF OIL ON BOILING INCIPIENCE

The effect of oil on the onset of nucleate boiling has been studied quite extensively in the past by Memory and Marto [Ref. 8], Chongrungreong et. al [Ref. 18], Stephan and Mitrovic [Ref. 22], Wanniarachi et. al. [Refs. 31 and 32], Stephan [Ref. 40], Daugherty and Sauer [Ref. 41], Sauer et al. [Ref. 42], Karasabun [Ref. 43], Reilley [Ref. 44], Sugiyama [Ref. 45], and Bertsch [Ref. 6]. The effect of oil on incipient wall superheat can best be explained by the use of equation (2.5) and the corresponding nucleation parameter given by:

$$N = \frac{\sigma T_{sat}}{\rho_v h_{fg}} \qquad (5.1)$$

It can be seen from equation (2.5) that the incipient wall superheat depends on the parametric group inside the bracket as discussed by Bergles and Roshenow [Ref. 35]. Saturation temperature, surface tension and viscosity increase with

increasing oil concentration as pointed out by Bar-Cohen [Ref. 9]. Sauer et al. [Ref. 42] said:

> Several thermodynamic properties of the refrigerant are significantly changed by the addition of oil. The vapor pressure of the refrigerant-oil mixture is lower than that for the pure refrigerant at the same temperature. Both viscosity and surface tension are increased when oil goes into solution with the refrigerant....An increase in surface tension decreases bubble formation for a given wall superheat. Increased liquid viscosity tends to reduce turbulence and dampen out eddy formations in the liquid flow to the surface. These may be the principal factors which account for the various effects of oil on nucleate boiling.

In the present study, however, there are no available thermodynamic properties of the oil (Zerol 300) to determine the mixture's latent heat of vaporization, specific volume and other thermodynamic properties, therefore, it is impossible at this time to predict precisely the incipient boiling superheat with the use of equations (2.5).

1. Smooth Tube

Figures 5.16 5.17, and 5.18 are plots of seven increasing heat flux runs for pure R-124, R-124/3% oil mixture and R-124/10% oil mixture respectively. These figures demonstrate the scattering of the data in the natural convection region, particularly at lower heat fluxes due to reasons given earlier. In Figure 5.16, the data points tend to merge towards the Churchill-Chu [Ref. 46] correlation prior to the onset of nucleate boiling. The highest heat fluxes reached prior to boiling for 0%, 3% and 10% oil

concentrations were 12.2 Kw/m^2, 12.2 Kw/m^2, and 14.9 Kw/m^2 respectively. It should be noted that once nucleation occurred, very few data points in the nucleate region were taken as can be seen from the figures. For the few data points taken, excellent repeatability were always obtained. Apart from the repeatability/comparison data presented in Figures 5.1 to 5.15, no decreasing heat flux data were taken. For the pure R-124 case, incipient wall superheats ranged from 30.2 K to 35.3 K with corresponding thermal overshoots from 21.0 K to 25.8 K. For the 3% oil/R-124 mixture, incipient superheats were from 31.2 K to 37.3 K with thermal overshoots of 24.0 K to 28.7 K. The 10% oil/R-124 mixture resulted in incipient superheats of 36.2 K to 40.1 K with thermal overshoots ranging from 27.0 K to 30.1 K (see Table 5.1). Hence, ONB was fairly consistent and only varied typically by 5 °C for numerous tests runs under identical conditions. In Figures 5.17 and 5.18, the Churchill and Chu correlation is not given as it is strictly valid for pure substances. However, the data still tend to converge as heat flux is increased in the convection region for similar reasons as those already given.

Figure 5.19 is a probabilistic summary of the onset of nucleate boiling. This form of presentation for incipient superheat was introduced by You et al. [Ref. 7] as the most convenient way to display the randomness behavior of the onset of nucleate boiling. Figure 5.19 shows the incipient wall

Table 5.1 ONSET OF NUCLEATE BOILING COMPARISON

Tube Type	q''_{max} attained prior to incipience (kW/m^2)			Incipient Superheat Range (K)			Thermal Overshoots Range (K)		
	0%	3%	10%	0%	3%	10%	0%	3%	10%
SM	9.7 - 12.2	9.6 - 12.2	11.8 - 14.9	30.2 - 35.3	31.2 - 37.3	36.2 - 40.1	21.0 - 25.8	24.0 - 28.7	27.0 - 30.1
GK 19	8.3 - 12.3	10.5 - 22.5	13.1 - 24.5	9.4 - 11.6	10.0 - 19.6	14.0 - 20.2	7.2 - 9.4	7.3 - 16.4	11.0 - 16.3
GK 26	24.1 - 33.9	16.7 - 28.6	31.5 - 38.4	17.5 - 22.4	12.9 - 21.1	20.4 - 23.7	13.0 - 17.3	9.2 - 17.0	14.6 - 17.8
HF	3.0 - 3.3	1.8 - 4.1	3.5 - 7.3	9.2 - 11.5	6.5 - 11.2	13.8 - 21.6	8.6 - 11.0	6.7 - 10.6	8.6 - 11.6

NOTE: SM - SMOOTH
GK 19 - GEWA-K 19 fpi
GK 26 - GEWA-K 26 fpi
HF - HIGH FLUX

superheats attained for the 7 tests conducted with pure R-124, 3% and 10% oil concentrations as percent probability of nucleation occurring. For example, for the 3% oil curve, all seven runs reached 31.5 °C without nucleating. Three of the seven runs nucleated at a wall superheat less than 32.8 °C and four of seven reached nucleation point at a higher wall superheat; this means that the probability of nucleation occurring at 32.8 °C is between 3/7 and 4/7 or 3.5/7 (50%). At a wall superheat of 37.3 °C all seven runs reached the nucleation point so that a probability of 100% exists. Notice that with this probabilistic representation, it is easy to see that the presence of oil delays the onset of nucleation. Figure 5.20 is a comparison between the smooth tube data of Bertsch [Ref. 6] with the present data. The difference can be attributed to factors such as degassing (which is discussed in more detail later) and data gathering techniques, by the two investigators. One thing in common, however, is that increasing oil concentration definitely seems to result in an increase in incipient wall superheat, but the effect may be small in comparison to the large probabilistic variations due to operating procedures.

2. GEWA-K 19 Tube

Figures 5.21, 5.22, and 5.23 show the effect of oil for seven increasing heat flux runs for pure R-124, R-124/3% oil mixture and R-124/10% oil mixture respectively while

boiling from a 19 fpi finned tube (GEWA-K). As before, data scattering was evident at low heat fluxes, with a merging trend at mid-range heat fluxes. The Churchill/Chu correlation is also given in Figure 5.21 and appears to be well to the right of the data. However, the reason for this is due to the choice of tube surface area in the heat flux calculation, where root diameter has been used. Memory and Marto [Ref. 8] have shown that if the actual wetted area were used in the calculation of heat flux, then the data would drop back very close to the correlation. Therefore, one must be careful when interpreting such results. The maximum heat fluxes attained prior to ONB were 12.3 kW/m^2, 22.5 kW/m^2 and 24.5 kW/m^2 for 0%, 3% and 10% oil respectively. For pure R-124, incipient wall superheats ranged from a minimum value of 9.4 K to a maximum of 11.6 K with thermal overshoots ranging from 7.2 K to 9.4 K. These are significantly lower than the smooth tube, demonstrating the improved heat transfer performance from these enhanced tubes. At 3% oil, the incipient wall superheats were more dispersed from 10.0 K to 19.6 K with thermal overshoots ranging from 7.3 K to 16.4 K. Increasing the oil concentration to 10% yielded incipient wall superheats ranging from 14.0 K to 20.2 K with thermal overshoots from 11.0 K to 16.3 K. On a probabilistic basis, Figure 5.24 shows a wide variation in the incipient wall superheats for the 3% and 10% oil mixtures which re-affirms the randomness of ONB.

Also, the figure demonstrates the increase in ONB as oil concentration increases, as from the smooth tube.

3. GEWA-K 26 Tube

Figures 5.25, 5.26, and 5.27 show the results of oil on seven increasing heat flux runs for pure R-124, R-124/3% oil mixture and R-124/10% oil mixture respectively, while boiling from a 26 fpi finned tube (GEWA-K). Just like the smooth and 19 fpi GEWA-K plots, scattering at low heat fluxes is clearly evident. The maximum heat fluxes attained prior to ONB were 33.9 kW/m^2, 28.6 kW/m^2 and 38.4 kW/m^2 for 0%, 3% and 10% oil respectively. Incipient wall superheats were from 17.5 K to 22.4 K with thermal overshoots ranging from 13.0 K to 17.3 K for pure R-124. These values were much larger than those noted earlier for the GEWA-K 19 fpi tube (see Table 5.1). The reason for this difference is not known but may be due either to different surface roughness effects or different micro-convection effects within the channels between the fins. With 3% oil, the incipient wall superheats ranged from 12.9 K to 21.1 K, giving thermal overshoots of 9.2 K to 17.0 K. At 10% oil concentrations, incipient wall superheats ranged from 20.4 K to 23.7 K with corresponding thermal overshoots from 14.6 K to 17.8 K. Figure 5.28 summarizes probabilistically the ONB data for 0%, 3% and 10% oil concentrations. Note that for 3% oil, the data are to the left of the data for 0% oil. This shift was not obtained with the GEWA-K 19 fpi tube (see

Figure 5.24). However, this shift is very repeatable as these curves are data taken from 7 identical tests. The reason for the shift is not clear but could be a combination of changes in the thermophysical properties (when oil is added) together with favorable conditions for bubble growth from the vapor nuclei trapped in the cavities. It may be that the 26 fpi tube, with its narrow gap width between fins, is conducive to bubble growth whereas the 19 fpi tube is not; there may be a critical bubble diameter which can grow on the 26 fpi tube (due to its narrow channels) but which condenses and collapses on the 19 fpi and smooth tubes. This of course is conjecture and requires further thought. Further addition of oil (up to 10% oil) causes a delay due to the change in nucleation parameter properties as noted in equation (5.1).

4. HIGH FLUX Tube

Figures 5.29, 5.30, and 5.31 present the seven runs conducted for 0%, 3% and 10% oil concentrations respectively for the HIGH FLUX tube. Lower incipient points and significantly larger thermal overshoots were obtained for all oil concentrations (see Table 5.1). Incipient wall superheats ranged from 9.2 K to 11.5 K with resulting thermal overshoots of 8.6 K to 11 K for 0% oil. The scatter is slightly more evident for this tube in the convection region but is still converging as heat flux increases. The data fall very close to the Churchill/Chu correlation, demonstrating that in this

region, a HIGH FLUX tube behaves in a similar way to a smooth tube. At 3% oil concentration, lower incipient wall superheats were obtained than for 0% oil (like the GEWA-K fpi tube) from 6.5 K to 11.2 K with corresponding thermal overshoots ranging from 6.7 K to 10.6 K. The 10% oil concentration showed a large increase of incipient wall superheat compared to pure R-124 values. Incipient points ranged from 13.8 K to 21.6 K, and thermal overshoots ranging from 8.6 K to 11.6 K. Figure 5.32 displays the variation in incipient wall superheats in a probabilistic way. Note again the decrease in incipient superheat at 3% oil concentration, similar to that found for the GEWA-K 26 fpi tube. It may be that the nucleating cavities on these tubes are similar. Figure 5.33 compares the incipient wall superheats of Bertsch [Ref. 6] with the present data for the HIGH FLUX tube for all oil concentrations. It can be seen that the present data have consistently much higher wall superheats than those of Bertsch. The reason for this is thought to be due to the different degassing procedures, which is discussed later.

C. EFFECT OF SURFACE ON BOILING INCIPIENCE

Figures 5.34 shows a comparison of representative data for GEWA-K 19 fpi and a smooth tube. It can be seen that in the natural convection region the GEWA-K 19 fpi tube has a higher heat transfer coefficient (lower wall superheat) than the smooth tube. As mentioned earlier, this is because the heat

flux was computed using a surface area based on the tube's root diameter instead of the actual finned area. Dividing the heat flux by 2.66 (ratio of the actual finned area to the area using the root diameter) shifts the curve closer to the smooth tube (and the Churchill/Chu correlation). An enhancement still is evident, indicating that the presence of the fins affects the local convection currents around the tube. In Figure 5.35, using an area conversion ratio of approximately four for the GEWA-K 26 fpi tube, the resulting actual finned area heat flux curve also behaves more like a smooth tube in the natural convection region. This is similar to that reported by Memory and Marto [Ref. 8] for R-114. Perhaps fin spacing is an important variable in studying these convective effects.

Figures 5.36, 5.37 and 5.38 are probabilistic comparisons of ONB from each enhanced tube (GEWA-K 19, GEWA-K 26 and HIGH FLUX) with the smooth tube. As shown in Figure 5.36, both the GEWA-K 19 fpi finned tube and the smooth tube display an increasing incipient point as oil increases. At 50% probability (using the smooth tube data as the basis of comparison), the onset of nucleate boiling decreased by about 60% for all oil concentrations in comparing the 19 FPI finned tube to a smooth tube. Figure 5.37 shows a similar decrease of approximately 40% for all oil concentrations for the 26 FPI finned tube. As shown in Figure 5.38, with the HIGH FLUX tube, the incipient wall superheat decreased by as much as 75% when compared to a smooth tube. This more

pronounced decrease can be attributed to the increase in nucleation sites on enhanced surfaces and their greater propensity to nucleate at lower wall superheat due to their larger relative size.

D. EFFECT OF DISSOLVED GASES

Dissolved gases in the refrigerant can significantly lower the point of incipience as described by Bar-Cohen [Ref. 9], Murphy and Bergles [Ref. 24] and Sugiyama [Ref. 44]. The effect of dissolved gases can be seen in Figures 5.16 and Figure 5.39. Degassing procedure A (as described in Chapter IV) was used initially for all tubes tested. With degassing procedure B, incipient wall superheats of about twice those obtained using degassing procedure A were obtained. Figure 5.40 is a probabilistic plot of the effect of degassing procedures for a smooth tube with 0% 3% and 10% oil concentrations. In Figure 5.41, the effect of dissolved gases over a long period of settling time (time between runs) can be seen. For overnight settling time (greater than 10 hours), about 73% lower incipient wall superheats were obtained compared to those obtained with just 0.5 hours or greater settling time. It is reasonable to assume that dissolved gases over long settling time will tend to be absorbed back into the refrigerant pool. Figure 5.41 clearly shows the trend of earlier incipience for longer times between runs.

E. EFFECT OF PRESSURE

The desire to be able to conduct more runs per day during the early part of the research led to pressurization of the system prior to a run. Bergles and Roshenow [Ref. 35], Bar-Cohen [Ref. 9], and Hooper and Abdelmessih [Ref. 37] discovered that creasing pressure above saturation pressure at operation tends to delay the incipient superheat. Pressurizing the system prior to a run deactivates more of the nucleation sites by flooding them out (i.e. rewetting the cavities).

Pressurization was achieved by pre-boiling the pool using maximum heat flux (around 90 kW/m^2) without running the condenser until a system pressure of 30 psig was reached. The heater was then secured and the pool was allowed to settle for the desired period. Figures 5.42 and 5.43 display the effect of pressurization on 0% and 3% oil/R-124 mixture respectively. The number of hours displayed in both figures corresponds to the settling time of the pool. It can be seen from these figures that there is a noticeable significant delay in the incipient wall superheat when the system was pre-pressurized.

F. EFFECT OF TUBE CLEANING

During the early runs conducted with the HIGH FLUX tube surface, the tube was cleaned (after tests with oil) following the cleaning procedure of Bertsch [Ref. 6] by spraying it with acetone and allowing it to air-dry before installation

(Cleaning Procedure A). These tests resulted in higher incipient wall superheats similar to the smooth tube for pure R-124, 3% and 10% oil concentrations. It seems that the use of alkylbenzene oil tends to clog the reentrant cavities of the HIGH FLUX tube making the tube behave more like a smooth tube. These effects were not found for the R-114 tests and maybe the mineral oil used there was easier to clean off the tubes. A new cleaning procedure (procedure B) was established which entailed brushing the porous surface with a soft bristle brush (i.e. toothbrush) using ethyl alcohol and then with acetone. The tube was then allowed to air-dry prior to installation and resulted in incipient wall superheats that were approximately 50% lower than those obtained using cleaning procedure A. Figure 5.44 shows the difference between the two cleaning procedures for 0% oil runs on a HIGH FLUX tube. Figure 5.45 is a probabilistic comparison between the cleaning procedures for 0%, 3%, and 10% oil concentrations.

G. EFFECT OF SUBCOOLING

Figure 5.46 and 5.47 demonstrate the effect of subcooling on a smooth tube with pure R-124 and 10% oil/R-124 mixture respectively. Subcooling was conducted by lowering the pool temperature below saturation by opening valve VC (see Figure 3.1) fully, thus allowing maximum flow of coolant through the condenser. The subcooling value is the difference between the

saturation temperature of the pool (i.e. 2.22 °C for R-124) and the measured pool temperature that can be obtained from running either SETUP71 program or the data acquisition program (DRPGB). It can be seen from Figure 5.46 that subcooling the pool below the saturation temperature for as long as one hour resulted in an incipient wall superheat close or even higher than the value obtained when the pool was allowed to settle overnight. This is because by subcooling, many of the potential nucleation sites are deactivated by condensation, similar to what happens by leaving the pool to settle for long periods (i.e. rewetting).

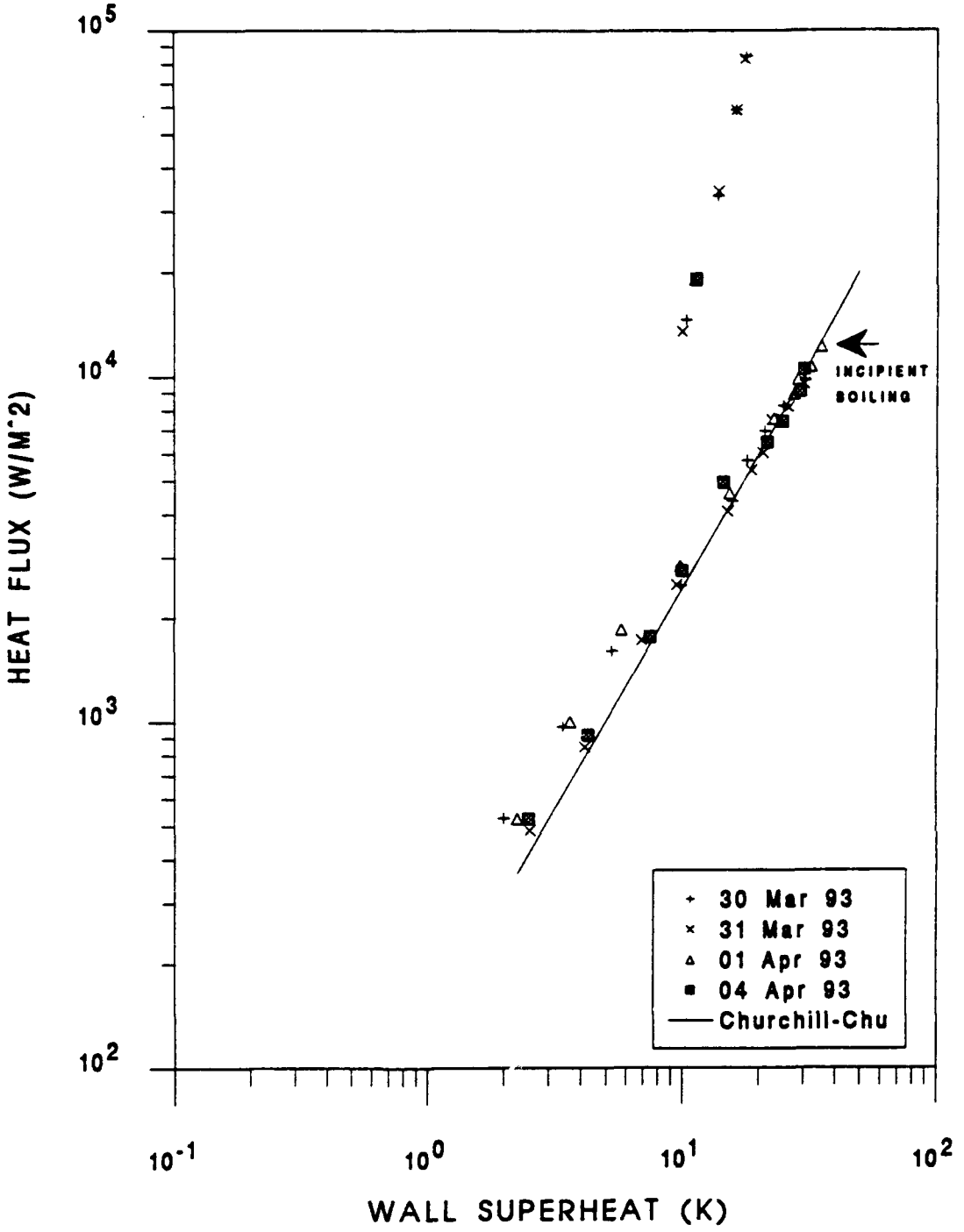

Figure 5.1 Smooth Tube 0% oil degassing procedure B repeatability runs

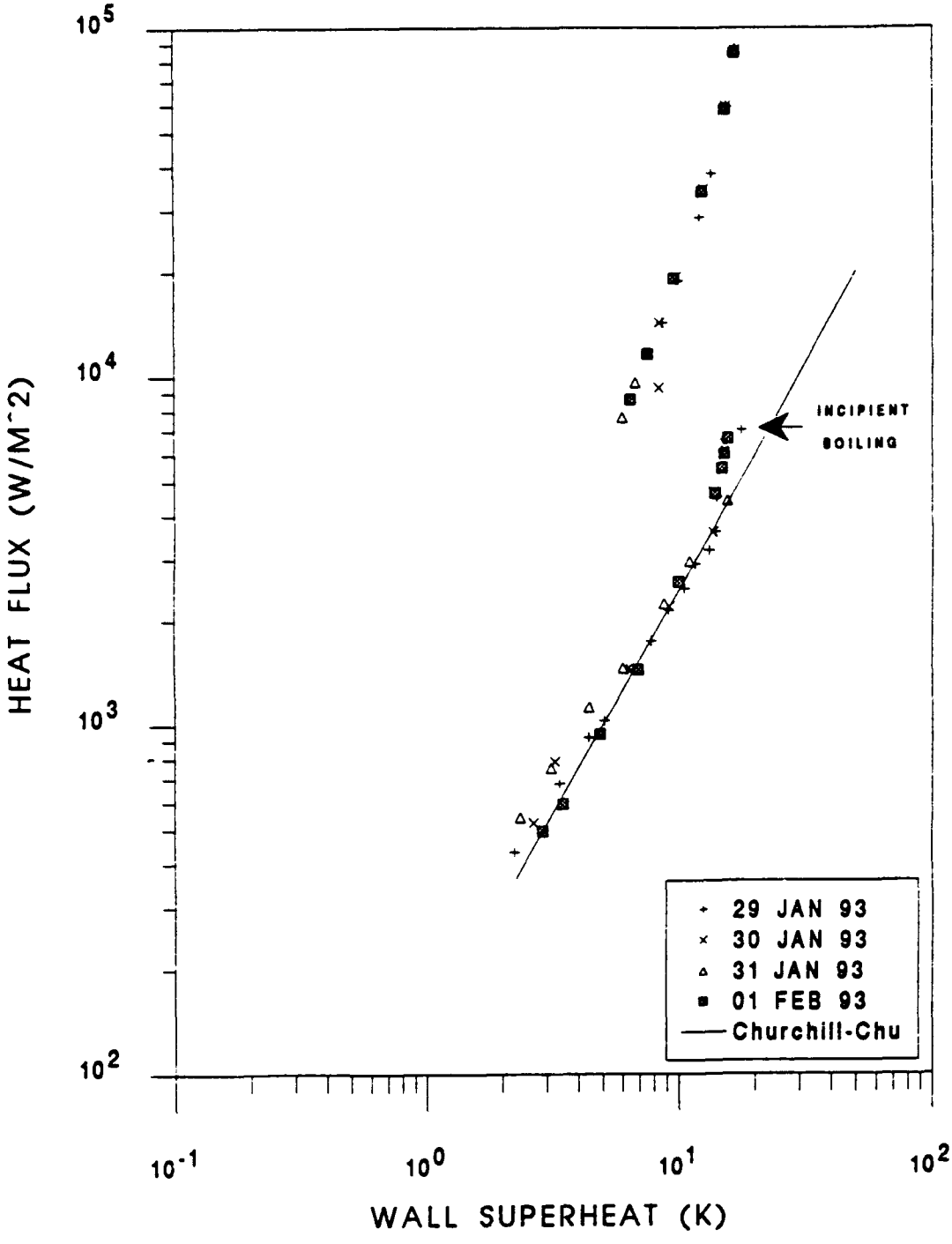

Figure 5.2 Smooth Tube 0% oil, degassing procedure A increasing heat flux repeatability runs

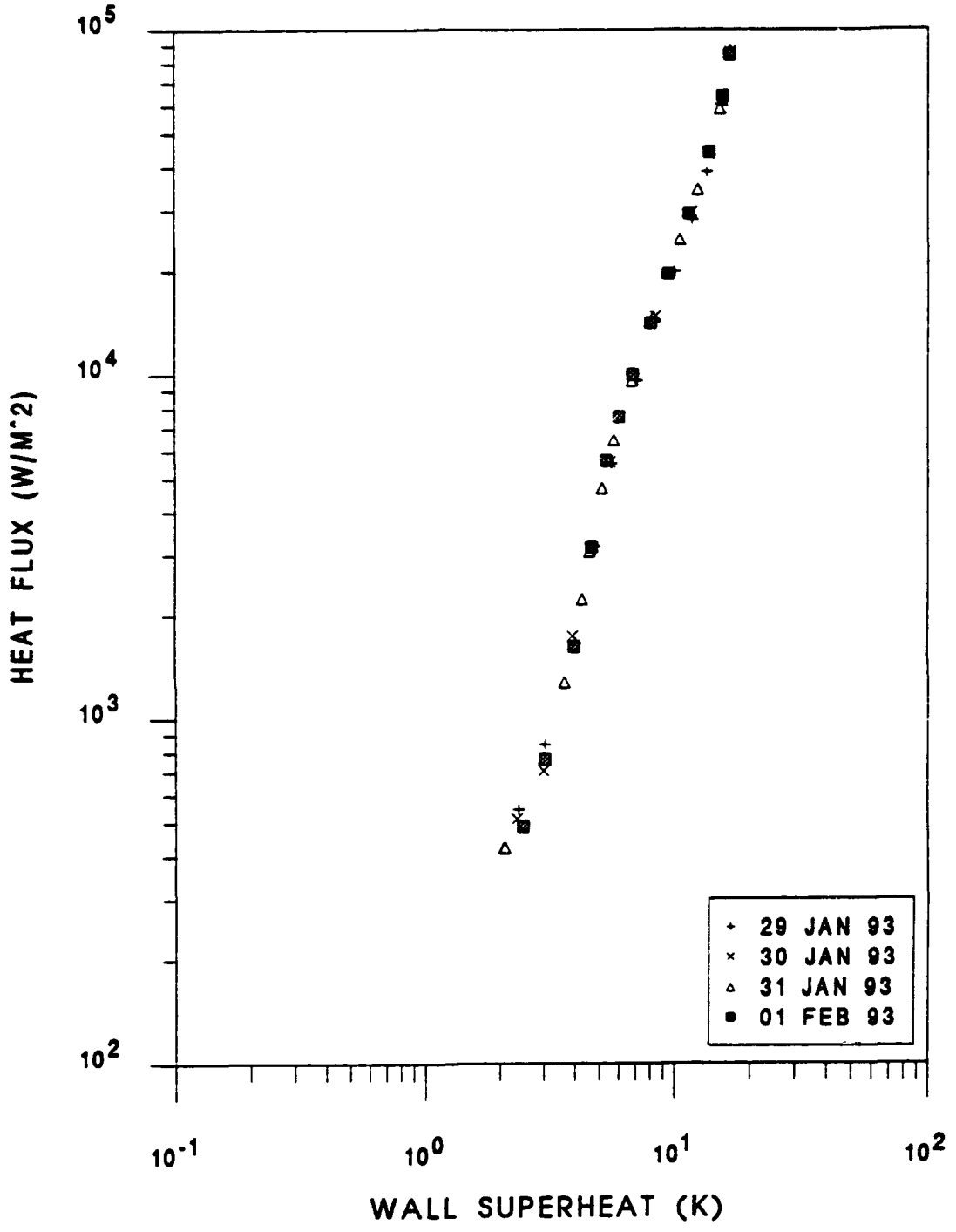

Figure 5.3 Smooth Tube 0% oil, degassing procedure A decreasing heat flux repeatability runs

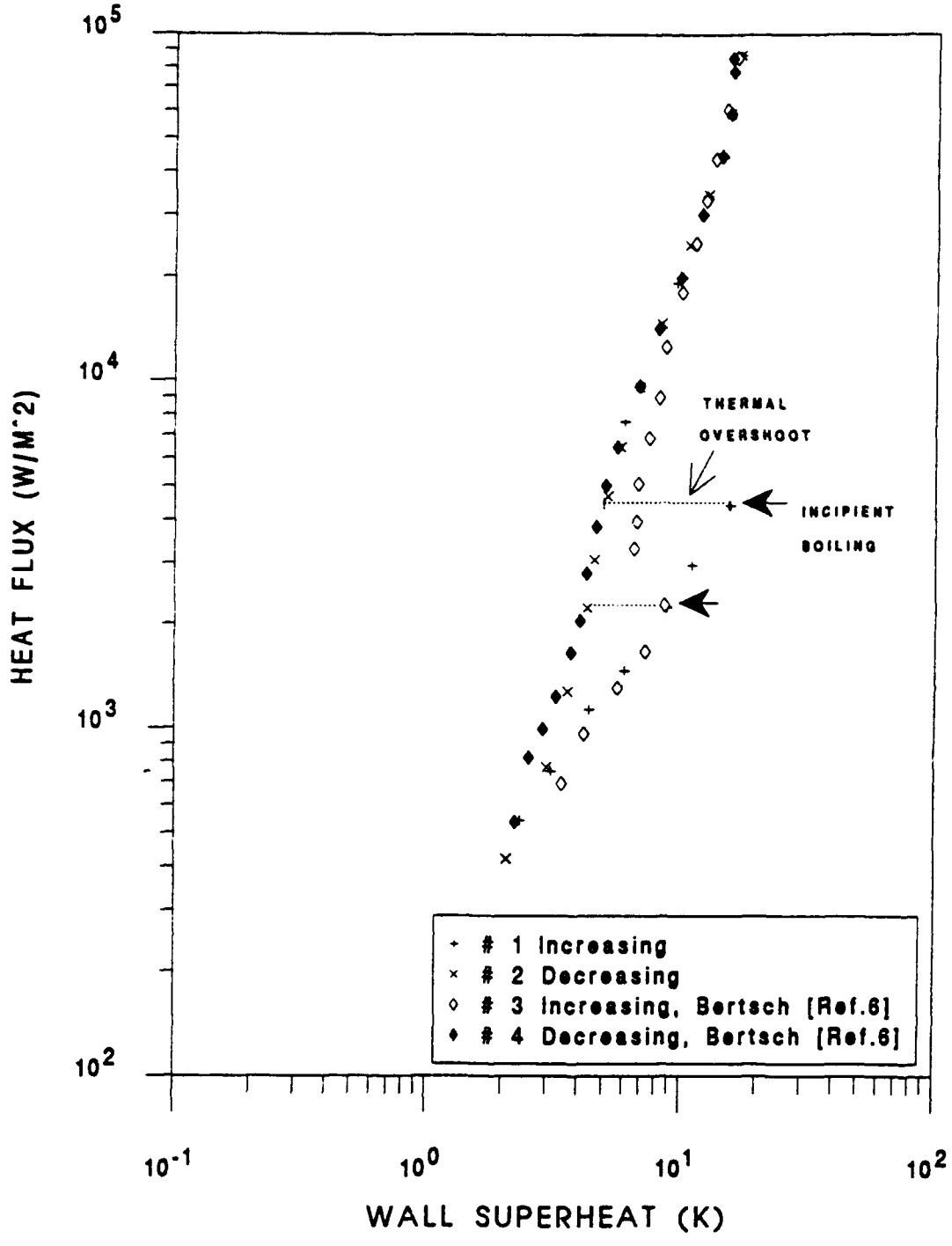

Figure 5.4 Comparison of smooth tube data with 0% oil (increasing and decreasing heat flux)

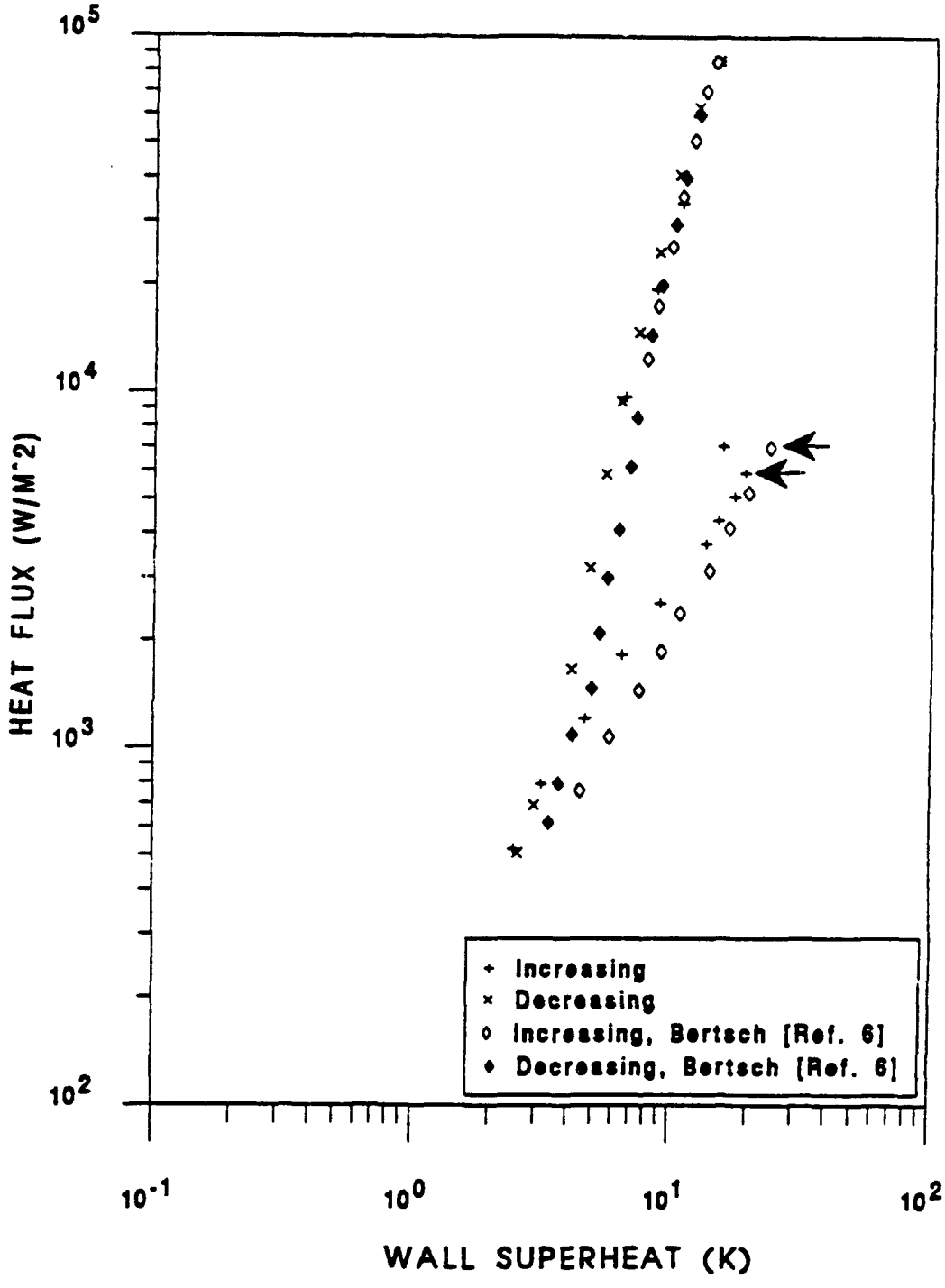

Figure 5.5 Comparison of Smooth tube 3% oil data (increasing and decreasing heat flux)

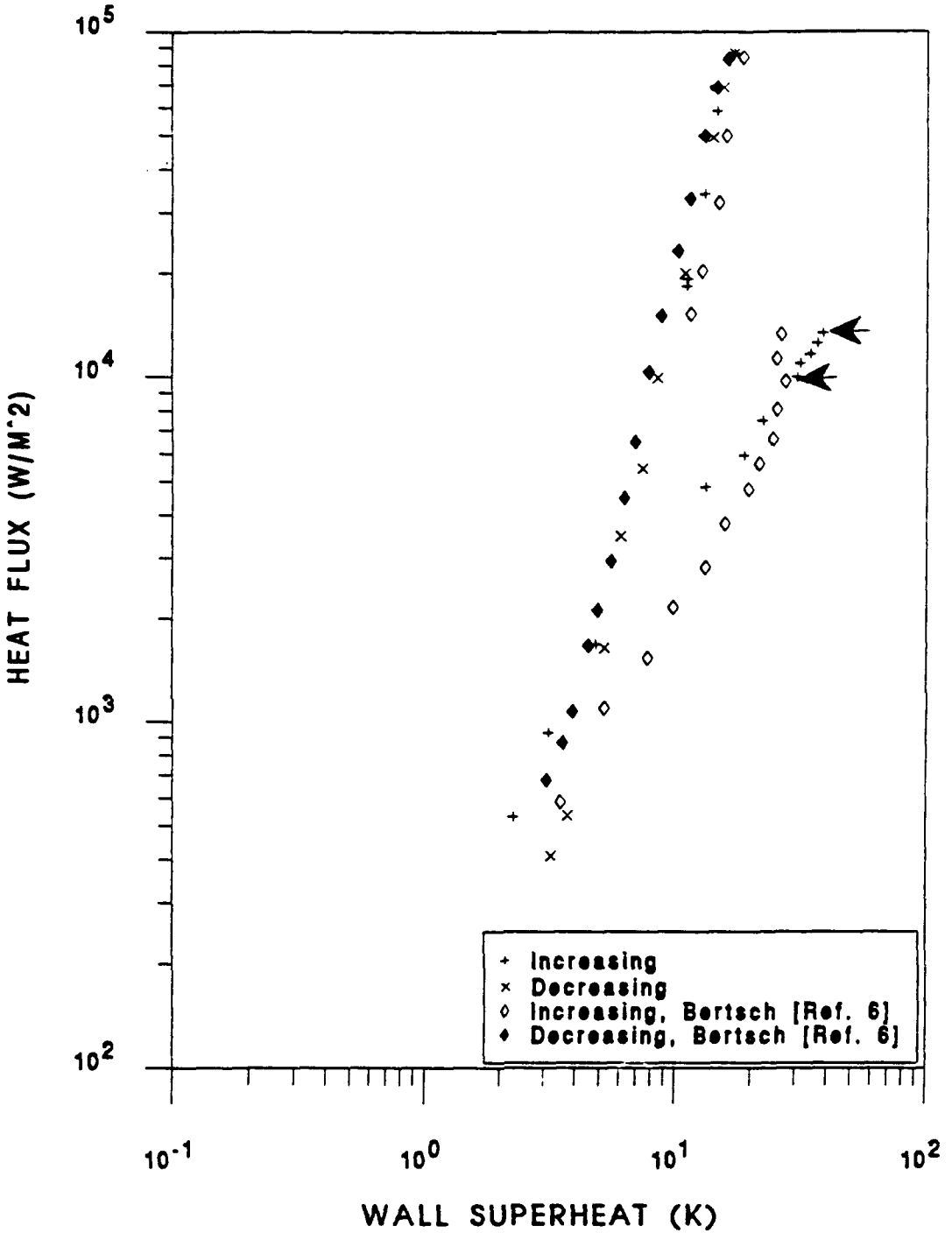

Figure 5.6 Comparison of smooth tube 10% oil data (increasing and decreasing heat flux)

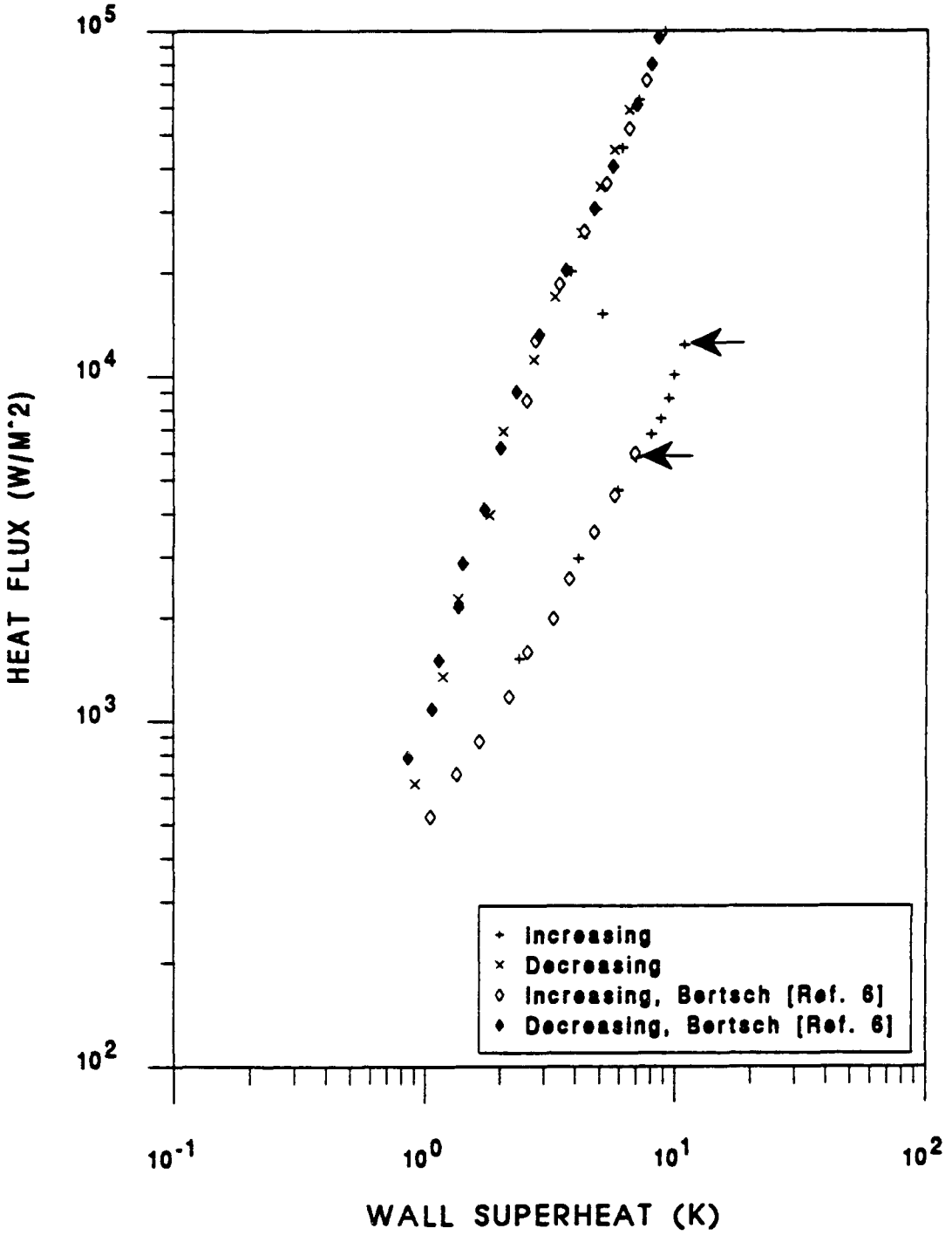

Figure 5.7 GEWA-K 19 fpi 0% oil data comparison

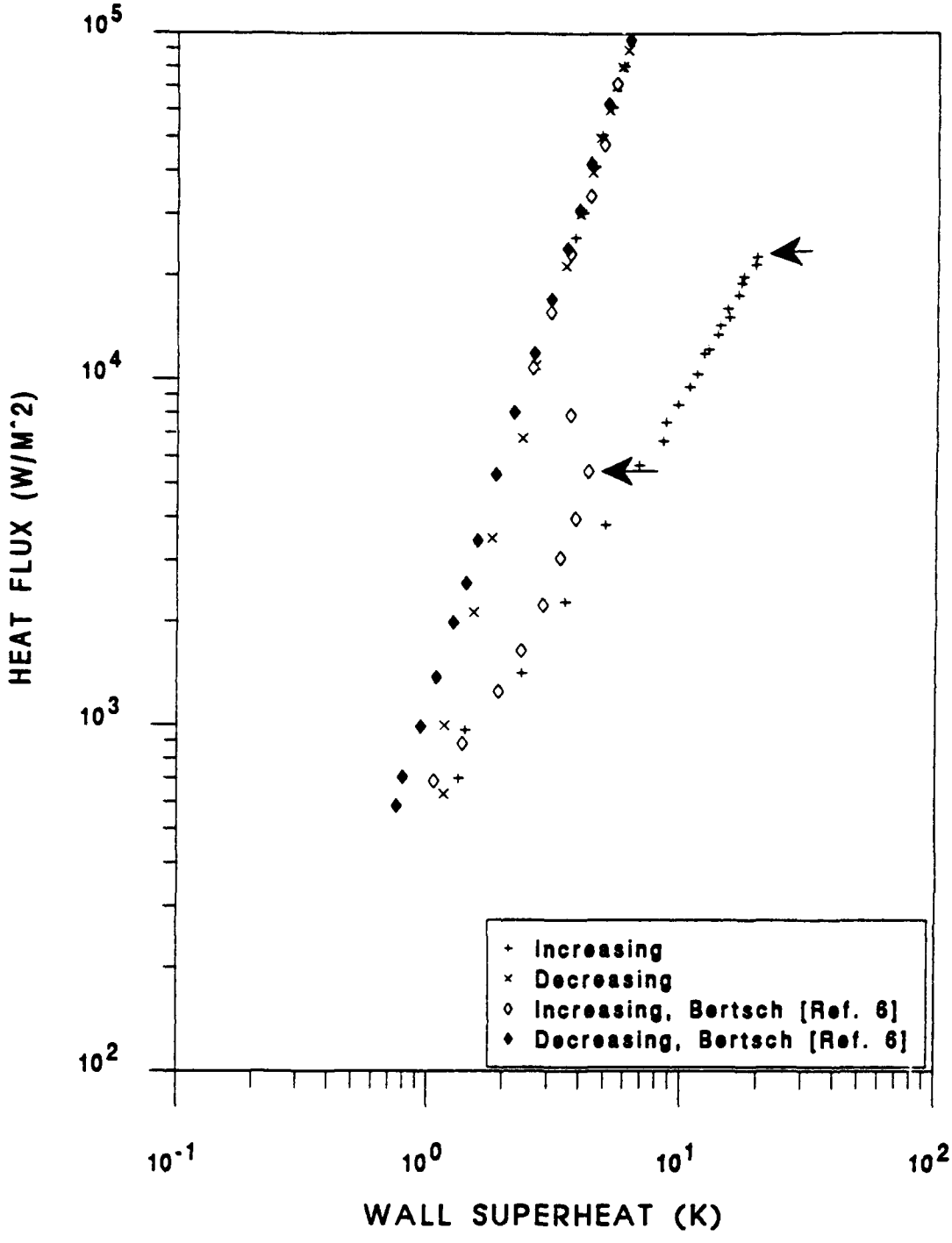

Figure 5.8 GEWA-K 19 fpi 3% oil data comparison

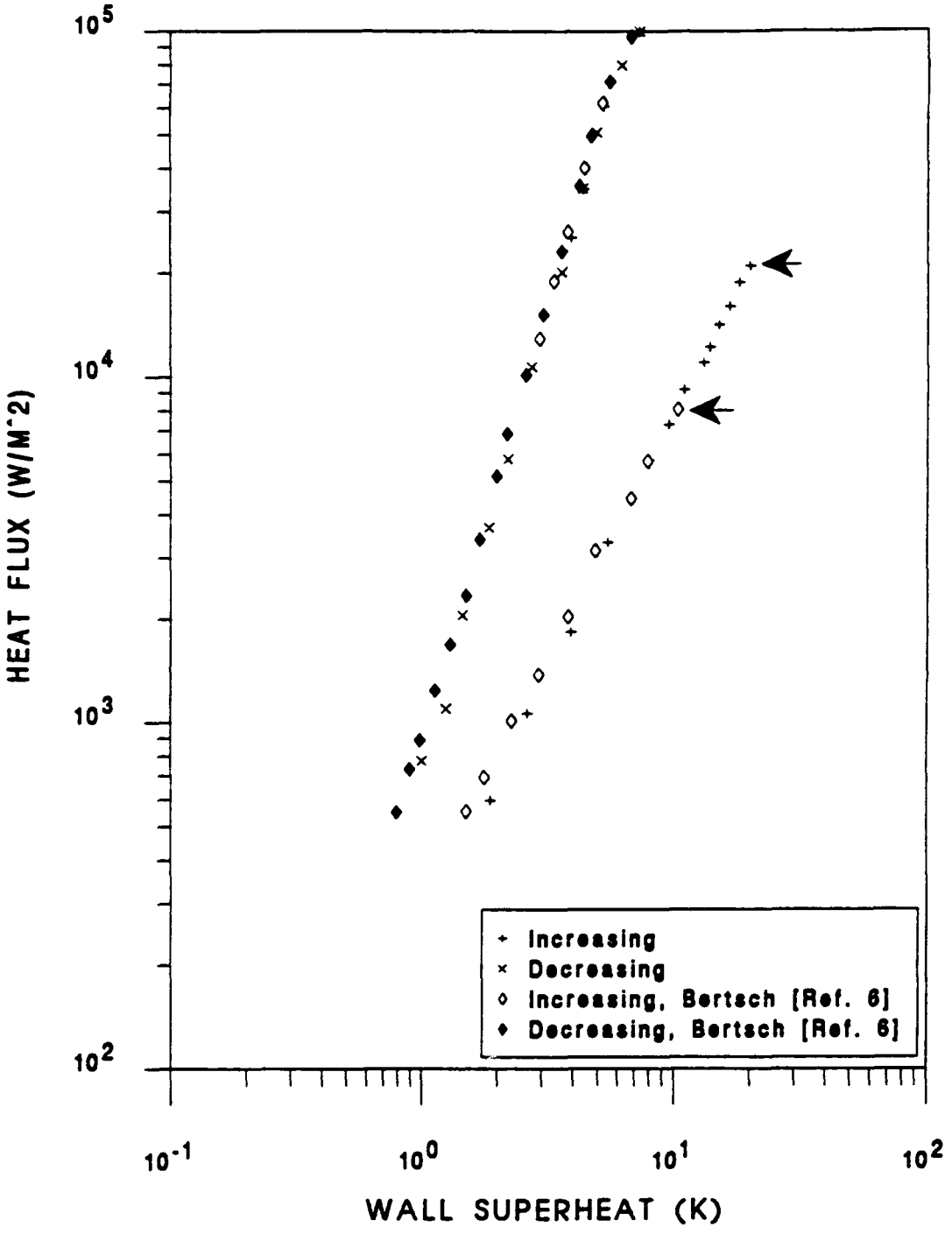

Figure 5.9 GEWA-K 19 fpi 10% oil data comparison

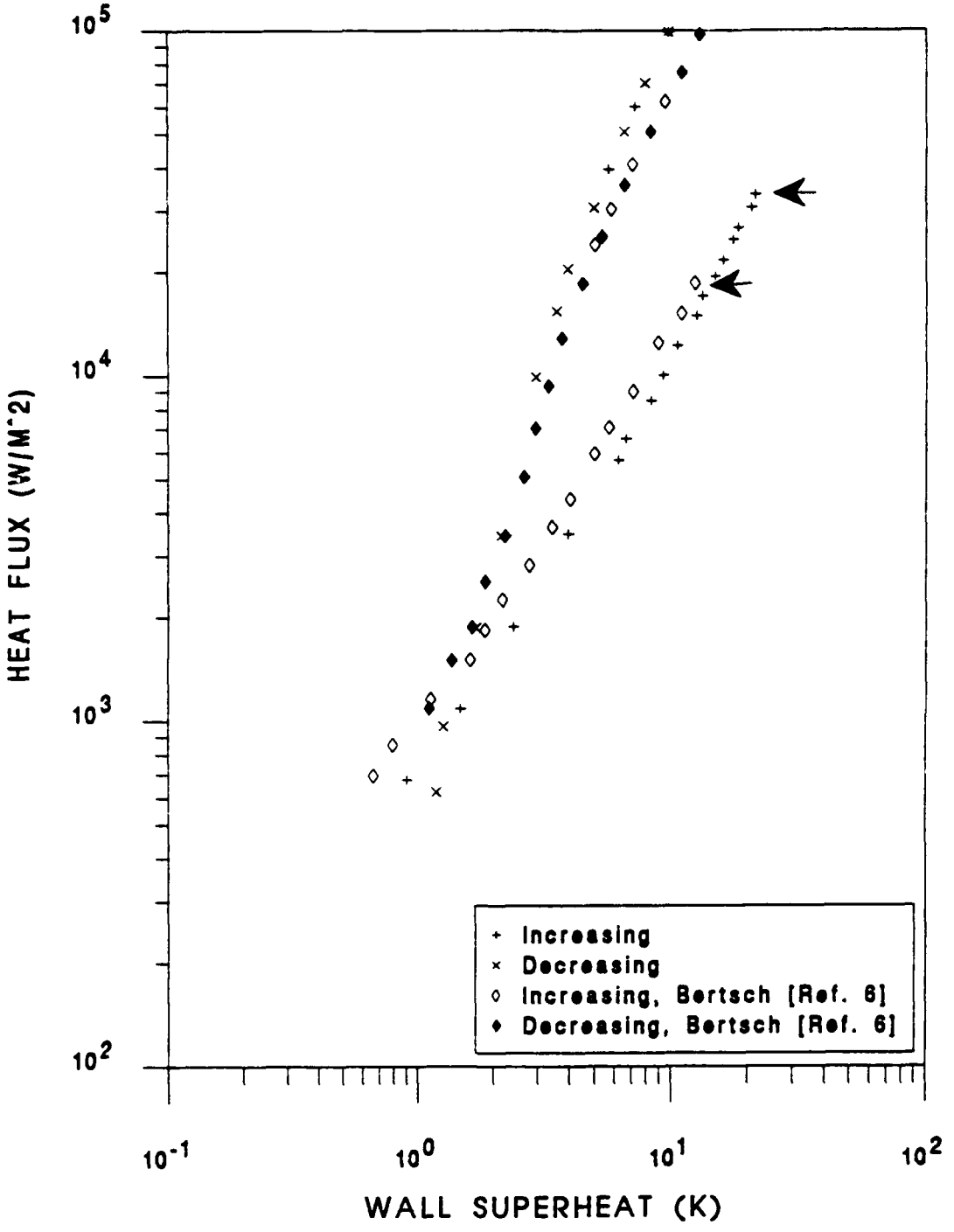

Figure 5.10 GEWA-K 26 fpi 0% oil data comparison

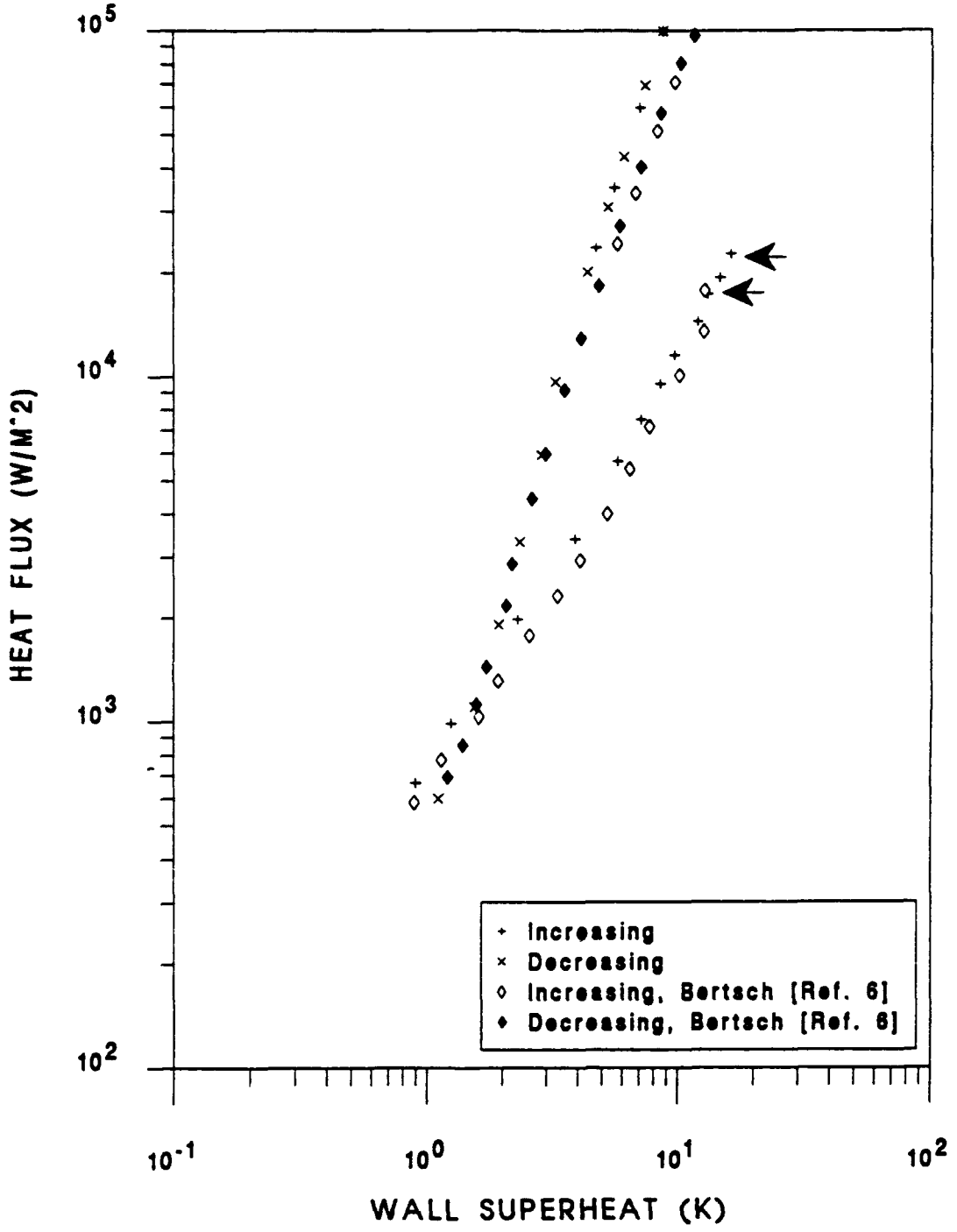

Figure 5.11 GEWA-K 26 fpi 3% oil data comparison

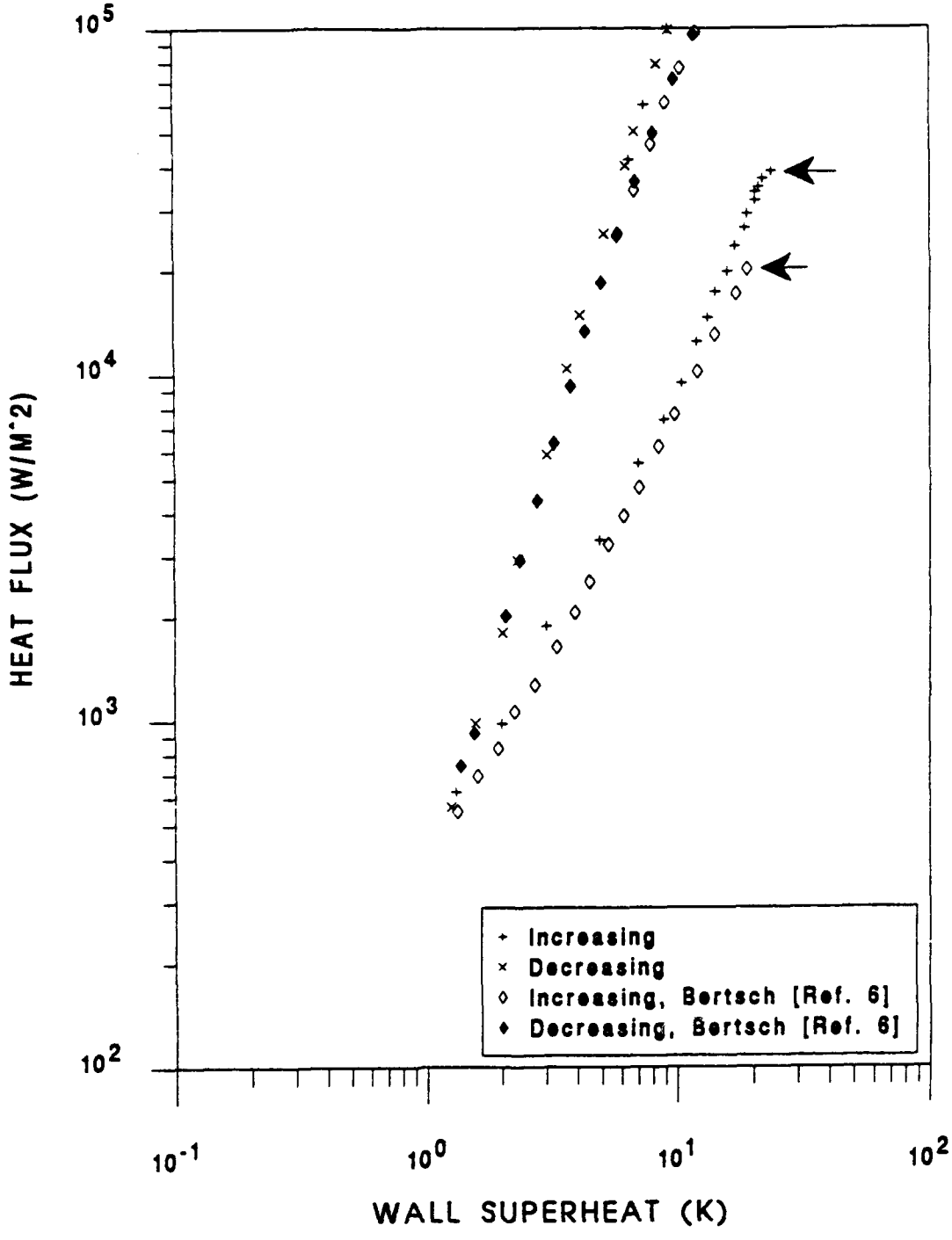

Figure 5.12 GEWA-K 26 fpi 10% oil data comparison

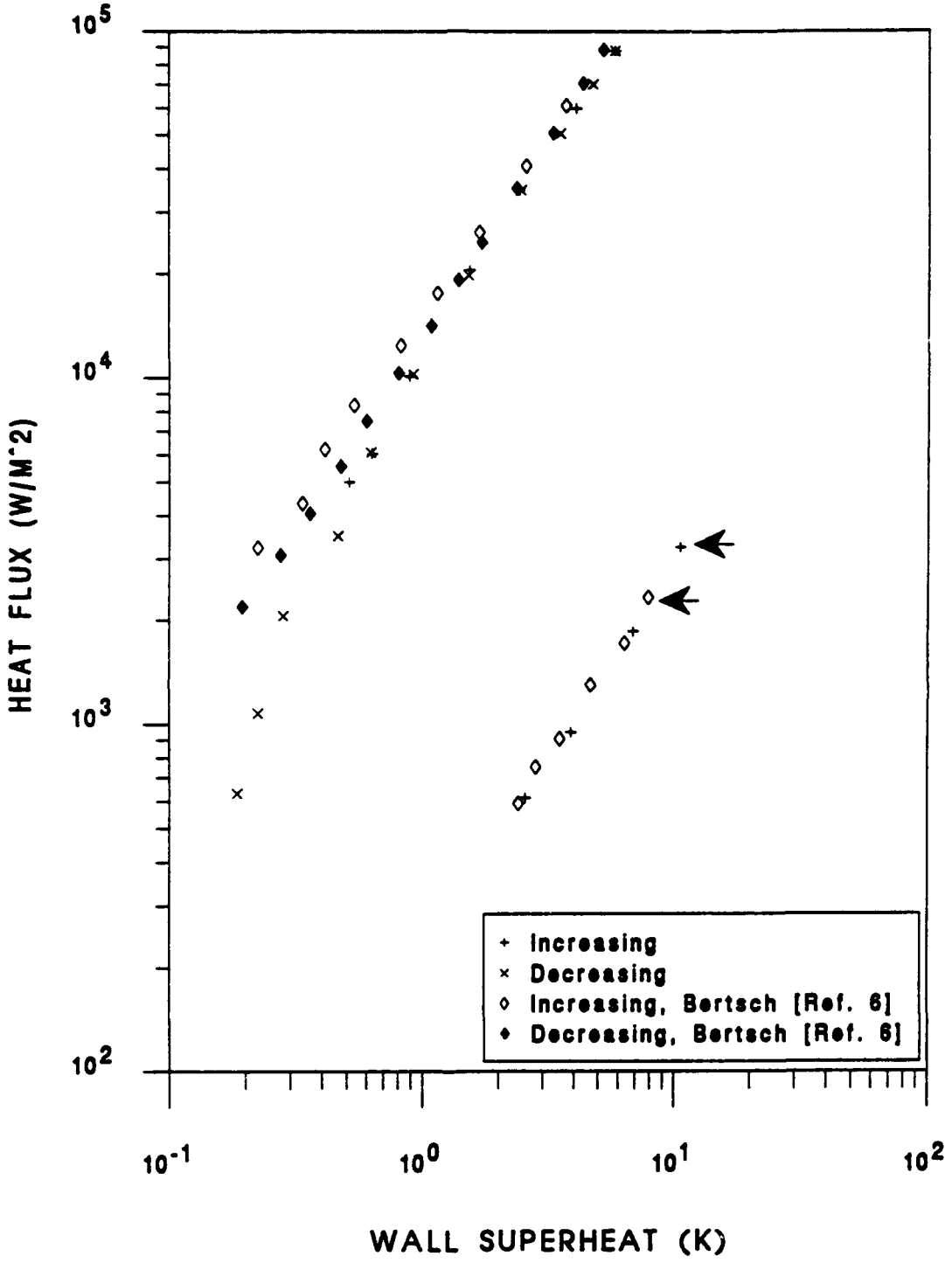

Figure 5.13 HIGH FLUX 0% oil data comparison

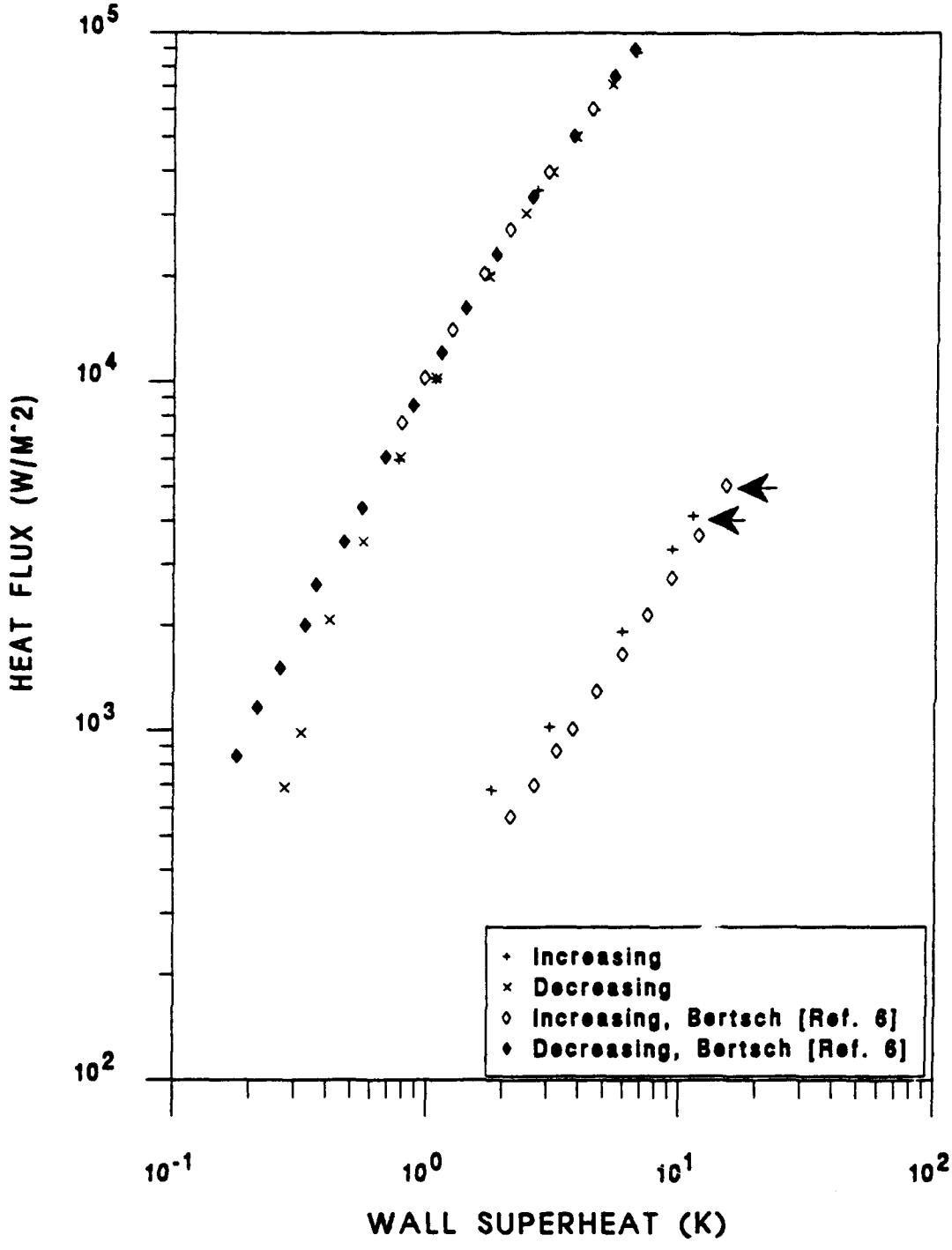

Figure 5.14 HIGH FLUX 3% oil data comparison

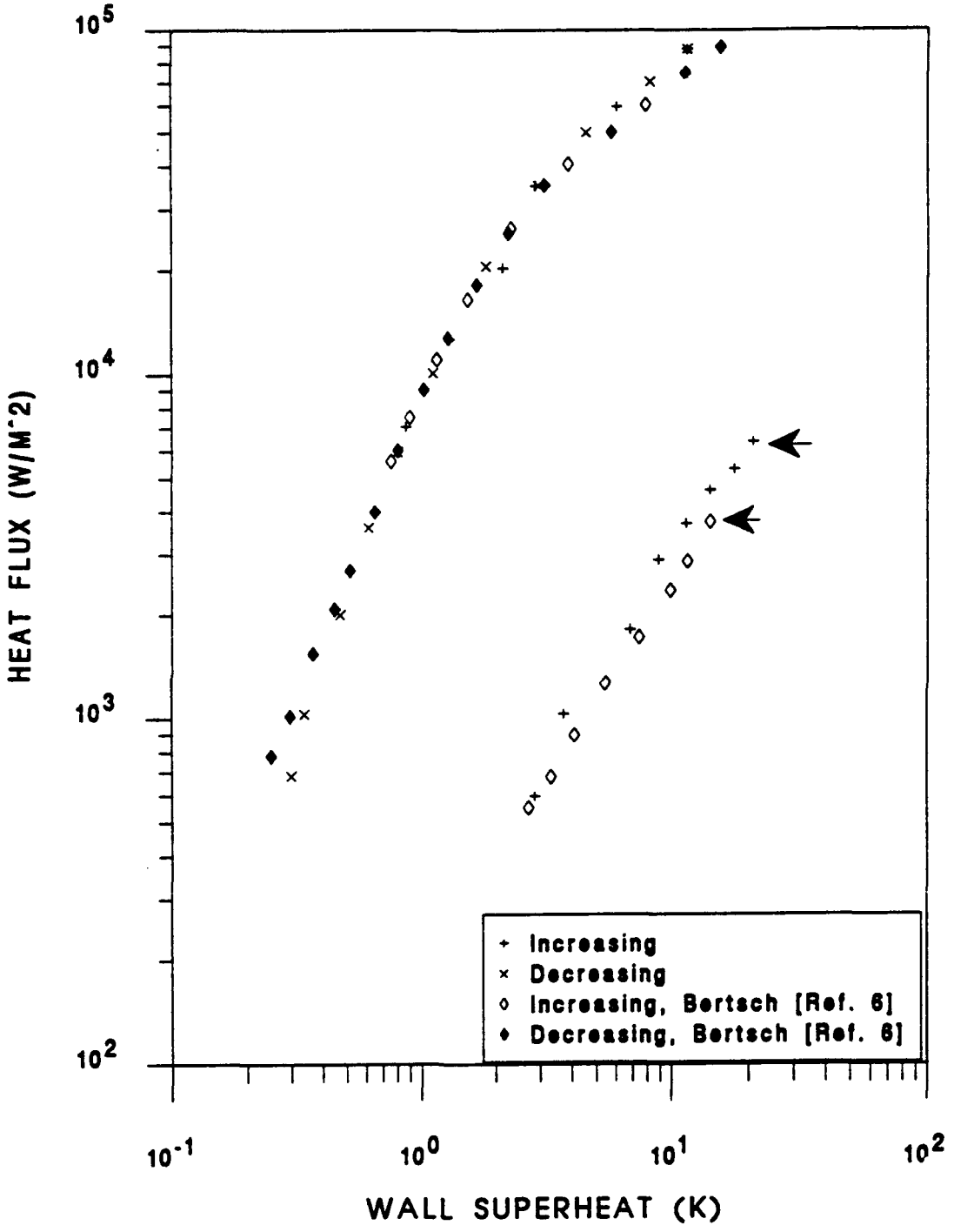

Figure 5.15 HIGH FLUX 10% oil data comparison

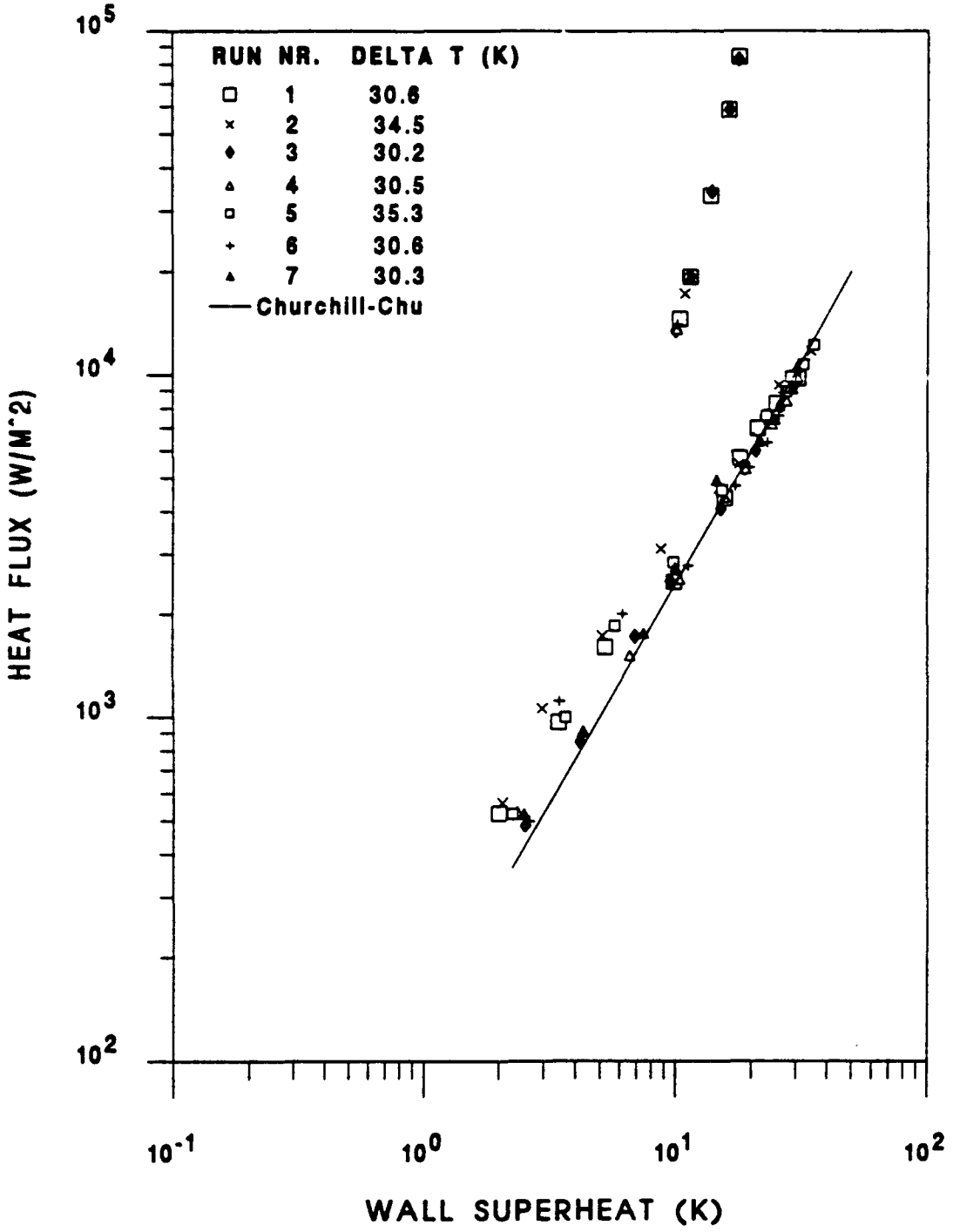

Figure 5.16 Smooth tube 0% oil incipience tests

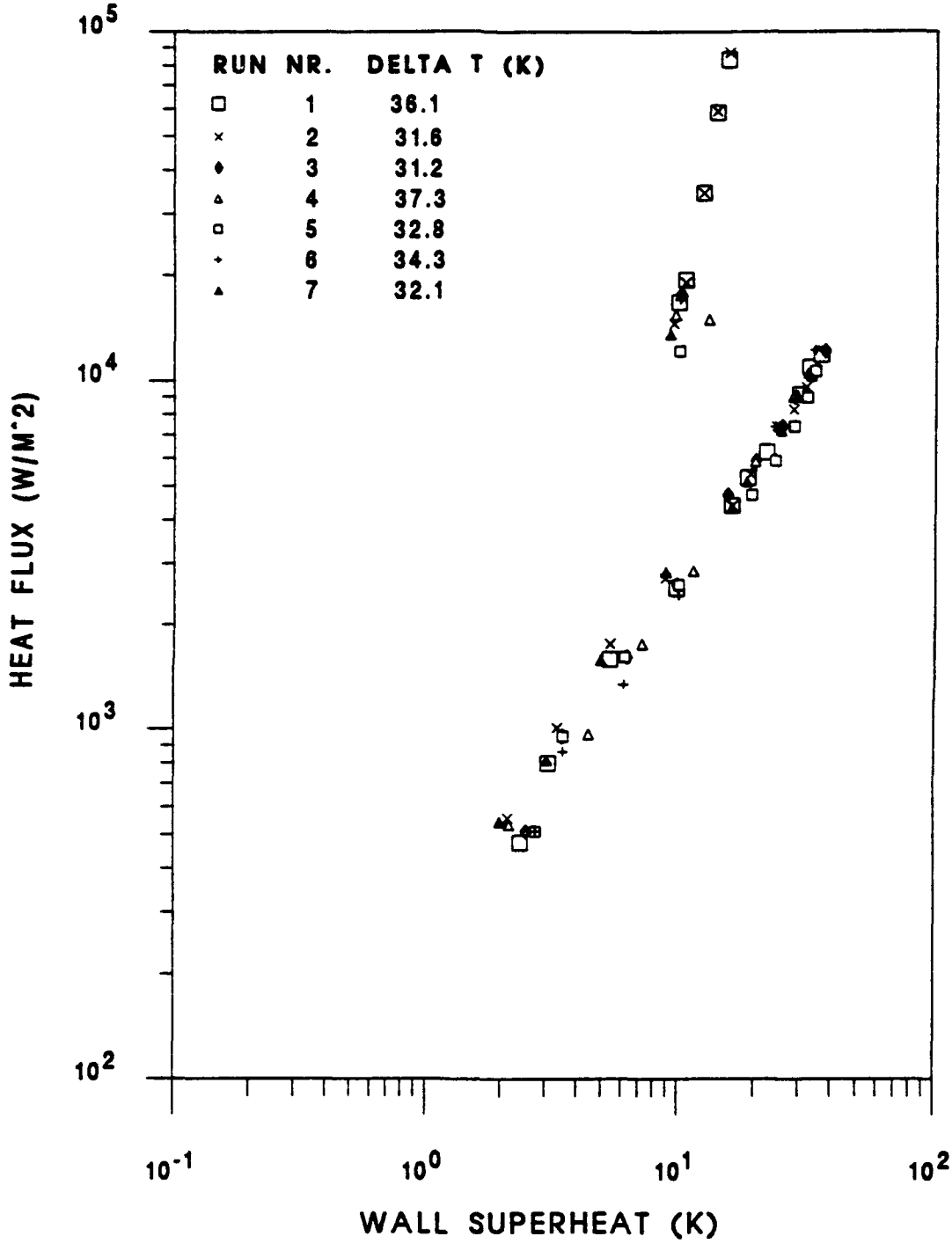

Figure 5.17 Smooth tube 3% oil incipience tests

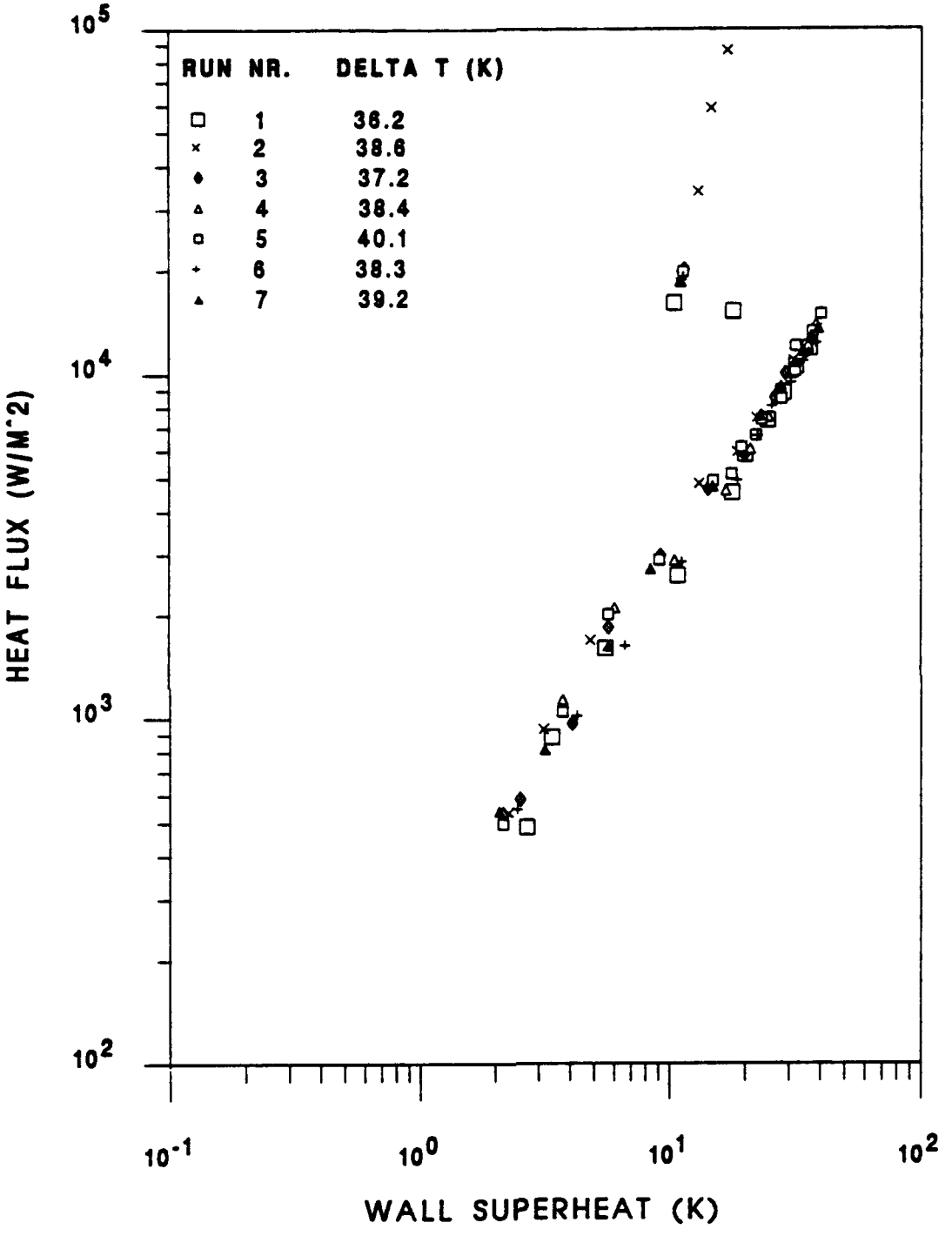

Figure 5.18 Smooth tube 10% oil incipience tests

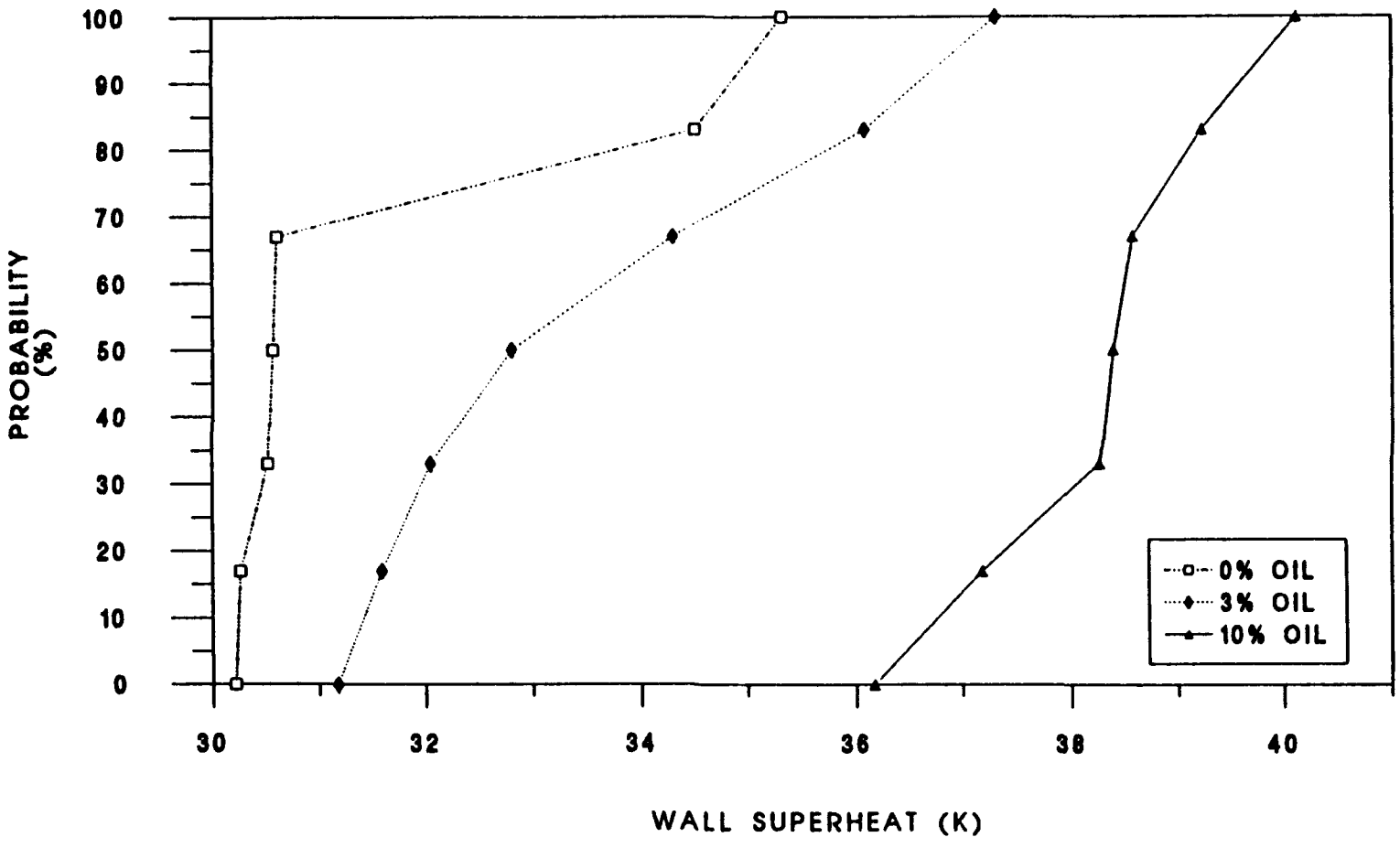

Figure 5.19 Probability of Incipience of Smooth tube with 0%, 3% and 10% oil concentrations

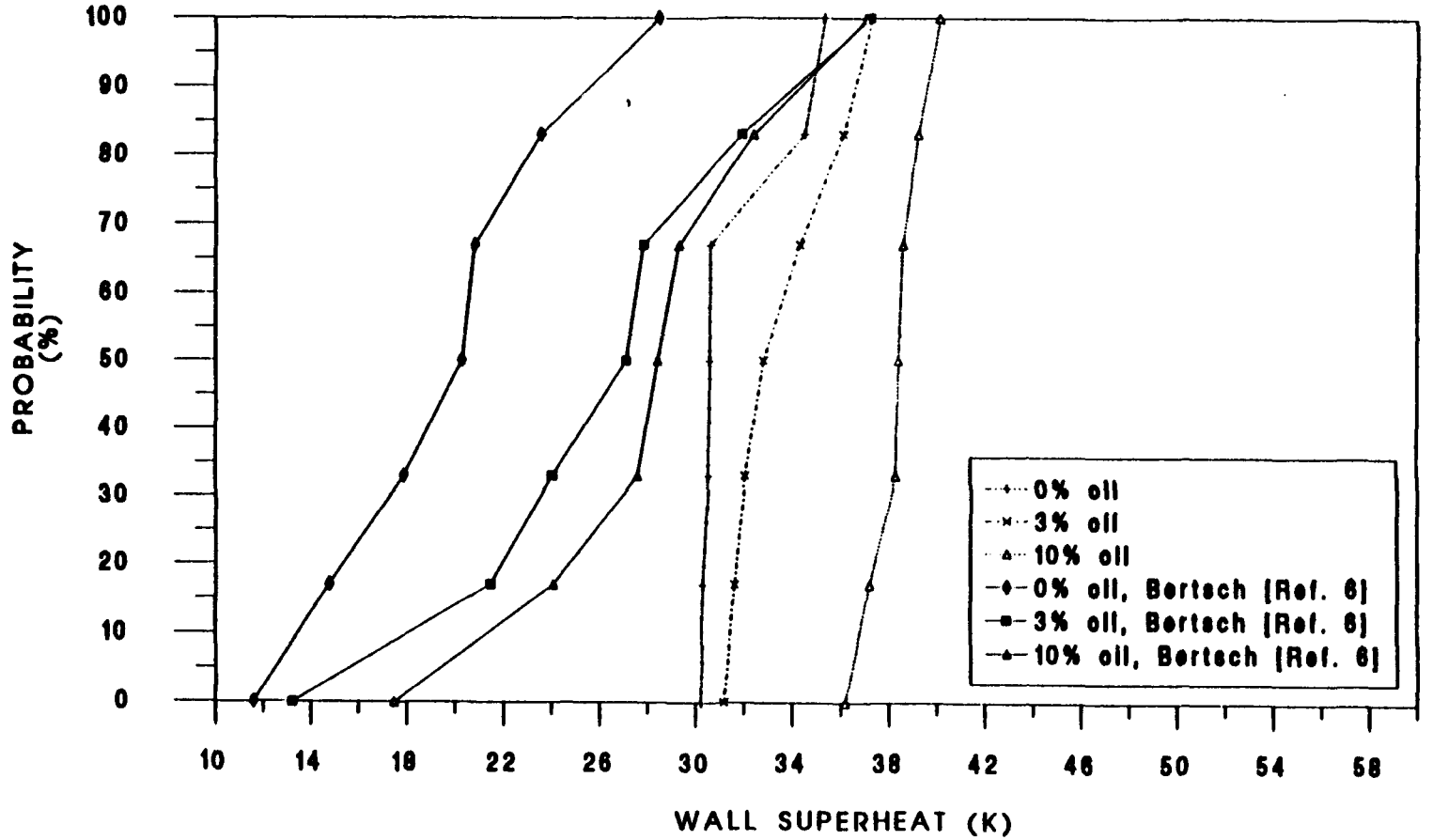

Figure 5.20 Smooth tube probability of incipience comparison

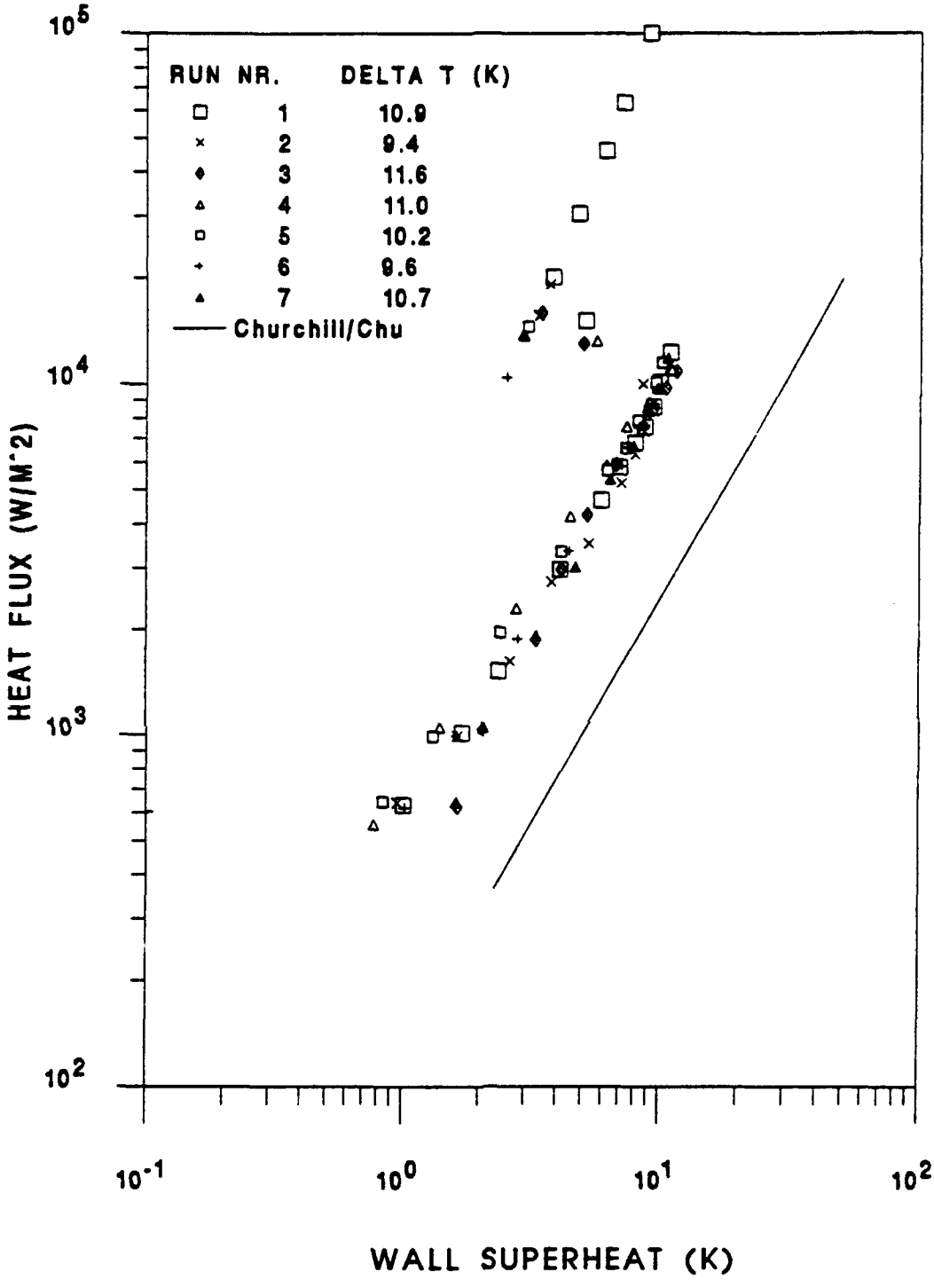

Figure 5.21 GEWA-K 19 fpi 0% oil incipience tests

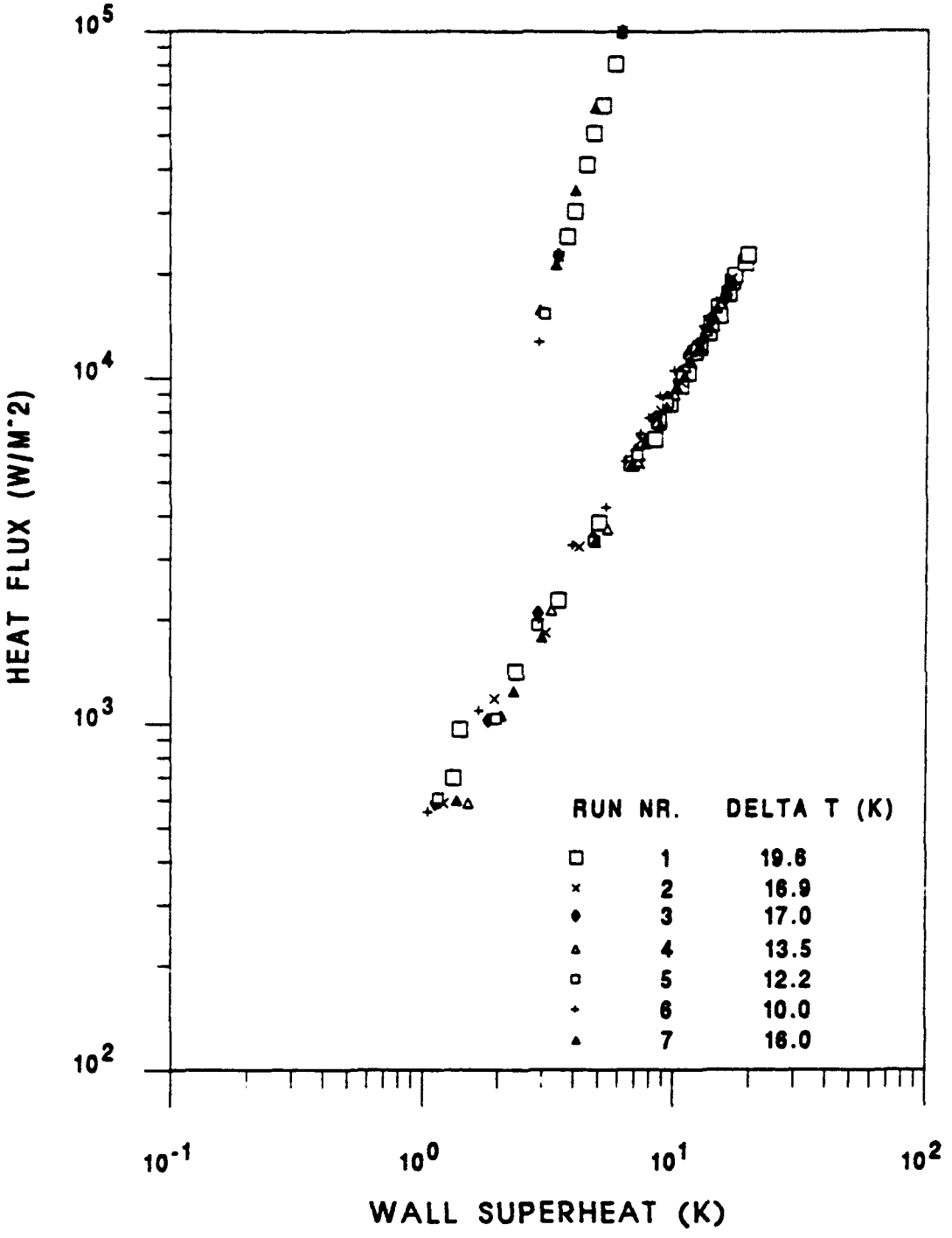

Figure 5.22 GEWA-K 19 fpi 3% oil incipience tests

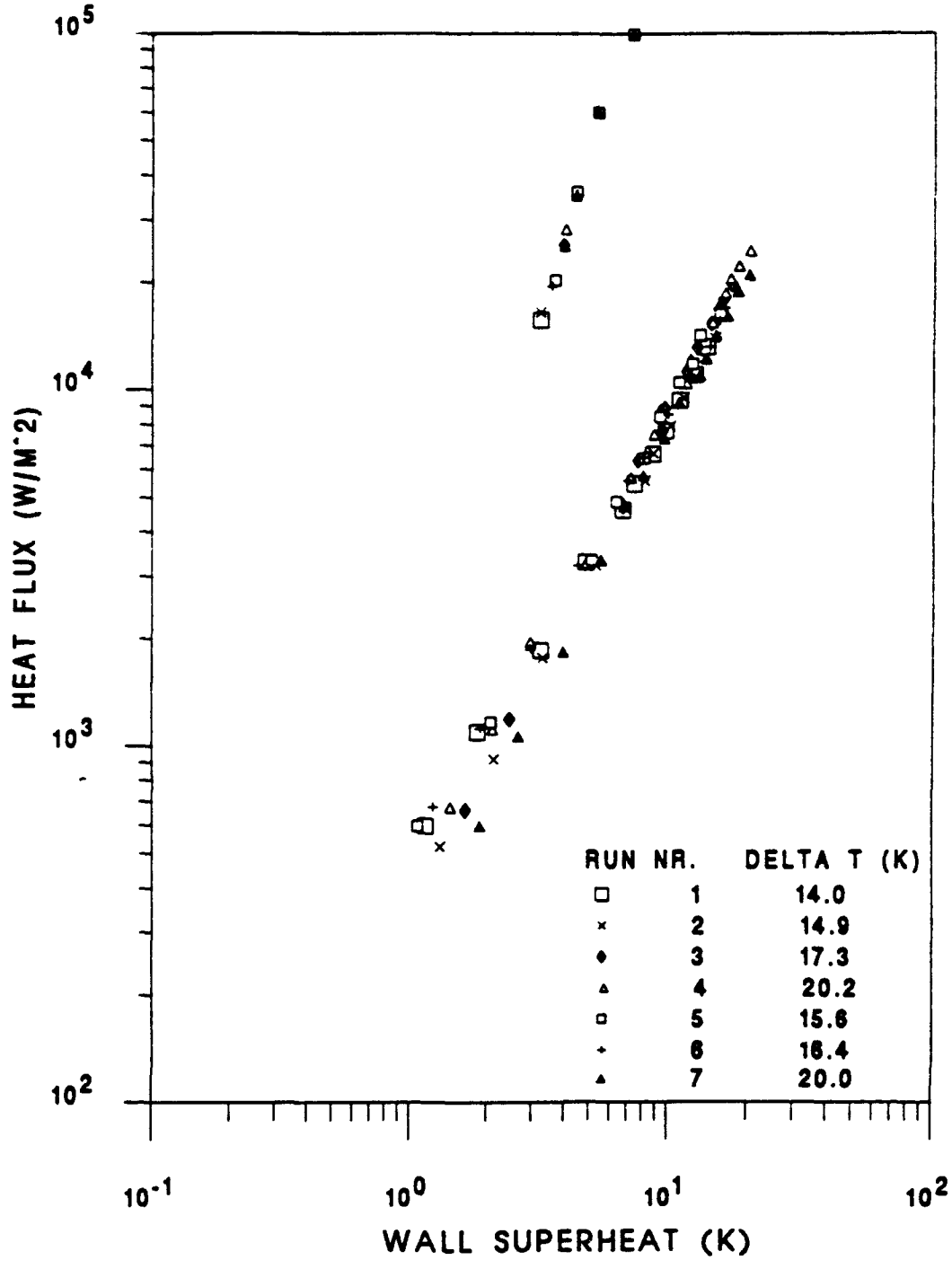

Figure 5.23 GEWA-K 19 fpi 10% oil incipience tests

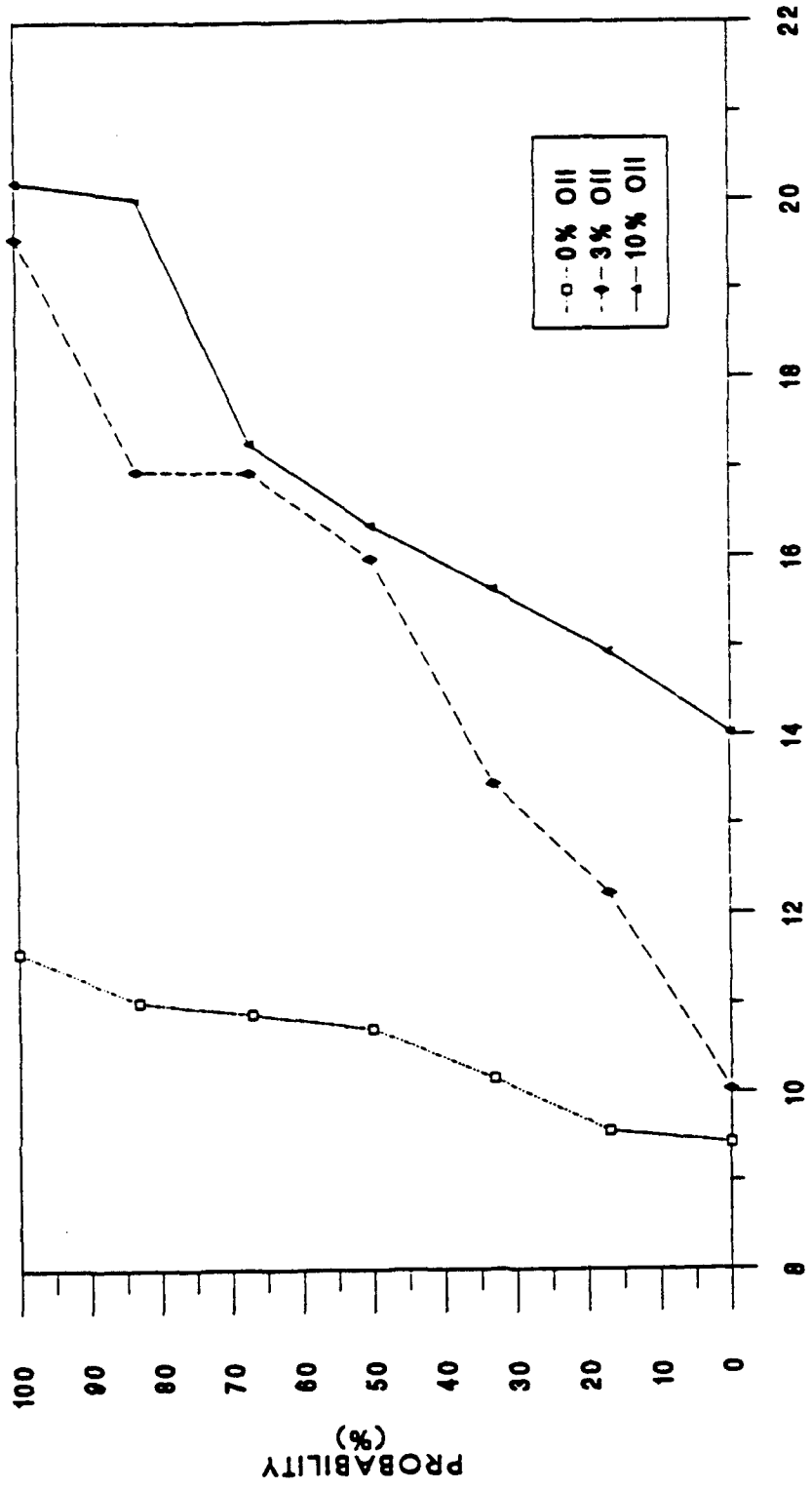

Figure 5.24 GEWA-K 19 fpi tube probability of incipience with 0%, 3% and 10% oil concentrations

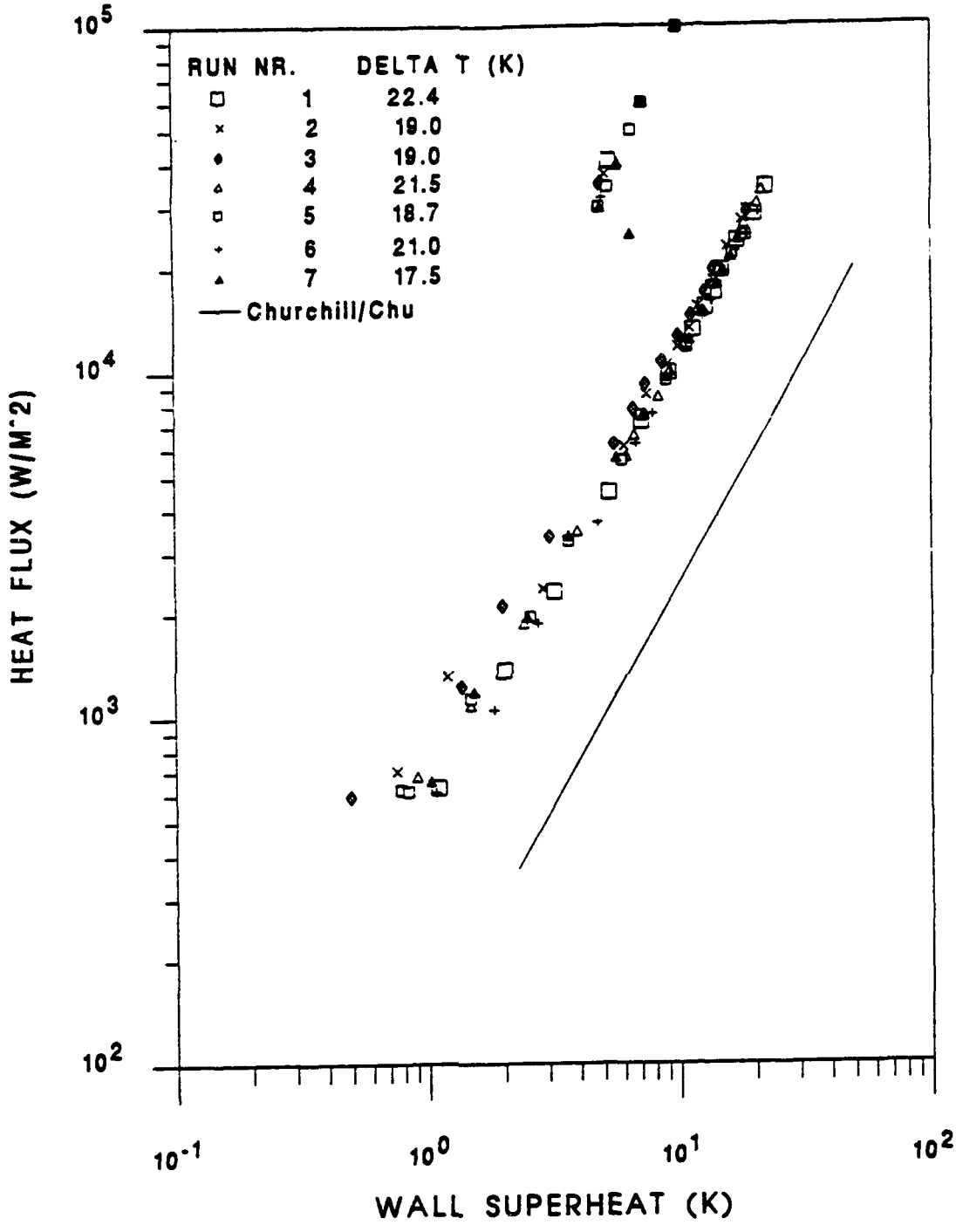

Figure 5.25 GEWA-K 26 fpi 0% oil incipience tests

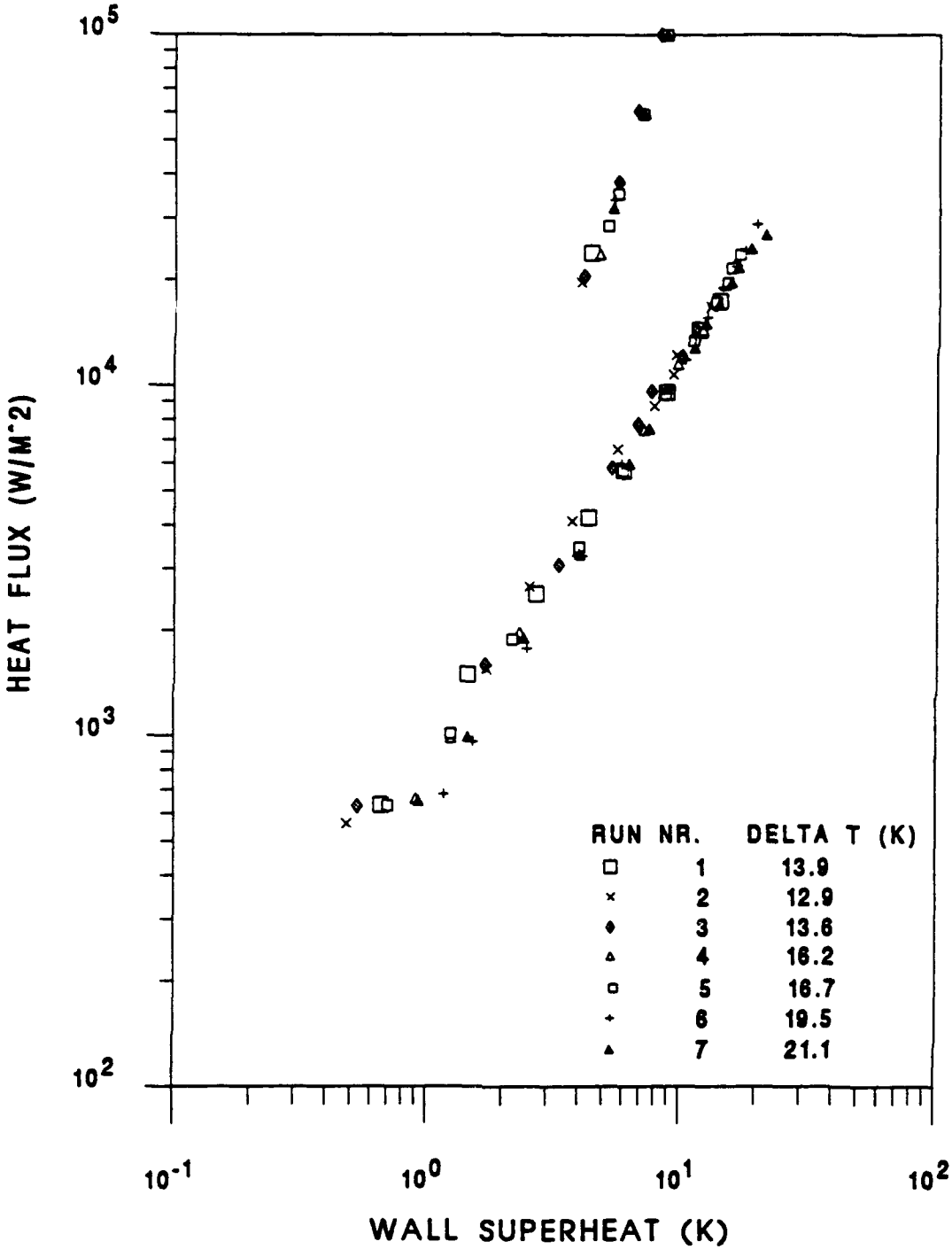

Figure 5.26 GEWA-K 26 fpi 3% oil incipience tests

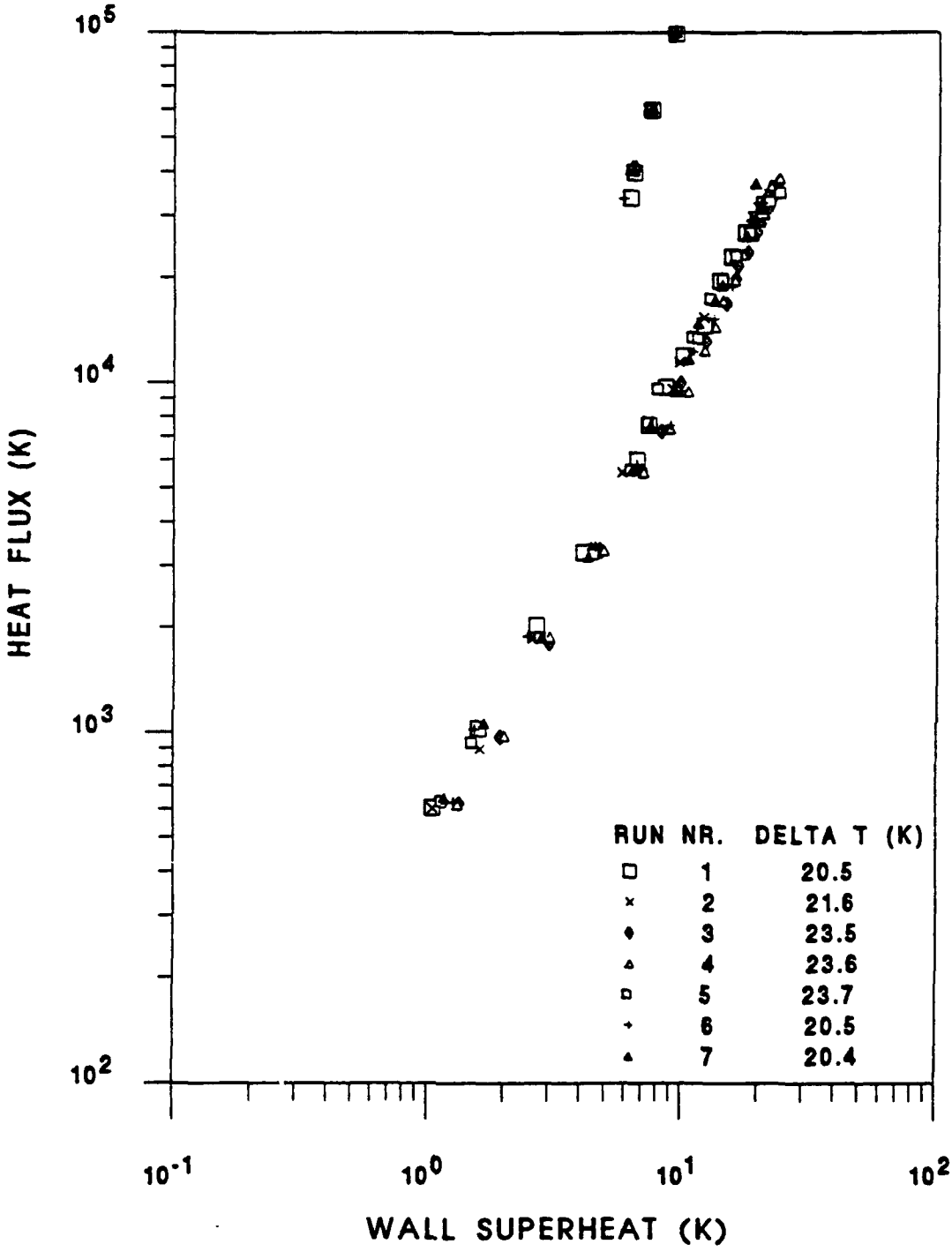

Figure 5.27 GEWA-K 26 fpi 10% oil incipience tests

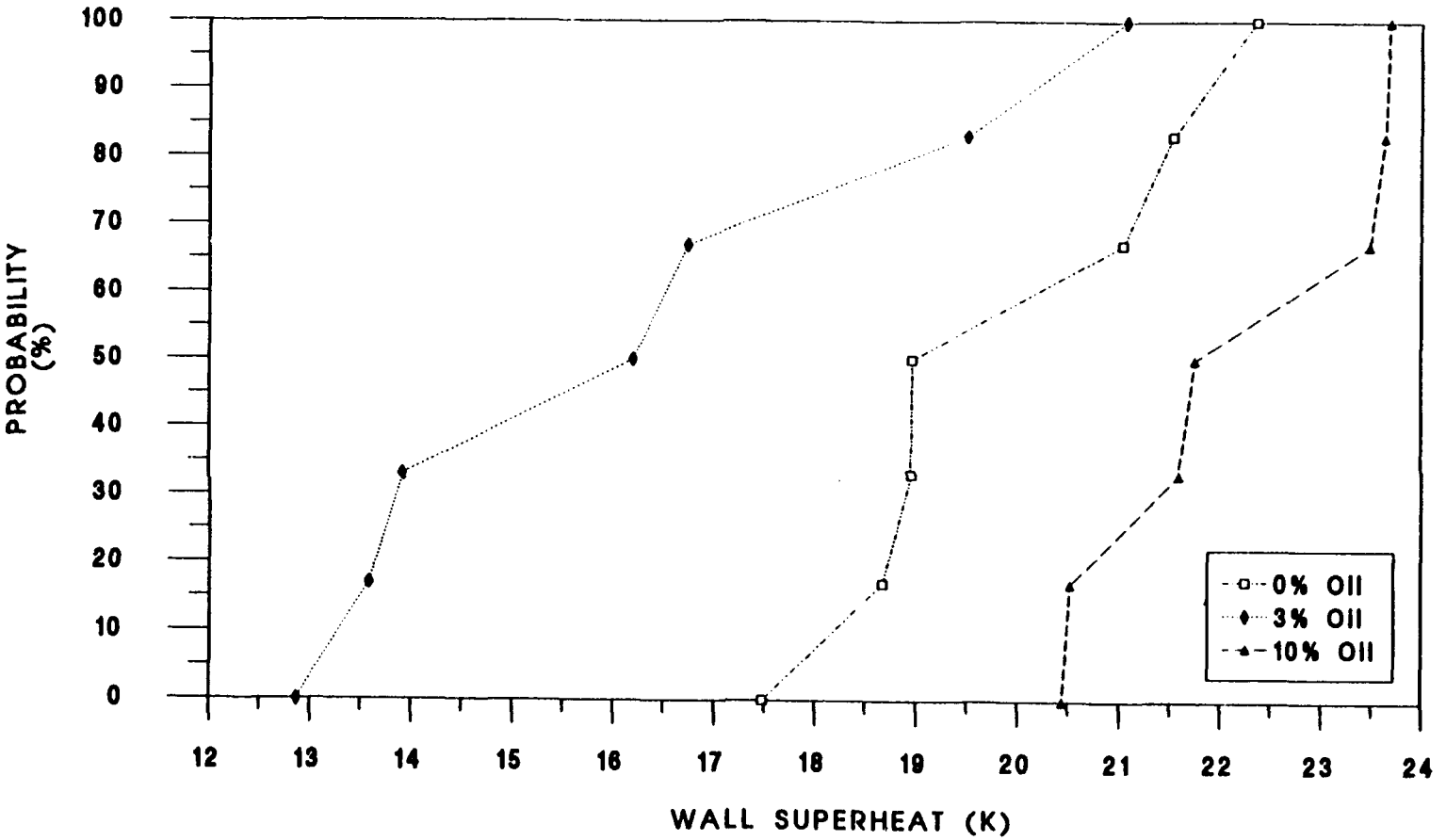

Figure 5.28 GEWA-K 26 fpi tube probability of incipience with 0%, 3% and 10% oil concentrations

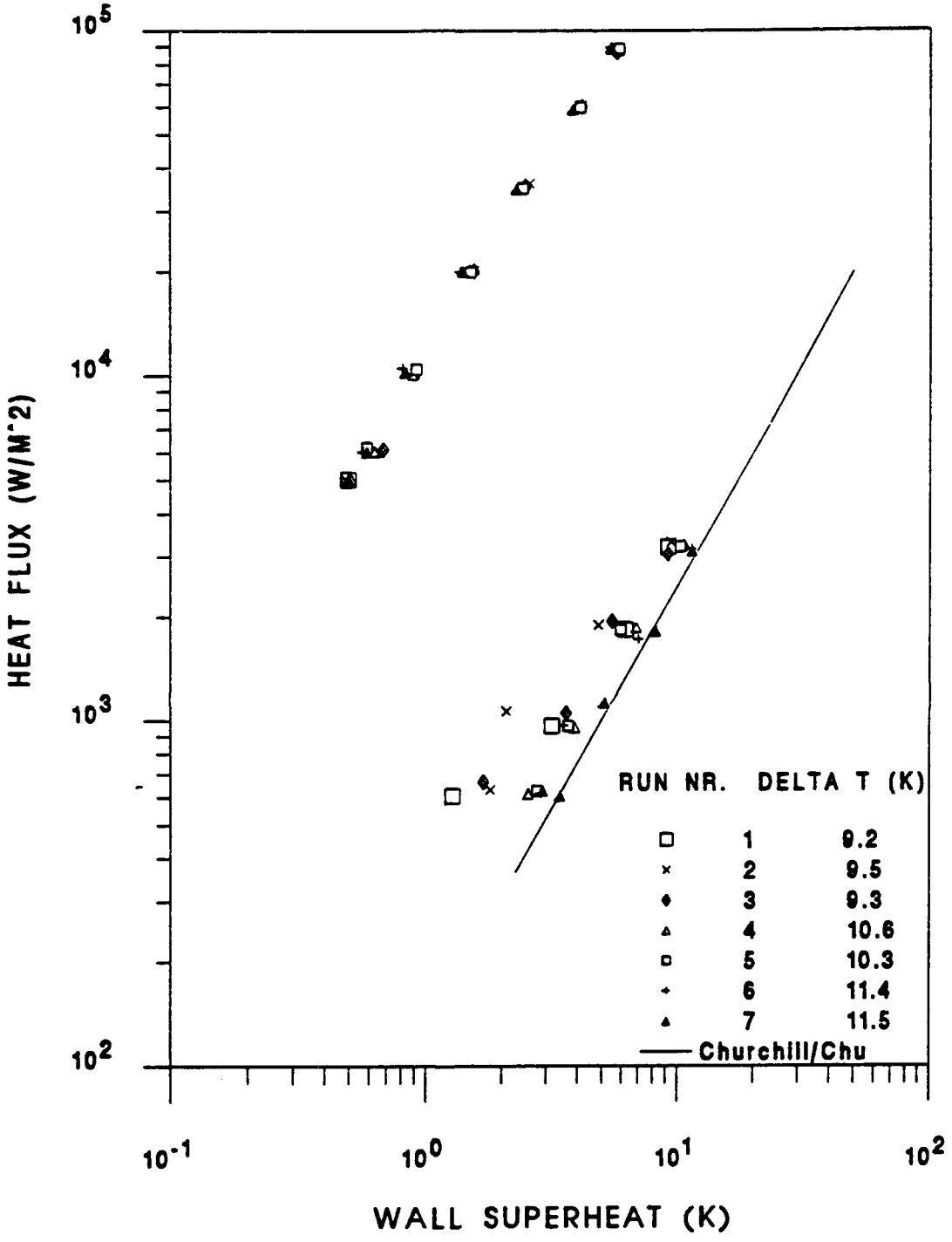

Figure 5.29 HIGH FLUX 0% oil incipience tests

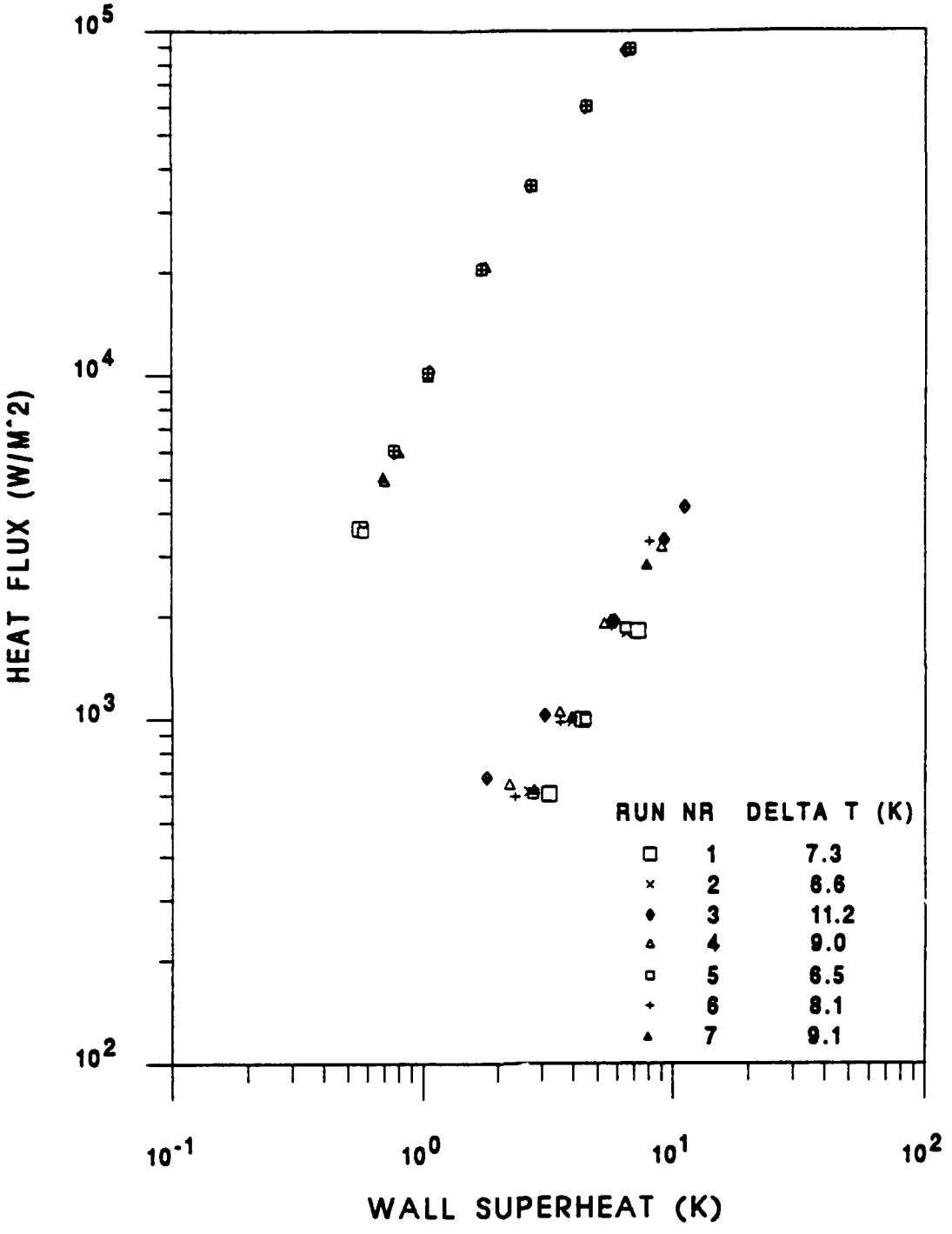

Figure 5.30 HIGH DELTA T 3% oil incipience tests

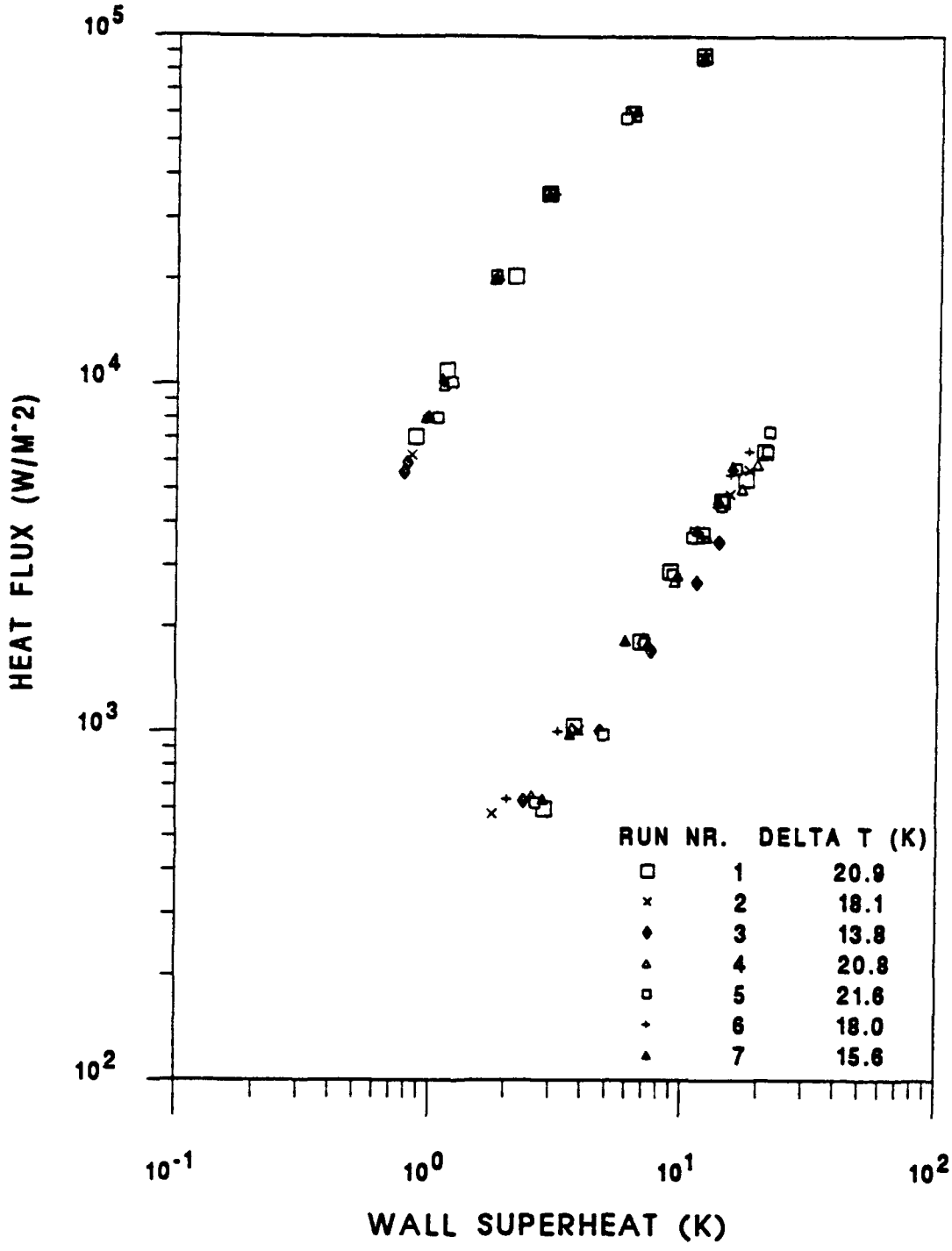

Figure 5.31 HIGH FLUX 10% oil incipience tests

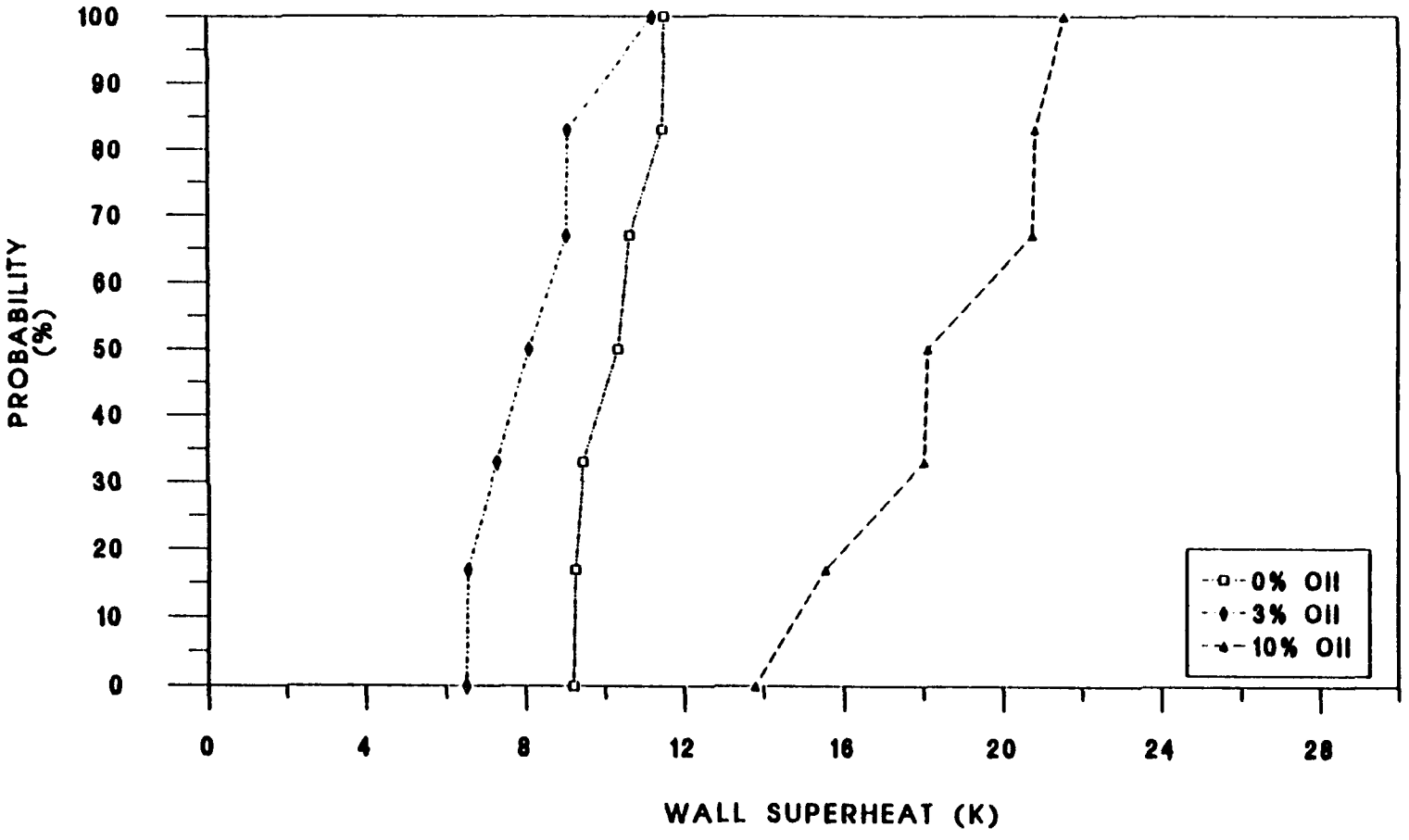

Figure 5.32 HIGH FLUX Probability of Incipience at 0%, 3% and 10% Oil Concentrations

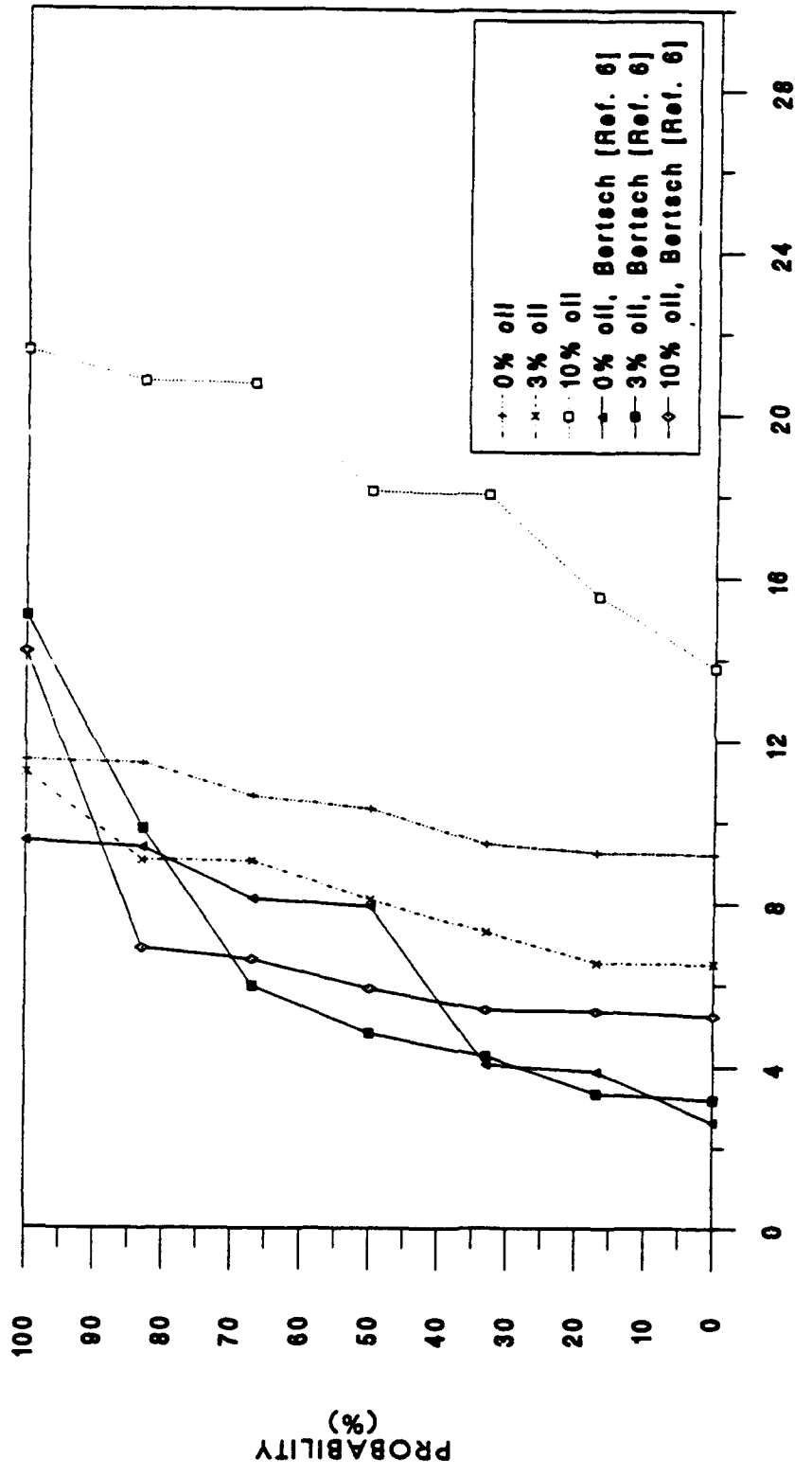

Figure 5.33 HIGH FLUX tube probability of incipience comparison

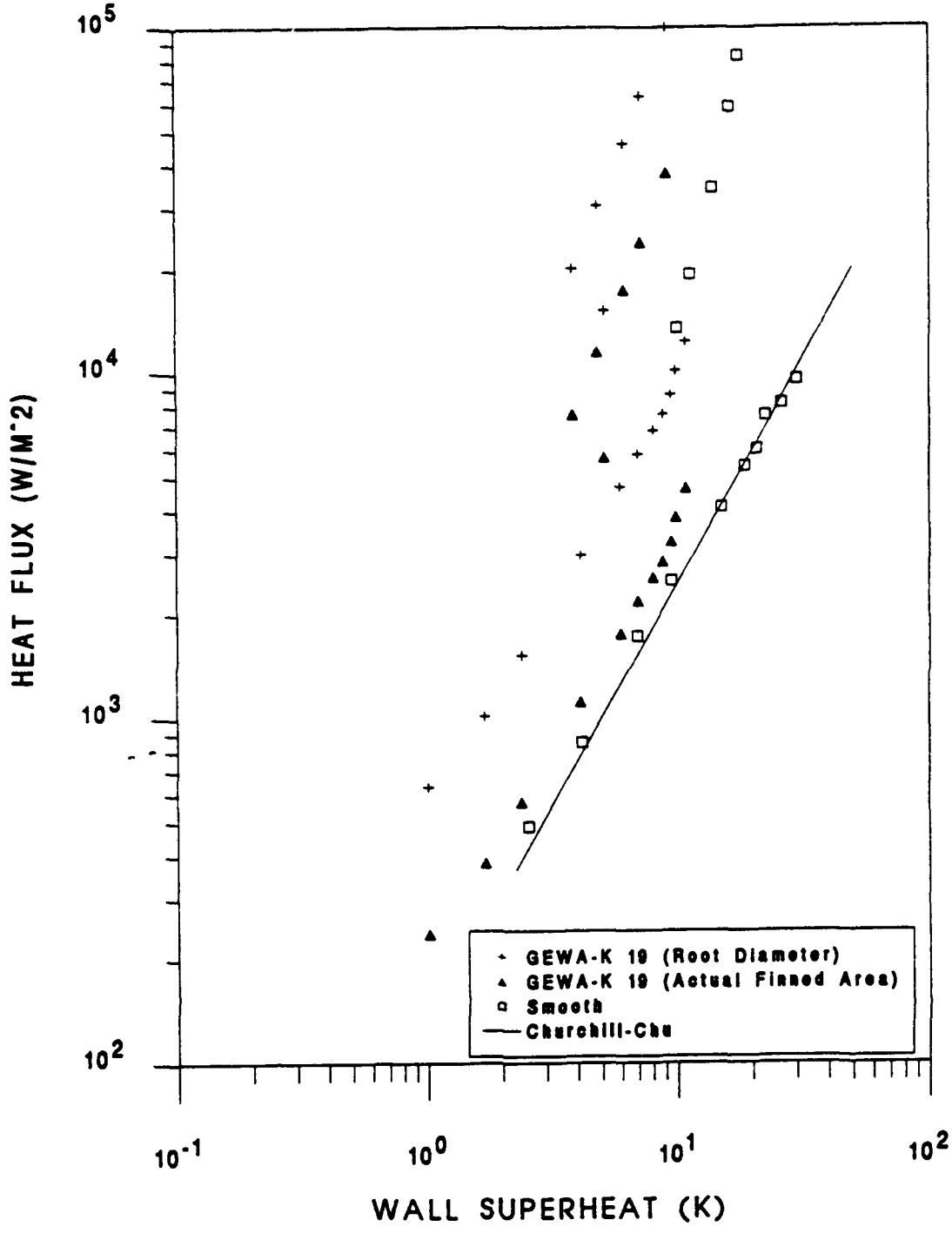

Figure 5.34 GEWA-K 19 fpi actual finned area and root diameter comparison with smooth tube at 0% Oil.

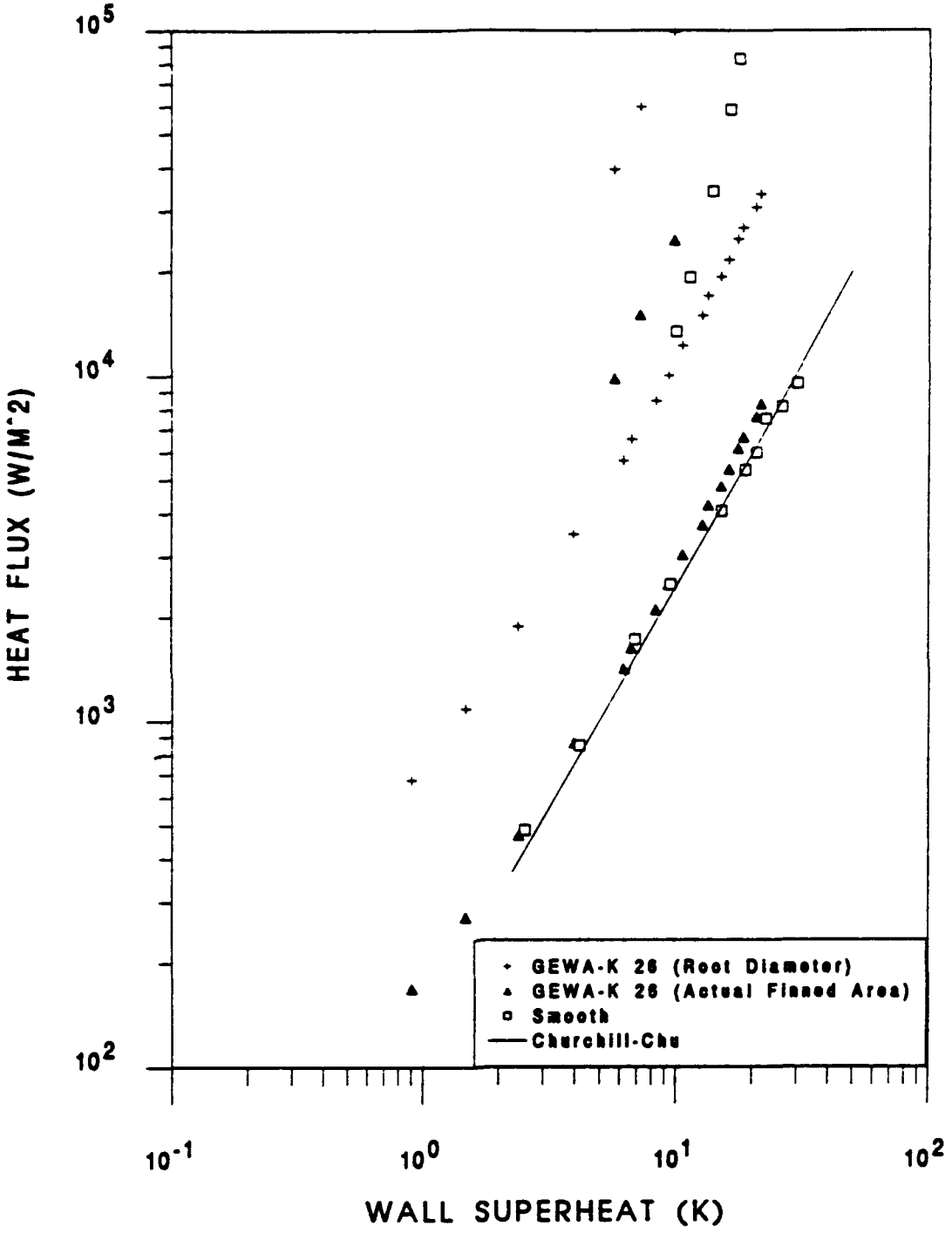

Figure 5.35 GEWA-K 26 fpi actual finned area and root diameter comparison with smooth tube at 0% oil

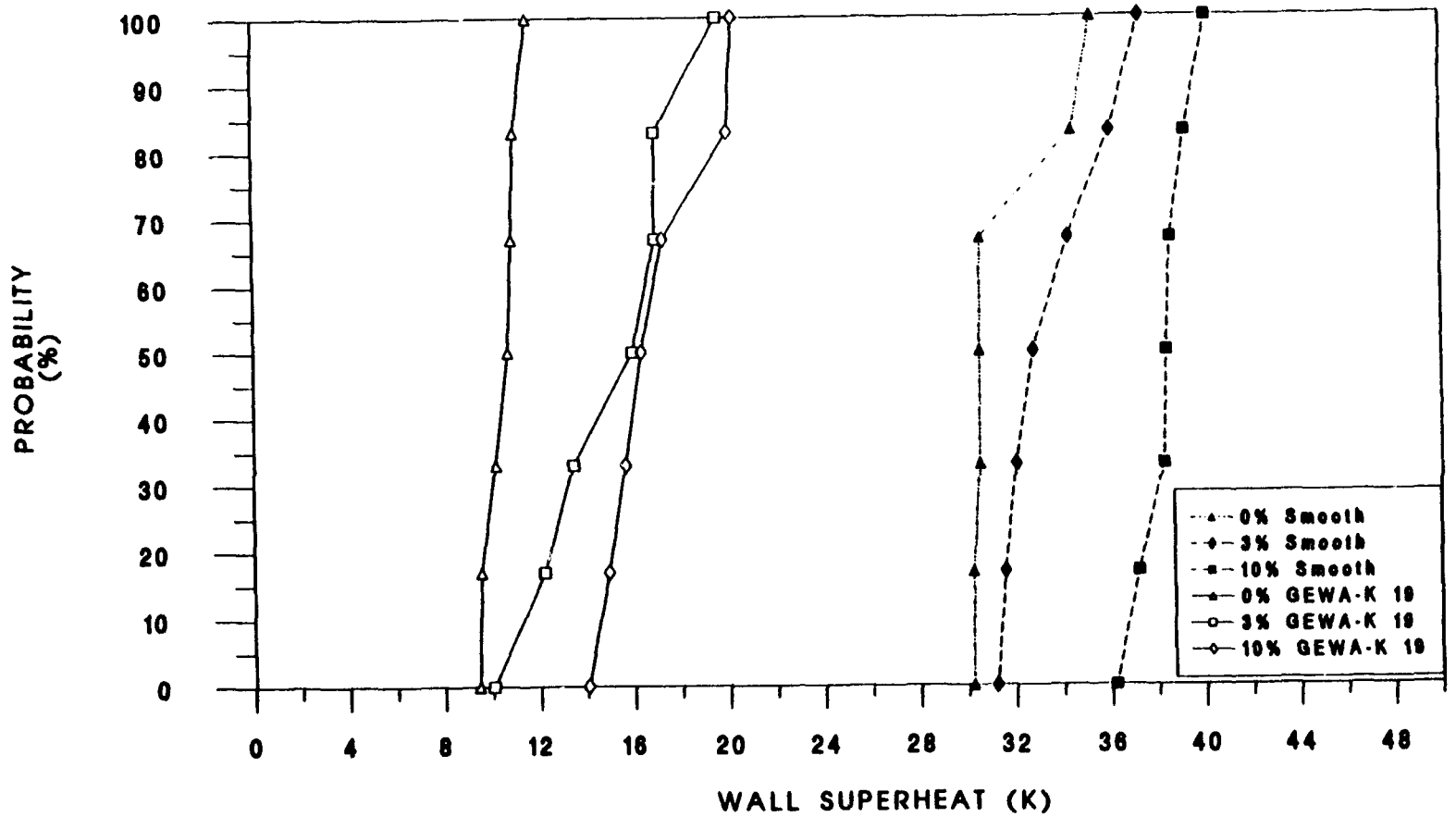

Figure 5.36 Smooth Tube and GEWA-K 19 fpi probability of incipience comparison with 0%, 3% and 10% oil concentrations

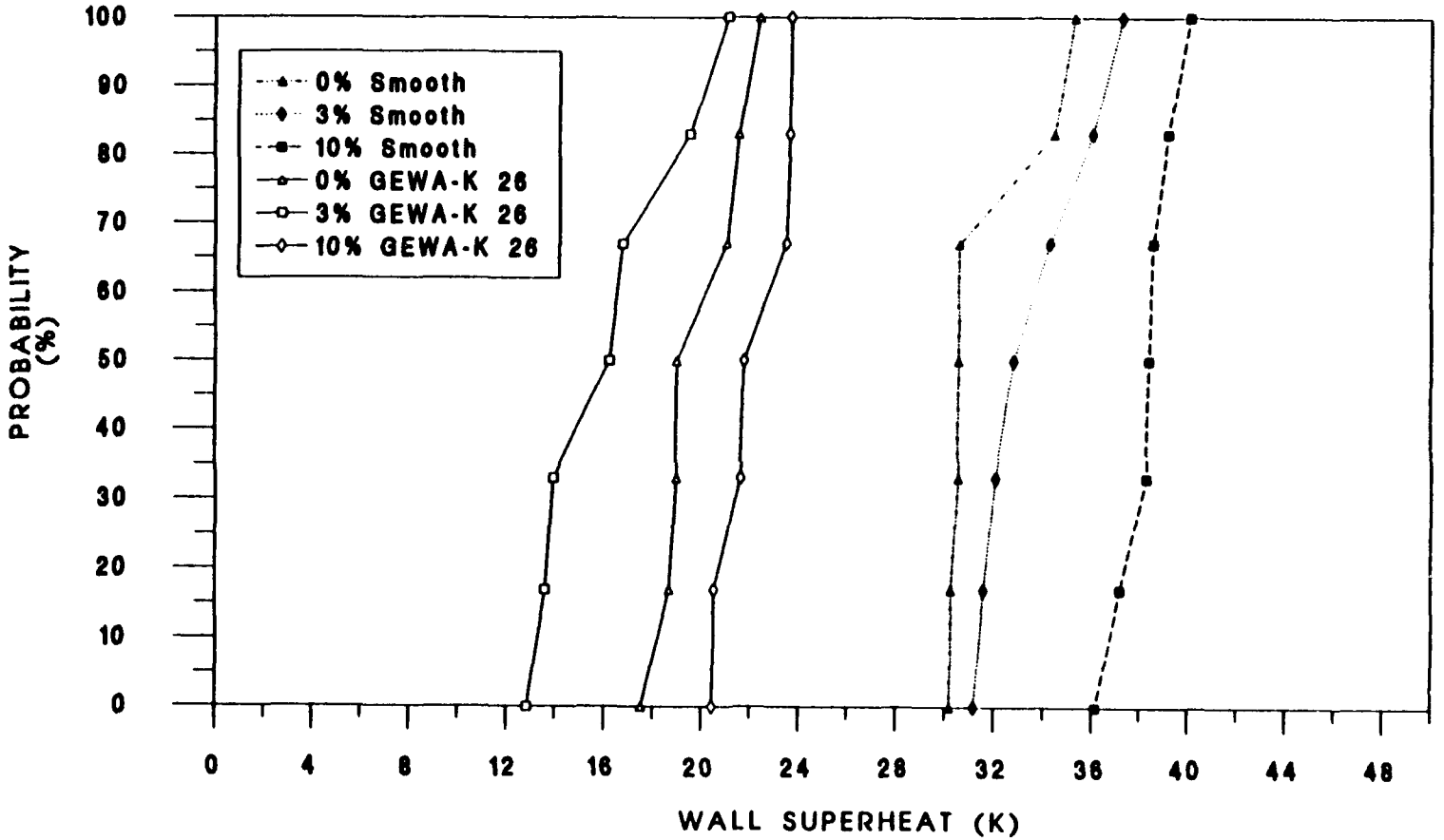

Figure 5.37 Smooth tube and GEWA-K 26 fpi tube probability of incipience comparison

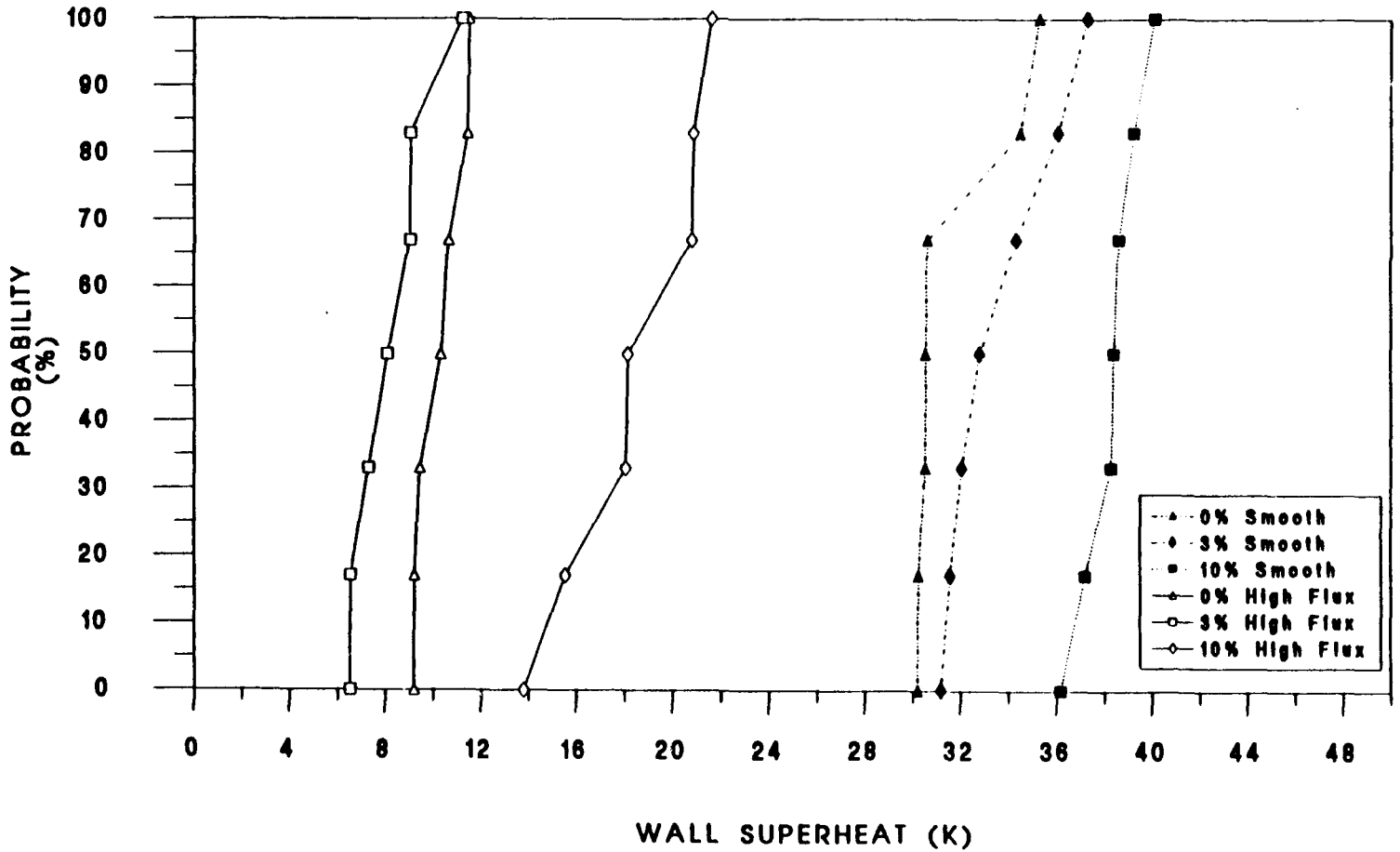

Figure 5.38 Smooth tube and HIGH FLUX tube probability of incipience comparison

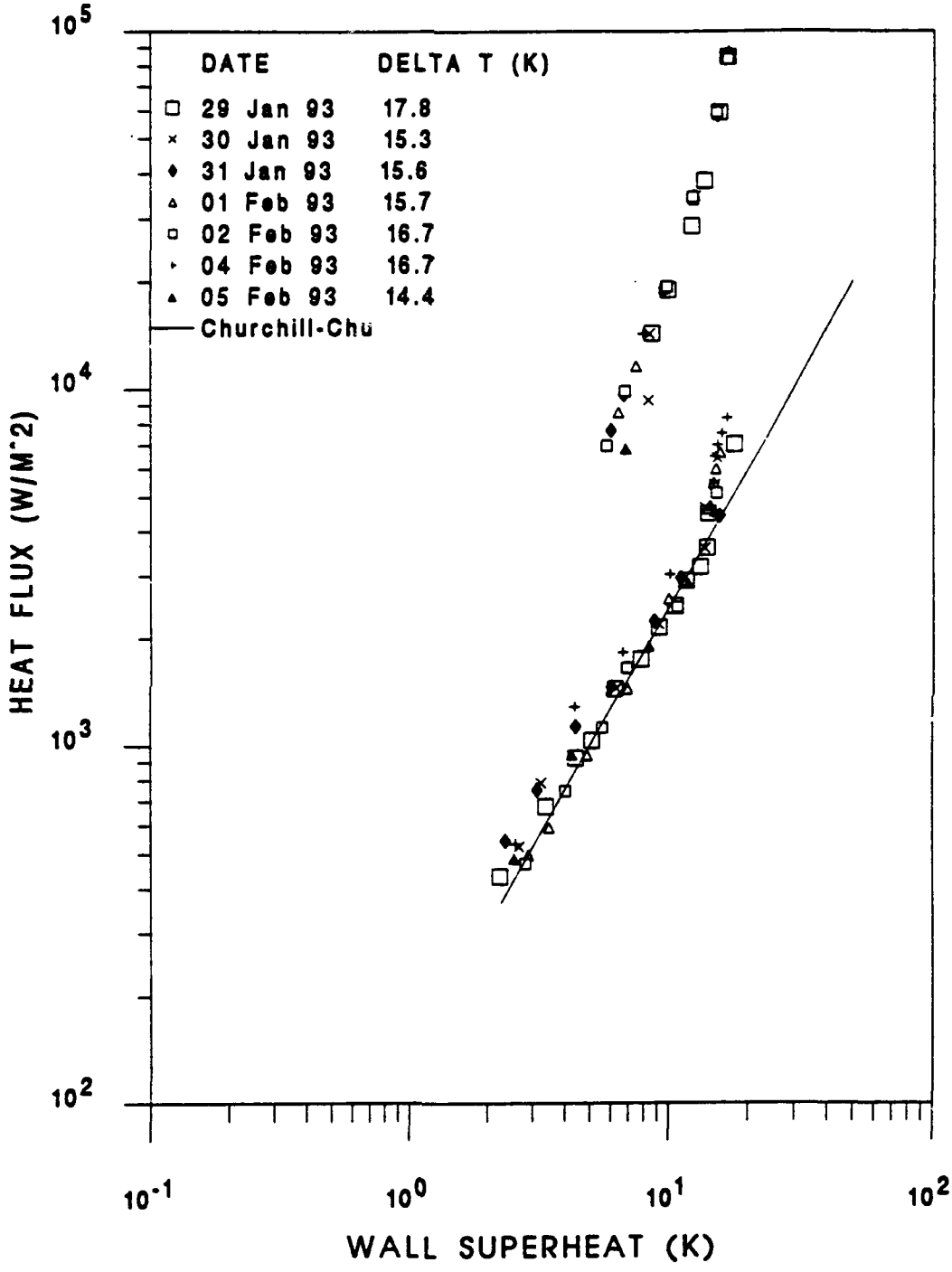

Figure 5.39 Smooth Tube 0% oil, degassing procedure A incipience tests

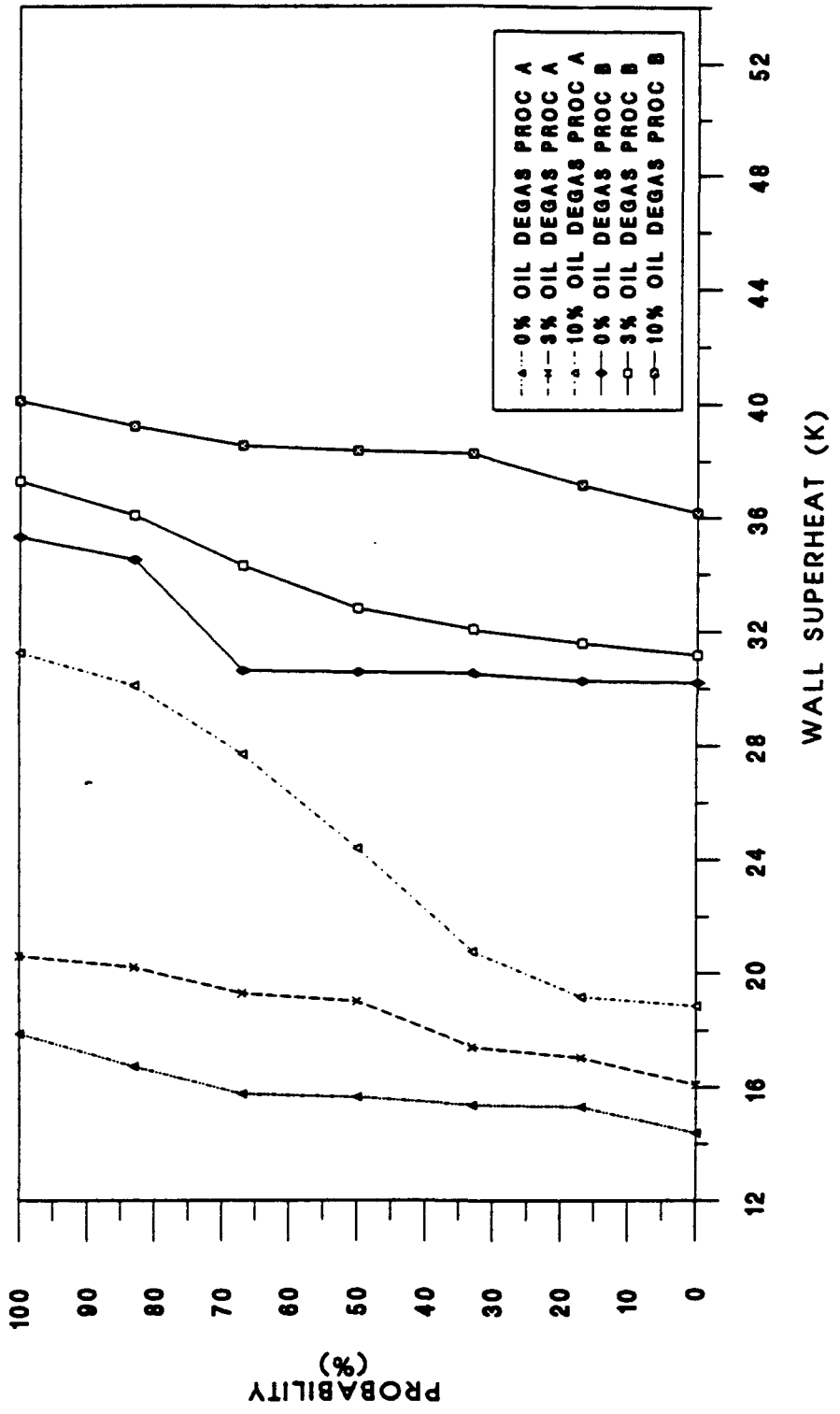

Figure 5.40 Effect of dissolved gases on incipient wall superheats on smooth tube

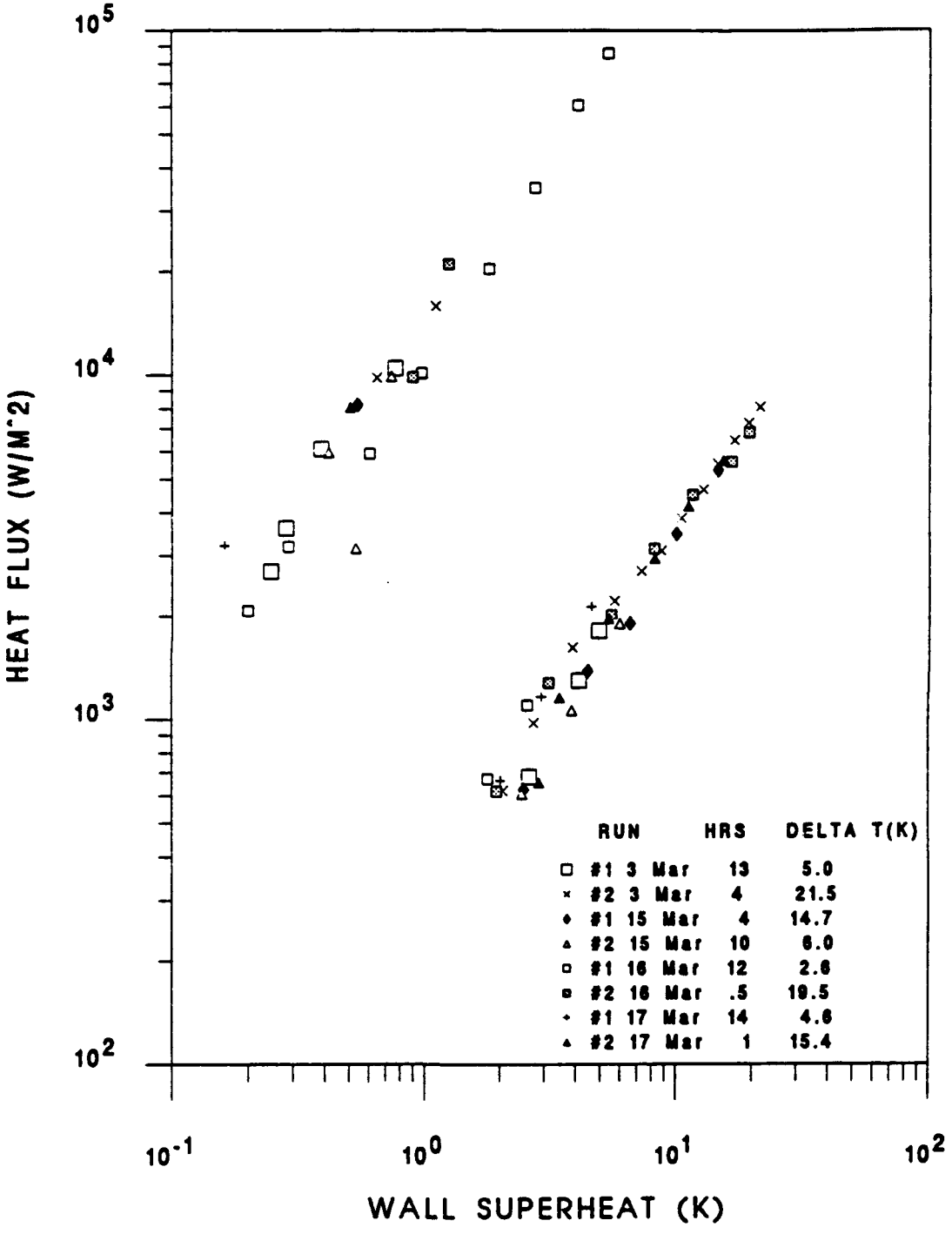

Figure 5.41 Effect of dissolved gases on incipient wall superheats on HIGH FLUX tube (varying settling time)

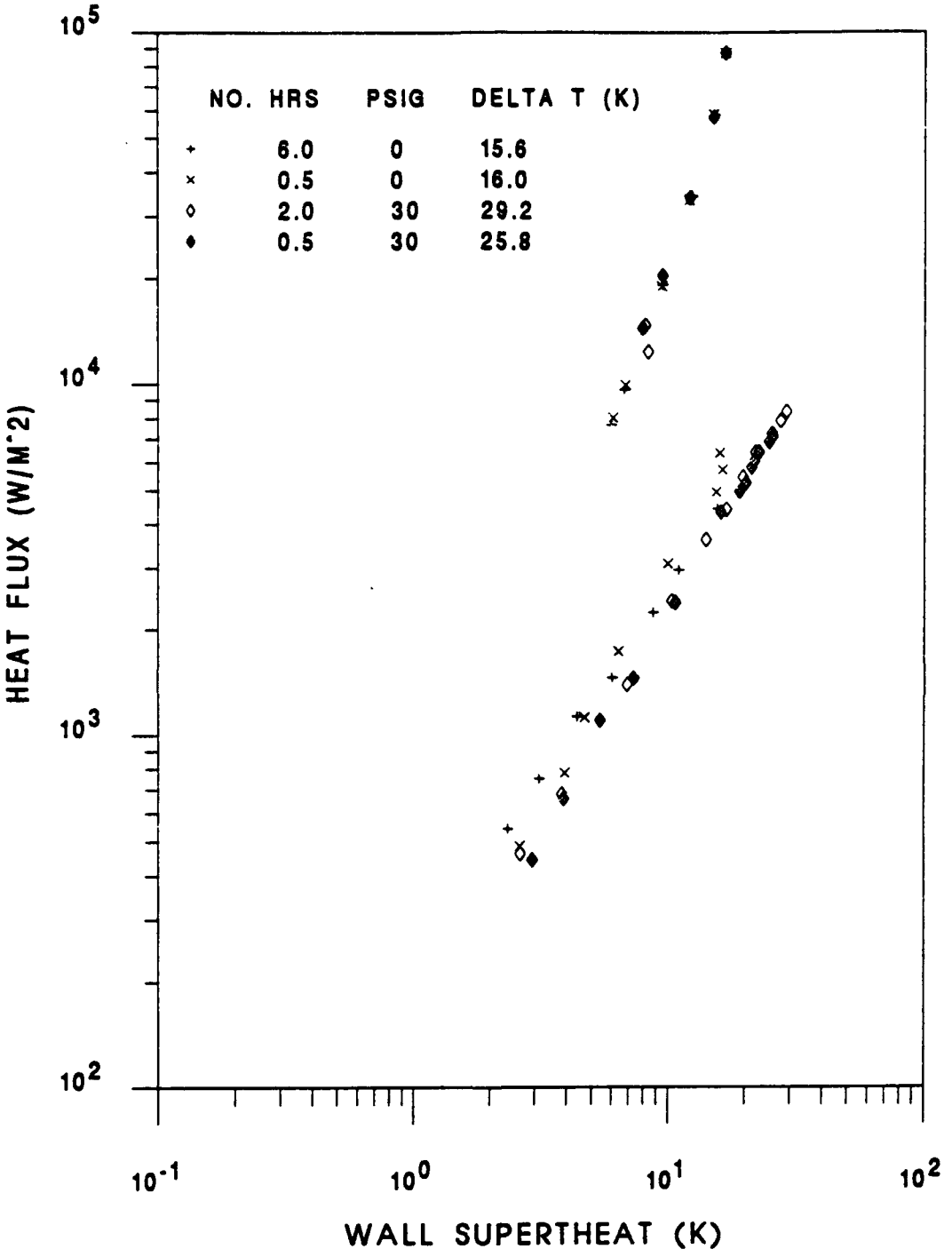

Figure 5.42 Pressure effect on incipient wall superheats on a smooth tube with 0% oil

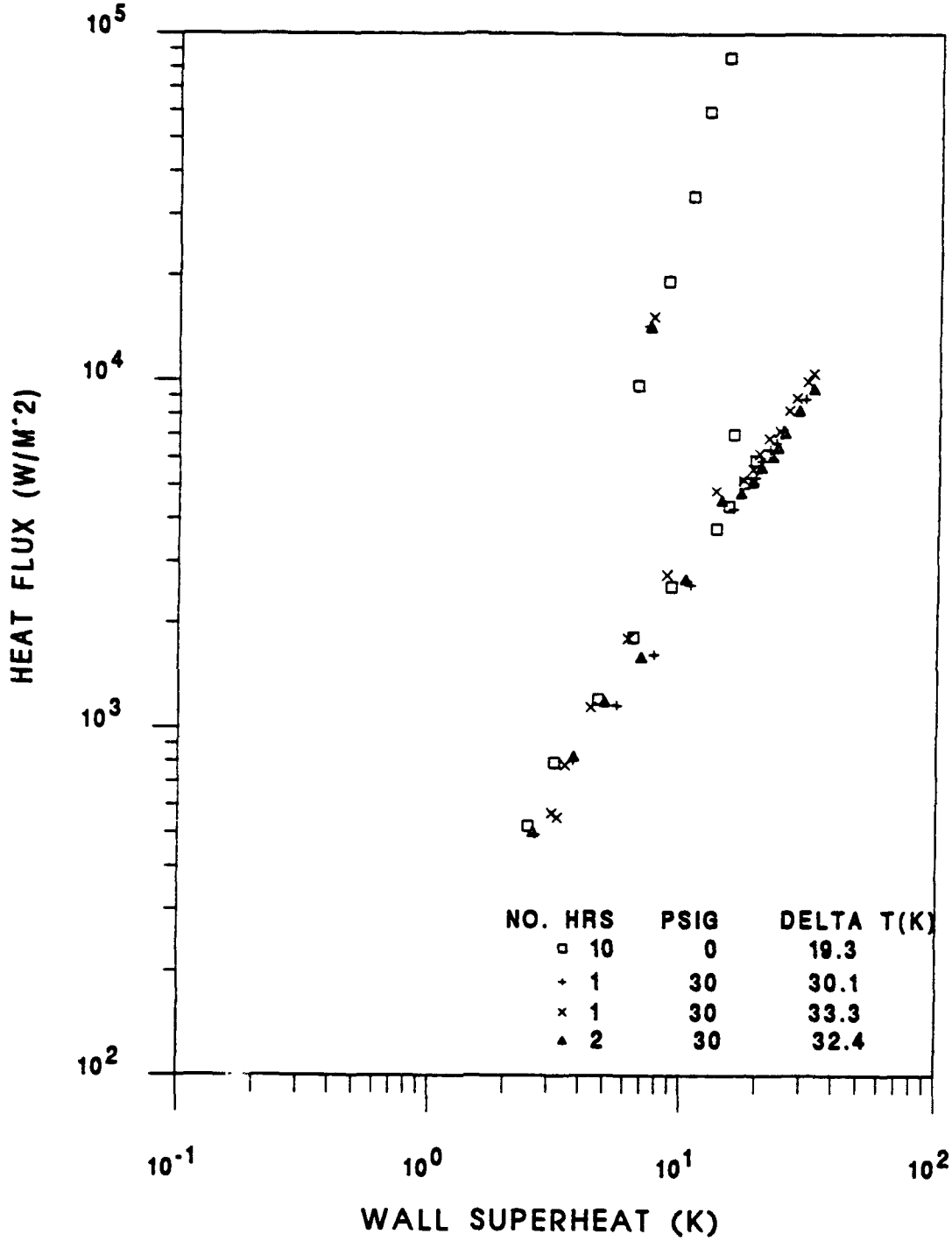

Figure 5.43 Pressure effect on incipient wall superheats on a smooth tube with 3% oil

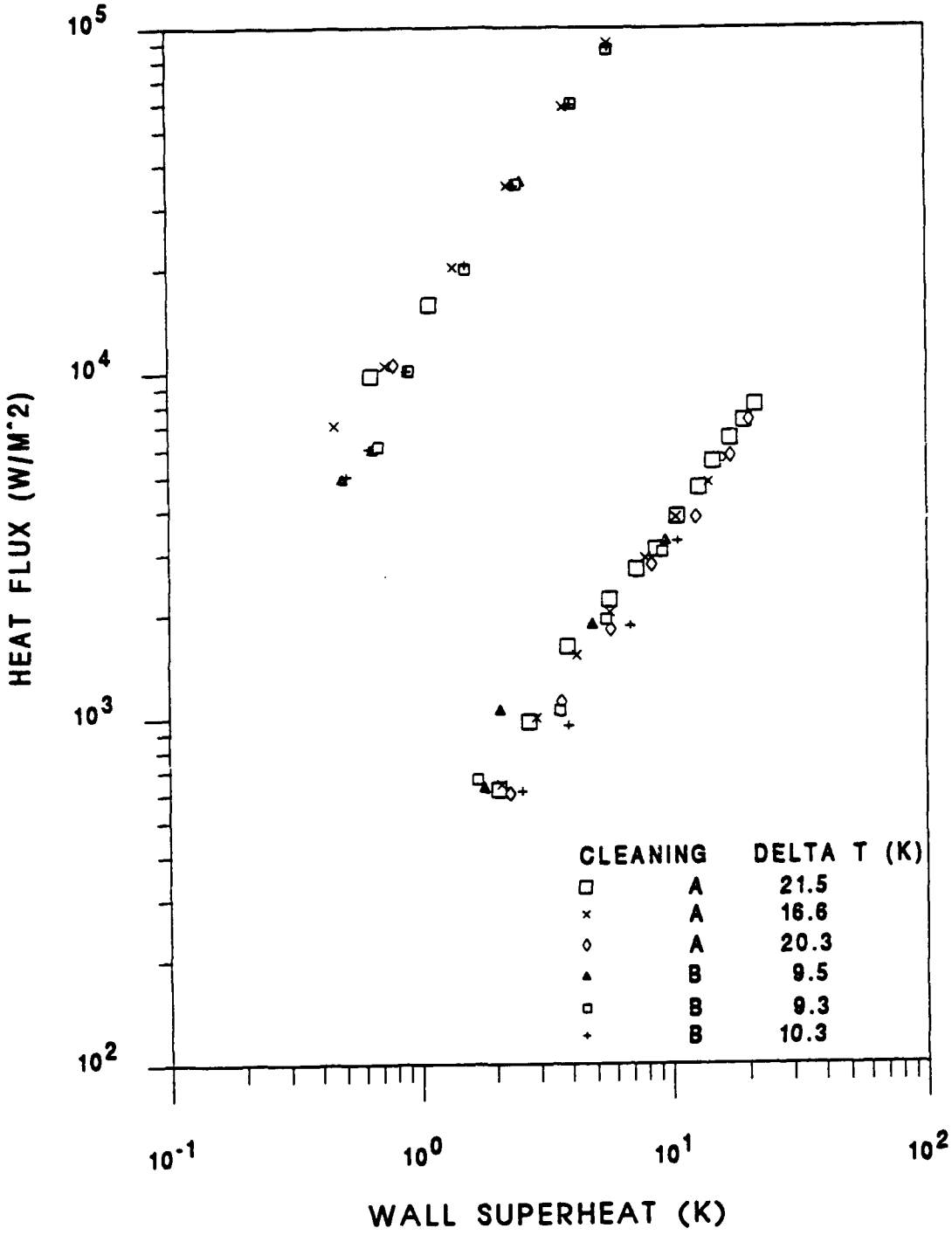

Figure 5.44 Cleaning procedure effect comparison on incipient wall superheat on a HIGH FLUX tube with 0% oil

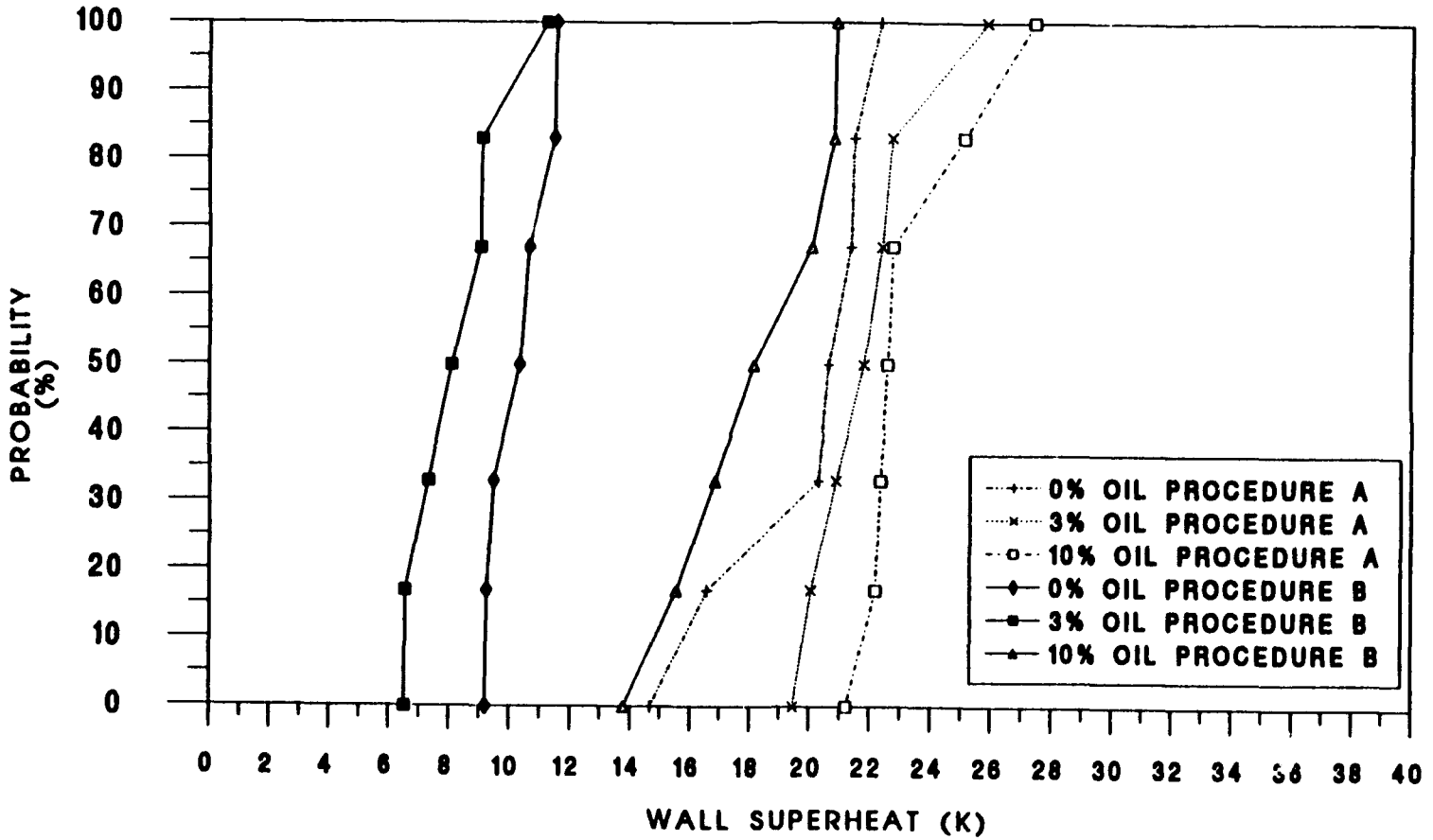

Figure 5.45 Probability of incipience comparison of cleaning procedures A and B on a HIGH FLUX Tube

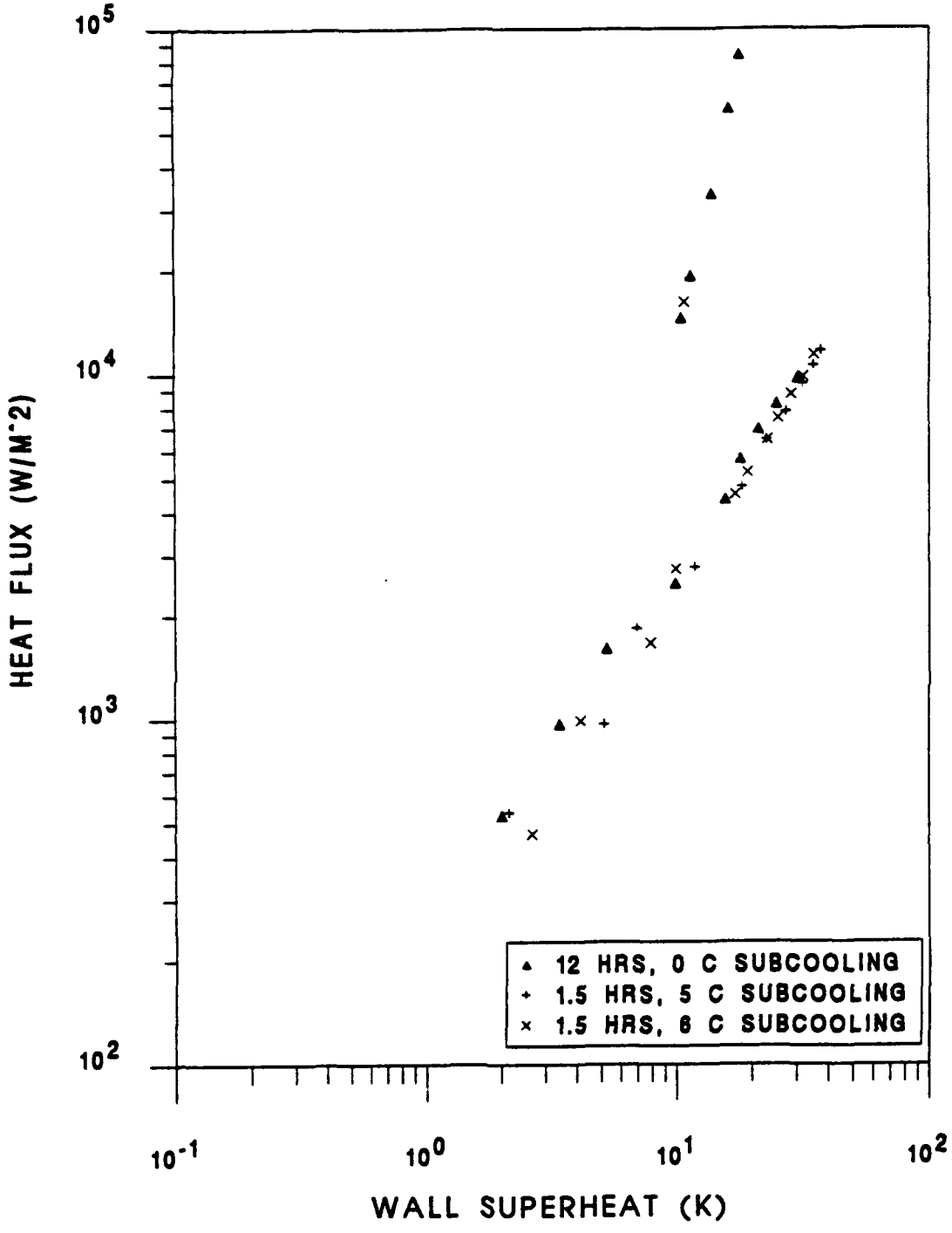

Figure 5.46 Subcooling effect on incipient wall superheat from a smooth tube with pure R-124

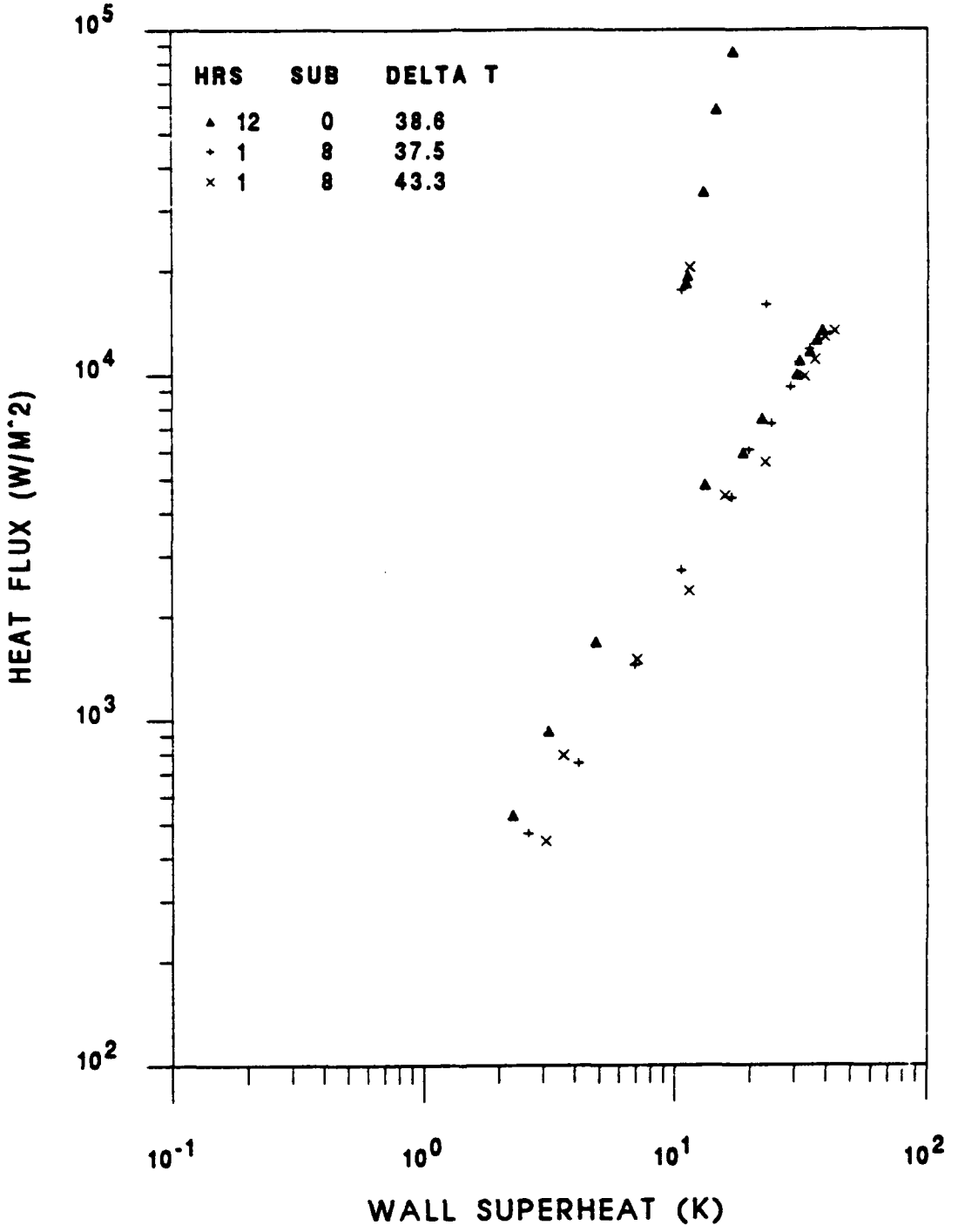

Figure 5.47 Subcooling effect on incipient wall superheat from a smooth tube with 10% oil/R-124 mixture

VI. CONCLUSIONS

1. Onset of nucleate boiling is very random.

2. An oil concentration of 3% tends to delay the onset of nucleate boiling (compared to pure R-124) on a smooth tube and GEWA-K 19 fpi tube, but tends to lower the onset of nucleate boiling on a GEWA-K 26 fpi and HIGH FLUX tube. The reason for this is not precisely known, but is very repeatable.

3. An oil concentration of 10% delayed the onset of nucleate boiling for all tubes.

4. Presence of dissolved gases in the refrigerant tends to lower the onset of nucleate boiling by increasing the number of entrapped vapor nuclei of the surface.

5. Pre-pressurization of the system increases the incipient superheat by dislodging or deactivating potential nucleation sites (flooding the cavities).

6. Subcooling the refrigerant pool for a short period (<1 hr) increases the incipient wall superheat to a value close to or even higher than that obtained with overnight settling time. Again this is due to deactivation of potential nucleation sites.

7. Alkylbenzene oil tends to clog the re-entrant cavities of the HIGH FLUX tube, resulting in a higher incipient wall superheat. Cleaning the porous tubes with a brush to unclog the cavities returned the surface to its original state.

VII. RECOMMENDATIONS

1. Further studies should be conducted to verify the incipient behavior of 3% oil on the GEWA-K 19 and 26 fpi tubes and HIGH FLUX tube to try to see why incipient wall superheat was reduced.

2. Conduct similar incipient tests on other remaining enhanced tubes to better understand the effect of oil addition on enhanced surfaces.

3. Modify the existing system for multiple (2 and 3) tube bundle experiments and conduct tests to study the effects of tube arrangement position and orientation on incipience from other tubes.

4. Conduct further tests on effect of subcooling, dissolved gases and pressurization on incipient wall superheat.

5. Conduct studies of oil/R-124 mixture properties.

APPENDIX A: LIST OF DATA FILES

FILE NAME	TUBE TYPE	DEGASSING	PURPOSE
D0129SM0	Smooth	A	Repeatability
D0129BSM0	Smooth	A	Repeatability
D0130SM0	Smooth	A	Repeatability
D0131SM0	Smooth	A	Repeatability
D0131ASM0	Smooth	A	Repeatability
D0131BSM0	Smooth	A	Data
D0131CSM0	Smooth	A	Data
D0201SM0	Smooth	A	Data
D0201ASM0	Smooth	A	Data
D0201CSM0	Smooth	A	Data
D0201DSM0	Smooth	A	Data
D0202SM0	Smooth	A	Data
D0202ASM0	Smooth	A	Data
D0202CSM0	Smooth	A	Data
D0202DSM0	Smooth	A	Data
D0202ESM0	Smooth	A	Data
D0203SM0	Smooth	A	Data
D0203ASM0	Smooth	A	Data
D0203CSM0	Smooth	A	Data
D0203DSM0	Smooth	A	Data
D0203ESM0	Smooth	A	Data
D0203FSM0	Smooth	A	Data
D0203GSM0	Smooth	A	Data
D0204SM0	Smooth	A	Data

FILE NAME	TUBE TYPE	DEGASSING	PURPOSE
D0210ASM3	Smooth	A	Data
D0211SM3	Smooth	A	Data
D0211ASM3	Smooth	A	Data
D0215SM3	Smooth	A	Data
D0216SM3	Smooth	A	Data
D0216SM10	Smooth	A	Data
D0216A3M10	Smooth	A	Data
D0217SM10	Smooth	A	Data
D0217ASM10	Smooth	A	Data
D0217BSM10	Smooth	A	Data
D0218SM10	Smooth	A	Data
D0218ASM10	Smooth	A	Data
D0218BSM10	Smooth	A	Data
D0218CSM10	Smooth	A	Data
D0220GK190	GEWA-K 19	A	Repeatability
D0220GAK190	GEWA-K 19	A	Repeatability
D0221GK190	GEWA-K 19	A	Repeatability
D0221AGK190	GEWA-K 19	A	Repeatability
D0221BGK190	GEWA-K 19	A	Data
D0221CGK190	GEWA-K 19	A	Data
D0222GK190	GEWA-K 19	A	Data
D0222GK193	GEWA-K 19	A	Data
D0222GK193	GEWA-K 19	A	Data
D0223AGK193	GEWA-K 19	A	Data
D0223BGK193	GEWA-K 19	A	Data
D0223CK193	GEWA-K 19	A	Data

FILE NAME	TUBE TYPE	DEGASSING	PURPOSE
D0224GK193	GEWA-K 19	A	Data
D0224AGK193	GEWA-K 19	A	Data
D0225GK193	GEWA-K 19	A	Data
D0225AGK193	GEWA-K 19	A	Data
D0224AGK193	GEWA-K 19	A	Data
D0225GK193	GEWA-K 19	A	Data
D0225AGK193	GEWA-K 19	A	Data
D0225GK1910	GEWA-K 19	A	Data
D0225BGK1910	GEWA-K 19	A	Data
D0226GK1910	GEWA-K 19	A	Data
D0227GK1910	GEWA-K 19	A	Data
D0301GK1910	GEWA-K 19	A	Data
D0301AGK1910	GEWA-K 19	A	Data
D0301BGK1910	GEWA-K 19	A	Data
D0302GK1910	GEWA-K 19	A	Data
D0303GK260	GEWA-K 26	A	Data
D0303AGK260	GEWA-K 26	A	Data
D0304GK260	GEWA-K 26	A	Data
D0304AGK260	GEWA-K 26	A	Data
D0304BGK260	GEWA-K 26	A	Data
D0305GK260	GEWA-K 26	A	Data
D0305AGK260	GEWA-K 26	A	Data
D0306GK263	GEWA-K 26	A	Data
D0306AGK263	GEWA-K 26	A	Data
D0306BGK263	GEWA-K 26	A	Data
D0307GK263	GEWA-K 26	A	Data

FILE NAME	TUBE TYPE	DEGASSING	PURPOSE
D0307AGK263	GEWA-K 26	A	Data
D0307BGK263	GEWA-K 26	A	Data
D0307CGK263	GEWA-K 26	A	Data
D0308GK263	GEWA-K 26	A	Data
D0308AGK263	GEWA-K 26	A	Data
D0308GK2610	GEWA-K 26	A	Data
D0309GK2610	GEWA-K 26	A	Data
D0309AGK2610	GEWA-K 26	A	Data
D0309BGK2610	GEWA-K 26	A	Data
D0310GK2610	GEWA-K 26	A	Data
D0310AGK2610	GEWA-K 26	A	Data
D0310BGK2610	GEWA-K 26	A	Data
D0311GK2610	GEWA-K 26	A	Data
D0311AGK2610	GEWA-K 26	A	Data
D0311BGK2610	GEWA-K 26	A	Data
D0311CGK2610	GEWA-K 26	A	Data
D0312GK2610	GEWA-K 26	A	Data
D0312AGK2610	GEWA-K 26	A	Data
D0312BGK2610	GEWA-K 26	A	Data
D0312CGK2610	GEWA-K 26	A	Data
D0313GK2610	GEWA-K 26	A	Data
D0313HF0	HIGH-FLUX	A	Data
D0313AHF0	HIGH-FLUX	A	Data
D0313BHF0	HIGH-FLUX	A	Data
D0314AHF0	HIGH-FLUX	A	Data
D0315HF0	HIGH-FLUX	A	Data

FILE NAME	TUBE TYPE	DEGASSING	PURPOSE
D0321BHF10	HIGH-FLUX	B	Data
D0322HF10	HIGH-FLUX	B	Data
D0322AHF10	HIGH-FLUX	B	Data
D0322BHF10	HIGH-FLUX	B	Data
D0323HF10	HIGH-FLUX	B	Data
D0324HF10	HIGH-FLUX	B	Data
D0329HF10	HIGH-FLUX	B	Data
D0330SM0	SMOOTH	B	Data
D0330ASM0	SMOOTH	B	Data
D0330BSM0	SMOOTH	B	Data
D0330CSM0	SMOOTH	B	Data
D0330DSM0	SMOOTH	B	Data
D0330ESM0	SMOOTH	B	UNCERTAINTY
D0330FSM0	SMOOTH	B	Data
D0331SM0	SMOOTH	B	Data
D0331ASM0	SMOOTH	B	Data
D0331BSM0	SMOOTH	B	Data
D0331CSM0	SMOOTH	B	Data
D0331DSM0	SMOOTH	B	Data
D0401SM0	SMOOTH	B	Data
D0401ASM0	SMOOTH	B	Data
D0401BSM0	SMOOTH	B	Data
D0401CSM0	SMOOTH	B	Data
D0401DSM0	SMOOTH	B	Data
D0404SM0	SMOOTH	B	Data
D0404ASM0	SMOOTH	B	Data

FILE NAME	TUBE TYPE	DEGASSING	PURPOSE
D0405SM0	SMOOTH	B	Data
D0405ASM0	SMOOTH	B	Data
D0405BSM0	SMOOTH	B	Data
D0405CSM0	SMOOTH	B	Data
D0405DSM0	SMOOTH	B	Data
D0405ESM0	SMOOTH	B	Data
D0405ASM3	SMOOTH	B	Data
D0406SM3	SMOOTH	B	Data
D0406ASM3	SMOOTH	B	Data
D0406BSM3	SMOOTH	B	Data
D0406CSM3	SMOOTH	B	Data
D0406DSM3	SMOOTH	B	Data
D0406ESM3	SMOOTH	B	Data
D0406FSM3	SMOOTH	B	Data
D0407SM3	SMOOTH	B	Data
D0407ASM3	SMOOTH	B	Data
D0407BSM3	SMOOTH	B	Data
D0407CSM3	SMOOTH	B	Data
D0407DSM3	SMOOTH	B	Data
D0408SM3	SMOOTH	B	Data
D0408ASM3	SMOOTH	B	Data
D0408BSM3	SMOOTH	B	Data
D0408CSM3	SMOOTH	B	Data
D0408DSM3	SMOOTH	B	Data
D0409SM3	SMOOTH	B	Data
D0409SM10	SMOOTH	B	Data

FILE NAME	TUBE TYPE	DEGASSING	PURPOSE
D0409ASM10	SMOOTH	B	Data
D0409BSM10	SMOOTH	B	Data
D0410SM10	SMOOTH	B	Data
D0410ASM10	SMOOTH	B	Data
D0410BSM10	SMOOTH	B	Data
D0410CSM10	SMOOTH	B	Data
D0410DSM10	SMOOTH	B	Data
D0411SM10	SMOOTH	B	Data
D0411ASM10	SMOOTH	B	Uncertainty
D0411BSM10	SMOOTH	B	Data
D0412SM10	SMOOTH	B	Data
D0412ASM10	SMOOTH	B	Data
D0412GK190	GEWA-K 19	B	Data
D0412GK190	GEWA-K 19	B	Data
D0412AGK190	GEWA-K 19	B	Data
D0412CGK190	GEWA-K 19	B	Data
D0413GK190	GEWA-K 19	B	Data
D0413AGK190	GEWA-K 19	B	Data
D0413BGK190	GEWA-K 19	B	Data
D0413DGK190	GEWA-K 19	B	Data
D0414GK190	GEWA-K 19	B	Data
D0414AGK190	GEWA-K 19	B	Data
D0414BGK190	GEWA-K 19	B	Data
D0415GK193	GEWA-K 19	B	Data
D0415GK193	GEWA-K 19	B	Data
D0415BGK193	GEWA-K 19	B	Data

FILE NAME	TUBE TYPE	DEGASSING	PURPOSE
D0415CGK193	GEWA-K 19	B	Data
D0415DGK193	GEWA-K 19	B	Data
D0416GK193	GEWA-K 19	B	Data
D0416AGK193	GEWA-K 19	B	Data
D0416BGK193	GEWA-K 19	B	Data
D0417GK193	GEWA-K 19	B	Data
D0417GK1910	GEWA-K 19	B	Data
D0418GK1910	GEWA-K 19	B	Data
D0418AGK1910	GEWA-K 19	B	Data
D0418BGK1910	GEWA-K 19	B	Data
D0419GK1910	GEWA-K 19	B	Data
D0419AGK1910	GEWA-K 19	B	Data
D0419BGK1910	GEWA-K 19	B	Data
D0420GK1910	GEWA-K 19	B	Data
D0420AGK1910	GEWA-K 19	B	Data
D0420BGK1910	GEWA-K 19	B	Data
D0420HF0	HIGH-FLUX	B	Data
D0421HF0	HIGH-FLUX	B	Data
D0421AHF0	HIGH-FLUX	B	Data
D0421CHF0	HIGH-FLUX	B	Data
D0421DHF0	HIGH-FLUX	B	Data
D0421EHF0	HIGH-FLUX	B	Data
D0422HF0	HIGH-FLUX	B	Data
D0422AHF0	HIGH-FLUX	B	Data
D0422BHF0	HIGH-FLUX	B	Data
D0422CHF0	HIGH-FLUX	B	Uncertainty

FILE NAME	TUBE TYPE	DEGASSING	PURPOSE
D0422HF3	HIGH-FLUX	B	Data
D0423HF3	HIGH-FLUX	B	Data
D0423AHF3	HIGH-FLUX	B	Data
D0423BHF3	HIGH-FLUX	B	Data
D0423CHF3	HIGH-FLUX	B	Data
D0423DHF3	HIGH-FLUX	B	Data
D0424HF3	HIGH-FLUX	B	Data
D0424AHF3	HIGH-FLUX	B	Data
D0424BHF3	HIGH-FLUX	B	Data
D0424CHF3	HIGH-FLUX	B	Data
D0425HF10	HIGH-FLUX	B	Data
D0425BHF10	HIGH-FLUX	B	Data
D0425AHF10	HIGH-FLUX	B	Data
D0425CHF10	HIGH-FLUX	B	Data
D0426HF10	HIGH-FLUX	B	Data
D0426AHF10	HIGH-FLUX	B	Data
D0426BHF10	HIGH-FLUX	B	Data
D0427GK260	GEWA-K 26	B	Data
D0427GK260	GEWA-K 26	B	Data
D0427AGK260	GEWA-K 26	B	Data
D0428GK260	GEWA-K 26	B	Data
D0428AGK260	GEWA-K 26	B	Data
D0428BGK260	GEWA-K 26	B	Data
D0428GK263	GEWA-K 26	B	Data
D0428AGK263	GEWA-K 26	B	Data
D0429GK263	GEWA-K 26	B	Data

FILE NAME	TUBE TYPE	DEGASSING	PURPOSE
D0429AGK263	GEWA-K 26	B	Data
D0429GK2610	GEWA-K 26	B	Data
D0429AGK2610	GEWA-K 26	B	Data
D0430GK2610	GEWA-K 26	B	Data
D0430AGK2610	GEWA-K 26	B	Data
D0430BGK2610	GEWA-K 26	B	Data
D0430CGK2610	GEWA-K 26	B	Data
D0430DGK2610	GEWA-K 26	B	Data
D0503GK190	GEWA-K 19	B	Data
D0504GK190	GEWA-K 19	B	Data

The tabulated data was filed using the same filing system used by Bertsch [Ref. 6]. For example filename 'D0312AGK2610':

1. First letter D refers to data.
2. The next four numbers refer to the month and day.
3. The next letter represents the order data was taken for a particular day;

   no letter - first run of the day
   A - Second run
   B - Third run
   etc...

4. The next two to four letters indicate tube type;

   SM = Smooth
   GK19 = GEWA-K 19 fpi
   GK26 = GEWA-K 26 fpi
   HF = HIGH FLUX

5. The last one to two numbers indicate the percentage of oil used;

   0 = 0% oil
   3 = 3% oil
   10 = 10% oil

Thus, the example filename was a test data conducted on Mar 12, and was the second run for the day using a GEWA-K 26 fpi tube with 10% oil.

APPENDIX B. REPRESENTATIVE DATA SET

```
Date :    30 Mar 1993

NOTE: Program name : DRP6B
      Disk number  = 00
      New file name: D0330ESM0
      TC are defective at locations  7     8
      Tube Number:   4

Data Set Number =   1  Bulk Oil % =  0.0
TIME:      11:14:53
TC No:     1       2       3       4       5       6       7       8
Temp :   4.38    4.46    4.45    4.41    4.31    4.16 -99.99 -99.99
 Twa     Tliqd   Tliqd2  Tvapr   Psat    Tsump
  4.36    2.14    2.15    2.10   10.76   -11.1
 Rho    =  1425.494
 Mu     =  .0003326
 K      =  .07405
 Cp     =  1061.21519
 Tfilm  =  3.22636
 Hfg    =  158957.68568
 Tsat   =  2.09544
 Hbar   =  160.71038
 Thetab  Htube       Qdp
  2.262  2.448E+02  5.537E+02

Data Set Number =   2  Bulk Oil % =  0.0
TIME:      11:15:43
TC No:     1       2       3       4       5       6       7       8
Temp :   5.00    5.11    5.14    5.07    4.94    4.74 -99.99 -99.99
 Twa     Tliqd   Tliqd2  Tvapr   Psat    Tsump
  4.99    2.18    2.21    2.16   10.82   -11.1
 Rho    =  1424.482
 Mu     =  .0003312
 K      =  .07392
 Cp     =  1061.98365
 Tfilm  =  3.57395
 Hfg    =  158929.45867
 Tsat   =  2.15584
 Hbar   =  170.97572
 Thetab  Htube       Qdp
  2.836  3.205E+02  9.091E+02

Data Set Number =   3  Bulk Oil % =  0.0
TIME:      11:16:49
TC No:     1       2       3       4       5       6       7       8
Temp :   7.13    7.34    7.38    7.33    7.20    6.87 -99.99 -99.99
 Twa     Tliqd   Tliqd2  Tvapr   Psat    Tsump
  7.19    2.22    2.25    2.17   10.83   -11.1
 Rho    =  1421.247
 Mu     =  .0003268
 K      =  .07353
 Cp     =  1064.44863
 Tfilm  =  4.68168
 Hfg    =  158923.45200
 Tsat   =  2.16869
 Hbar   =  199.93379
 Thetab  Htube       Qdp
  5.026  3.240E+02  1.629E+03
```

```
Data Set Number =   4  Bulk Oil % =  0.0
TIME:      11:17:54
TC No:     1       2       3       4       5       6       7       8
Temp :  10.40   10.81   10.85   10.57   10.22    9.66 -99.99 -99.99
 Twa     Tliqd   Tliqd2  Tvapr   Psat    Tsump
 10.40    2.21    2.25    2.13   10.80   -11.2
 Rho    =  1416.588
 Mu     =  .0003207
 K      =  .07296
 Cp     =  1068.01306
 Tfilm  =  6.26510
 Hfg    = 158940.26987
 Tsat   = 2.13271
 Hbar   = 229.63708
 Thetab  Htube       Qdp
  8.265  3.358E+02  2.775E+03

Data Set Number =   5  Bulk Oil % =  0.0
TIME:      11:19:39
TC No:     1       2       3       4       5       6       7       8
Temp :  16.06   16.76   16.80   16.76   16.33   15.41 -99.99 -99.99
 Twa     Tliqd   Tliqd2  Tvapr   Psat    Tsump
 16.33    2.28    2.29    2.13   10.79   -11.2
 Rho    =  1407.746
 Mu     =  .0003096
 K      =  .07191
 Cp     =  1074.81715
 Tfilm  =  9.23281
 Hfg    = 158940.87046
 Tsat   = 2.13142
 Hbar   = 267.36095
 Thetab  Htube       Qdp
 14.203  3.077E+02  4.371E+03

Data Set Number =   6  Bulk Oil % =  0.0
TIME:      11:22:02
TC No:     1       2       3       4       5       6       7       8
Temp :  20.65   21.47   21.53   21.23   20.32   18.83 -99.99 -99.99
 Twa     Tliqd   Tliqd2  Tvapr   Psat    Tsump
 20.63    2.15    2.19    1.97   10.65   -11.2
 Rho    =  1401.495
 Mu     =  .0003023
 K      =  .07117
 Cp     =  1079.64687
 Tfilm  = 11.30039
 Hfg    = 159014.11805
 Tsat   = 1.97460
 Hbar   = 289.07728
 Thetab  Htube       Qdp
 18.652  3.258E+02  6.077E+03
```

```
Data Set Number =   7  Bulk Oil % =  0.0
TIME:      11:23:39
TC No:     1       2       3       4       5       6       7       8
Temp :  25.21   26.41   26.59   26.24   25.37   23.72 -99.99 -99.99
 Twa     Tliqd    TliqdZ   Tvapr   Psat    Tsump
 25.53    2.32     2.35     2.17   10.83   -11.3
 Rho    =  1393.680
 Mu     =  .0002935
 K      =  .07025
 Cp     =  1085.69564
 Tfilm  =  13.84961
 Hfg    =  158922.85131
 Tsat   =  2.16998
 Hbar   =  308.62237
 Thetab  Htube       Qdp
 23.359  3.272E+02  7.642E+03

Data Set Number =   8  Bulk Oil % =  0.0
TIME:      11:26:05
TC No:     1       2       3       4       5       6       7       8
Temp :  10.95   11.28   11.01   10.68   10.41   10.53 -99.99 -99.99
 Twa     Tliqd    TliqdZ   Tvapr   Psat    Tsump
 10.74    2.22     2.25     2.23   10.89   -11.3
 Rho    =  1415.933
 Mu     =  .0003198
 K      =  .07209
 Cp     =  1068.51554
 Tfilm  =  6.48669
 Hfg    =  158894.01454
 Tsat   =  2.23166
 Hbar   =  231.54919
 Thetab  Htube       Qdp

 Data Set Number =  10  Bulk Oil % =  0.0
 TIME:      11:30:45
 TC No:     1       2       3       4       5       6       7       8
 Temp :  13.12   13.60   13.34   12.61   12.24   12.44 -99.99 -99.99
  Twa     Tliqd    TliqdZ   Tvapr   Psat    Tsump
  12.78    2.28     2.33     2.28   10.93   -11.3
  Rho    =  1412.840
  Mu     =  .0003159
  K      =  .07251
  Cp     =  1070.89183
  Tfilm  =  7.52908
  Hfg    =  158872.38200
  Tsat   =  2.27791
  Hbar   =  245.59642
  Thetab  Htube       Qdp
  10.502  1.807E+03  1.897E+04
```

```
Data Set Number =  11  Bulk Oil % =  0.0
TIME:      11:36:29
TC No:      1       2       3       4       5       6       7       8
Temp :   15.67   16.20   15.79   15.02   14.69   15.11  -99.99  -99.99
 Twa     Tliqd    Tliqd2   Tvapr   Psat    Tsump
 15.21    2.21     2.24     2.19   10.85   -11.2
 Rho    =  1409.331
 Mu     =  .0003116
 K      =  .07209
 Cp     =  1073.59415
 Tfilm  =  8.70433
 Hfg    =  158911.43766
 Tsat   =  2.19439
 Hbar   =  260.88268
 Thetab  Htube       Qdp
 13.020  2.597E+03   3.382E+04

Data Set Number =  12  Bulk Oil % =  0.0
TIME:      11:38:21
TC No:      1       2       3       4       5       6       7       8
Temp :   18.04   18.31   18.06   17.47   17.19   17.85  -99.99  -99.99
 Twa     Tliqd    Tliqd2   Tvapr   Psat    Tsump
 17.49    2.25     2.31     2.26   10.91   -11.1
 Rho    =  1405.826
 Mu     =  .0003073
 K      =  .07168
 Cp     =  1076.29935
 Tfilm  =  9.87057
 Hfg    =  158882.59790
 Tsat   =  2.25607
 Hbar   =  272.90109
 Thetab  Htube       Qdp
 15.229  3.828E+03   5.829E+04

Data Set Number =  13  Bulk Oil % =  0.0
TIME:      11:41:04
TC No:      1       2       3       4       5       6       7       8
Temp :   19.57   19.54   19.48   18.96   18.74   19.51  -99.99  -99.99
 Twa     Tliqd    Tliqd2   Tvapr   Psat    Tsump
 18.81    2.22     2.25     2.19   10.85   -10.9
 Rho    =  1403.932
 Mu     =  .0003051
 K      =  .07145
 Cp     =  1077.76257
 Tfilm  =  10.49731
 Hfg    =  158915.04210
 Tsat   =  2.18668
 Hbar   =  279.76952
 Thetab  Htube       Qdp
 16.621  5.156E+03   8.570E+04
```

APPENDIX C. SAMPLE CALCULATIONS

Data set number 10 of Data file D0330ESM0 (smooth tube with 0% oil concentration) was used for the sample calculation.

A. TEST-TUBE DIMENSIONS

D_o = 0.015875 m

D_i = 0.0127 m

D_1 = 0.012446 m

L = 0.2032 m

L_u = 0.0762 m

B. MEASURED PARAMETERS

V = V_s x 25 = 4.444 x 25 = 203.25 volts

I = I_s x 1.9182 = 0.9536 x 1.9182 = 1.829 amps

T1 = 13.12 °C

T2 = 13.60 °C

T3 = 13.34 °C

T4 = 12.61 °C

T5 = 12.24 °C

T6 = 12.44 °C

Tsat = 2.28 °C

kc = 344 W/m·K

C. OUTER WALL TEMPERATURE OF THE BOILING TUBE

1. Surface Area of Smooth Tube (Ac):

$p = \pi \times Do = \pi \times .015875\ m = .04987\ m$

$Ac = \pi(Do^2-Di^2)/4 = \pi((.015875)^2-(.0127)^2)/4$

$Ac = 7.13 \times 10^{-5}\ m^2$

2. Heater Power (Q_h):

$Q_h = VI = 111.15\ volts \times 1.829\ amps = 203.25\ W$

3. Tube inside Temperature (Tavg):

$T_{avg} = \sum T_n/n = \sum T_n/6 = 12.89\ ^\circ C$

4. Tube outside wall temperature (T_{wo}):

T_{wo} is calculated by knowing the inside wall temperature using Fourier's Conduction Law, assuming uniform radial conduction.

$$T_{wo} = T_{avg} - [Qh \cdot (\ln(Do/D1)/(2\pi \cdot L \cdot kc))]$$

$$T_{wo} = 12.89 - [203.25 \cdot (\ln(.015875/.012446)/(2\pi \cdot L \cdot kc))]$$

$T_{wo} = 12.89 - .11 = 12.78\ ^\circ C$

5. Wall Superheat (ΔT):

$\Delta T = (T_{wo} - T_{sat}) = 12.78 - 2.28 = 10.5\ ^\circ C$

D. PROPERTIES OF R-124 AT FILM TEMPERATURE:

All thermophysical properties of R-124 were computed at film temperature using the REFPROP equations as provided by Bertsch [Ref. 6].

1. Film Temperature (T_f):

$Tf=(Two+Tsat)/2=(12.78+2.28)/2= 7.53\ ^\circ C$

2. Dynamic Viscosity (μ):

$$\mu = 3.4593-(.0426)T_f+(3.9485\times10^{-4})T_f^2-(4.193\times10^{-6})T_f^3+(2.0709\times10^{-8})T_f^4$$

Substituting T_f:

$$\mu = 3.4593-(.0426)\cdot 7.53+(3.9485\times10^{-4})\cdot(7.53)^2-(4.193\times10^{-6})\cdot(7.53)^3+(2.0709\times10^{-8})\cdot(7.53)^4$$

$$\mu = 3.159\times10^{-4}\ N\cdot s/m^2$$

3. Density (ρ):

$$\rho = 1434.8-(2.8619)T_f-(6.7267\times10^{-3})T_f^2-(7.2852\times10^{-5})T_f^3$$

$$\rho = 1434.8-(2.8619)\cdot 7.53-(6.7267\times10^{-3})\cdot(7.53)^2-(7.2852\times10^{-5})\cdot(9.2)^3$$

$$\rho = 1412.837\ kg/m^3$$

4. Kinematic Viscosity (υ):

$$\upsilon = \mu/\rho = 3.159\times10^{-4}/1412.837 = 2.236\times10^{-7}\ m^2/s$$

5. Thermal Conductivity (k):

$$k = 7.5191\times10^{-2}-(3.5436\times10^{-4}).T_f-(1.9545\times10^{-7})T_f^2+(3.1835\times10^{-9}).T_f^3$$

$$k = 7.5191\times10^{-2}-(3.5436\times10^{-4})\cdot(7.53)-(1.9545\times10^{-7})\cdot(7.53)^2+(3.1835\times10^{-9})\cdot(7.53)^3$$

$$k = 7.251\times10^{-2}\ W/m\cdot K$$

6. Specific Heat (C_p):

$$C_p = 1.0542+(2.1405\times10^{-3})Tf+(1.0709\times10^{-5})Tf^2-(6.4721\times10^{-8})Tf^3-(1.4324\times10^{-9})Tf^4+(4.136\times10^{-11})Tf^5$$

$$C_p = 1.0542+(2.1405\times10^{-3})\cdot(7.53)+(1.0709\times10^{-5})\cdot(7.532)^2-(6.4721\times10^{-8})\cdot(9.2)^3-(1.4324\times10^{-9})\cdot(9.2)^4+(4.136\times10^{-11})\cdot(9.2)5$$

C_p = 1070.89 J/kg·K

7. Thermal Diffusivity (α):

$\alpha = k/(\rho \cdot C_p) = 7.251x10^{-2}/(1412.84 \cdot 1070.89)$

$\alpha = 4.792x10^{-8}$ m^2/s

8. Volumetric Thermal Expansion Coefficient (β):

$\beta = -(\Delta\rho/\Delta T)/\rho = (\rho_{wo}-\rho_{sat})/(T_{wo}-T_{sat})$

$= -(1396.97 - 1428.24)/(12.78 - 2.28)$

$\beta = 2.107x10^{-3}$ (1/K)

9. Prandtl Number (Pr):

$Pr = \upsilon/\alpha = 4.666$

E. HEAT FLUX (Q_f) CALCULATION:

To find the average natural convection heat-transfer coefficient at the non-boiling ends of the test tube, the Churchill and Chu [Ref. 45] correlation was used:

For simplification let **R** represent the following in the correlation :

$$\mathbf{R} = [(g \cdot \beta \cdot Do^3 \cdot \Theta \cdot \tanh(m \cdot Lu))/(\vartheta \cdot \alpha \cdot Lu \cdot m)]^{1/6}$$

where: $m = [(h \cdot p)/(kc \cdot Ac)]^2$

then:

$$h = k/Do\left[.6+.387([\mathbf{R}/(1+(0.559/Pr)^{9/16})^{8/27}]^2)\right]$$

The value of h was computed iteratively. An initial value for h of 190 ($W/m^2 \cdot K$) was used. The following results were obtained:

h = 245.59 ($W/m^2 \cdot K$)

m = 24.93 (1/m)

therefore:

$$Q_f = (h \cdot p \cdot kc \cdot Ac)^{1/2} \cdot \theta \cdot \tanh(m.Lu) = 5.50 \text{ W}$$

F. HEAT FLUX THROUGH ACTIVE BOILING LENGTH

$$Q = Q_h - 2 \cdot Q_f = 203.25 - (2 \cdot 5.50) = 192.25 \text{ W}$$

$$A_b = \pi \cdot D_o \cdot L = \pi \cdot 0.015875 \cdot 0.2032 = 1.0134 \times 10^{-2} \text{ m}^2$$

$$q'' = Q/A_b = 192.25/1.0134 \times 10^{-2} = 18970.79 \text{ W/m}^2$$

$$h = q''/\Theta = 18970.79/10.5 = 1806.74 \text{ W/m}^2 \cdot \text{K}$$

The following results were obtained from the computer using the data acquisition and reduction program DRPGP:

$$q'' = 18970 \text{ W/m}^2$$

$$\Theta = 10.502 \text{ °C}$$

$$h = 1807 \text{ W/m}^2 \cdot \text{°K}$$

APPENDIX D. UNCERTAINTY ANALYSES

The same data run used for Appendix C for a heat flux of 18970 w/m^2 was used for uncertainty analyses, thus all the measured and most of the calculated results still apply. A higher heat flux of 85700 w/m^2 (data set number 13) was also analyzed to show the difference between the two heat fluxes. All uncertainties are presented as a percentage of the calculated parameter, i.e. a relative uncertainty. The uncertainty analysis method suggested by Kline and McClintock [Ref. 47] was used. for example: $R = R(x_1, x_2, x_3, \ldots x_n)$, then:

$$\delta R = \left[\left(\frac{\delta R}{\delta x_1}\delta x_1\right)^2 + \left(\frac{\delta R}{\delta x_2}\delta x_2\right)^2 + \ldots + \left(\frac{\delta R}{\delta x_3}\delta x_3\right)^2\right]^{\frac{1}{2}}$$

where:

δR = uncertainty of the desired dependent variable

x_n = measured variable

δx_n = uncertainty in the measured variable

A. HEAT TRANSFER RATE UNCERTAINTY:

$I_s = 0.9536$ amps $\qquad \delta I_s = 0.025$ amps

$V_s = 4.444$ volts $\qquad \delta V_s = 0.05$ volts

so we have:

$$\frac{\delta Q_h}{Q_h} = \left[\left(\frac{\delta V}{\delta V_s}\right)^2 + \left(\frac{\delta I}{\delta I_s}\right)^2\right]^{\frac{1}{2}}$$

$$\frac{\delta Q_h}{Q_h} = \left[\left(\frac{0.05}{4.444}\right)^2 + \left(\frac{0.025}{0.9536}\right)^2\right]^{\frac{1}{2}} = 2.85\%$$

B. SURFACE AREA UNCERTAINTY:

The following dimensions were taken from the manufacturer's data sheet, and from actual measurements:

D_o = 15.88 (mm) $\quad \delta D_o$= 0.1 (mm)

L = 203.2 (mm) $\quad \delta L$ = 0.1 (mm)

$A_b = D_o \times L$

$$\frac{\delta A_b}{A_b} = \left[\left(\frac{\delta D_o}{D_o}\right)^2 + \left(\frac{\delta L}{L}\right)^2\right]^{\frac{1}{2}}$$

$$\frac{\delta A_b}{A_b} = \left[\left(\frac{0.1}{15.88}\right)^2 + \left(\frac{0.1}{203.2}\right)^2\right]^{\frac{1}{2}} = 0.63\%$$

C. WALL SUPERHEAT UNCERTAINTY

The following temperatures were measured:

T_1 = 13.12 °C

T_2 = 13.60 °C

T_3 = 13.34 °C

T_4 = 12.61 °C

T_5 = 12.24 °C

T_6 = 12.44 °C

T_{avg}= 12.89 °C

Standard Deviation = 0.541 °C

T_{sat} = 2.28 °C and δT_{sat} = 0.01 °C

$$T_{wo} = T_{avg} - Q_h \left[\frac{\ln(\frac{D_o}{D_1})}{2 \Pi L k_c} \right]$$

Note: The second term on the right hand side of the above equation is the Fourier heat-transfer conduction term, and can be neglected for the uncertainty analysis since its value is much less compared to the temperature standard deviation, so:

$T_{wo} = T_{avg}$ = 12.89 °C

$\Delta T = T_{wo} - T_{sat}$ = 12.89 °C - 2.28 °C = 10.61 °C

$$\frac{\delta \Delta T}{\Delta T} = \left[\left(\frac{\Delta T_{wo}}{\Delta T} \right)^2 + \left(\frac{T_{sat}}{\Delta T} \right)^2 \right]^{\frac{1}{2}}$$

substituting values:

$$\frac{\delta \Delta T}{\Delta T} = \left[\left(\frac{0.541}{10.61} \right)^2 + \left(\frac{0.01}{10.61} \right)^2 \right]^{\frac{1}{2}} = 5.1\%$$

D. HEAT FLUX UNCERTAINTY:

$$q = \frac{(Q_h - 2 \times Q_f)}{A_b}$$

where: $Q_h = V \times I = 203.25$ watts

and $\delta Q_h = (203.25)(0.0285) = 5.793$ watts

$q = 18970$ w/m^2 (measured)

$A_b = 0.010137$ m^2

$Q_h - 2.Q_f = q.A_b = (18970)(0.010137) = 192.29$ W

solving for Q_f:

$Q_f = (203.25 - 192.29)/2 = 5.48$ W

assuming the same proportion uncertainty for Q_f, we have:

$\delta Q_f = (5.48)(0.0285) = 0.1562$ W

and now for the uncertainty, we have:

$$\frac{\delta q}{q} = \left[\left(\frac{\delta Q_h}{Q_h - 2.Q_f} \right)^2 + \left(\frac{2.\delta Q_f}{Q_h - 2.Q_f} \right)^2 + \left(\frac{\delta A_b}{A_b} \right)^2 \right]^{\frac{1}{2}}$$

and substituting the computed values:

$$\frac{\delta q}{q} = \left[\left(\frac{5.793}{192.29}\right)^2 + \left(\frac{2\ x\ 0.1562}{192.29}\right)^2 + \left(\frac{6.39\ x\ 10^{-5}}{0.010137}\right)^2\right]^{\frac{1}{2}} = 3.0\%$$

E. HEAT-TRANSFER COEFFICIENT UNCERTAINTY:

$$h = q/DT$$

and

$$\frac{\delta h}{h} = \left[\left(\frac{\delta q}{q}\right)^2 + \left(\frac{\delta \Delta T}{\Delta T}\right)^2\right]^{\frac{1}{2}}$$

and substituting computed values we have:

$$\frac{\delta h}{h} = [(0.003)^2 + (0.005)^2]^{\frac{1}{2}} = 5.11\%$$

The above series of calculation was also conducted on the higher heat flux for the same data filename, furthermore an uncertainty analyses was also conducted on a high flux run with 10% oil at both low and high flux, the results are tabulated in Table C.1.

Table C.1 RESULTS OF UNCERTAINTY ANALYSES

PARAMETER	SMOOTH 18970 W/m²	SMOOTH 85700 W/m²	HIGH-FLUX 19960 W/m²	HIGH-FLUX 19960 W/m²
$\delta Q_h/Q_h$	2.85	1.37	2.87	1.36
$\delta A_b/A_b$	0.63	0.63	0.634	0.634
$\delta \Delta T/\Delta T$	5.10	2.09	20.00	28.80
$\delta q/q$	3.00	0.62	2.93	1.49
$\delta h/h$	5.11	2.18	20.00	28.84

LIST OF REFERENCES

1. Ozone Protection Campaign Briefing Sheet, Friends of Earth, United Kingdom, June 1990.

2. Montreal Protocol on Substance That Deplete the Ozone Layer, Final Act, Montreal, Canada, United Nations Environment Program (UNEP), September 1987.

3. Montreal Protocol on Substance That Deplete the Ozone Layer, Amendments and Adjustments, London, England, UNEP, June 1990.

4. Montreal Protocol on Substance That Deplete the Ozone Layer, Amendments and Adjustments, Copenhagen, Denmark, UNEP, November 1992.

5. Cavallaro, T., *The Navy's Chlorofluorocarbon and Halon Program*, Private Communication, May 1993.

6. Bertsch G., *Nucleate Pool Boiling Characteristeics of R-124*, Master's Thesis, Naval Posgraduate School, Monterey, CA, March 1993.

7. You, S. M., Bar-Cohen, A.,Simon, T. W., and Tong, W., *Experimental Investigation of Nucleate Boiling Incipience with a Highly-wetting Dielectric Fluid (R-113)*, International Journal Heat Mass Transfer, Vol. 33, No. 1, pp. 105-117, 1990.

8. Memory, S. B.,and Marto, P. J., *The Influence of Oil on Boiling Hysteresis of R-114 from Enhanced Surfaces*, Proceedings of the Engineering Foundation Conference On Pool and External Flow Boiling, Santa Barbara, CA, pp. 63-71, 1992.

9. Bar-Cohen, A., *Hysteresis Phenomena at Onset of Nucleate Boiling*, Proceedings of the Engineering Foundation Conference On Pool and External Flow Boiling, Santa Barbara, CA, pp. 1-13, 1992.

10. Thome, J. R., Enhanced Boiling of Mixtures, *Enhanced Boiling Heat Transfer*, Hemisphere Publishing Corp, pp.4-13, 1990.

11. Corty C.,and Foust A. S., *Surface variables in Nucleate Boiling*, Chem. Eng. Progr. Symp. Ser., No. 17, pp. 1-12,1955.

12. Bankoff, S. G., *Entrapment of Gas in the Spreading of a Liquid over a Rough Surface*, AIChE Journal., Vol. 4, No. 1 pp. 24-26, 1958.

13. Bergles, A. E., and Chyu, M. C.,*Characteristics of Nucleate Pool Boiling From Porous Metallic Coatings*, Journal of Heat Transfer, Vol. 104, pp. 279-285,May 1982.

14. Marto, P. J. and Lepere, V. J., *Pool Boiling Heat Transfer from Enhanced Surfaces to Dielectric Fluids*, ASME Journal of Heat Transfer, Vol. 104, pp. 292-299, May 1992.

15. Bar-Cohen, A. and Simon, T. W., *Wall Superheat Excursions in the Boiling Incipience of Dielectric Fluids*, Heat Transfer Engineering Vol 9. No.3 pp 19-31, 1988.

16. Brauer, H. and Mayinger, F., *Onset of Nucleate Boiling and Hysteresis Effects under Forced Convection and Pool Boiling*, Pool and External Flow Boiling, ASME 1992.

17. Carey, V. P., *Liquid-Vapor Phase-Change Phenomena*, Hemisphere Publishing Corp, pp. 176-180, 1992.

18. Chongrungreong, S., and Sauer, H.J. Jr., *Nucleate Boiling Performance of Refrigerants and Refrigrerant-Oil Mixtures*, Transactions of the ASME, Vol. 102, pp. 701-705,Nov. 1980.

19. Hsu, Y. Y. and Graham, R. W.,*Transport Processes in Boiling and Two-Phase Systems*, Hemisphere, Washington, 1976.

20. Thome, J. R., *Enhanced Boiling of Mixtures*, "Enhanced Boiling Heat Transfer", Hemisphere Publishing Corp, pp. 91-124, 1990.

21. Thome, J. R., *Mechanisms of Enhanced Nucleate Pool Boiling*, Pool and External Flow Boiling, ASME, pp. 337-343, 1992.

22. Stephan, K., and Mitrovic, J., *Heat Transfer in Natural Convective Boiling of Refrigerants and Refrigerant-Oil Mixtures in Bundles of T-shaped Finned Tubes*, Advances in Enhanced Heat Transfer, ASME HTD Vol. 18, pp. 131-146, 1981.

23. Roshenow, W. M., *Pool Boiling*, Handbook of Multiphase Systems, Hetsroni, G.,ed., McGraw-Hill, New York, 1983.

24. Murphy, R. W., Bergles, A. E., *Subcooled Flow Boiling of Flourocarbons - Hysteresis and Dissolved Gas Effects*, Proceedings Heat Transfer and Fluid Mechanics Inst., pp. 400-416, Stanford University Press, Stanford, CA, 1972.

25. Marsh, W.M., and Mudawar, I., *Effect of Surface Tension and Contact Angle on Sensible Heating and Boiling Incipience in Dielectric Falling Film*, ASME Nat. Heat Transfer Conference Proceedings, HTD-Vol. 96, pp. 543-550, 1988.

26. Tong, W., Bar-Cohen, A.,Simon, T. W., You, S. M.; *Contact Angle Effects on Boiling Incipience of Highly-wetting Liquids*, International Journal Heat Mass Transfer, Vol. 33, No. 1, pp. 91-103, 1990.

27. Griffith, P., and Wallis, J. D., *The Role Of Surface Conditions in Nucleate Boiling*, Chemical Engineering Progress Symposium Series, Vol. 56, pp. 49-63, 1960.

28. Cornwell K., *On Boiling Incipience Due to Contact Angle Hysteresis*, International Journal Of Heat and Mass Transfer, Vol. 25, No.2, pp. 205-211, 1982.

29. Chowdhury, S. K. R., and Winterton, R. H. S., *Surface Effects in Pool Boiling*, International Journal Heat Mass Transfer 28, pp 1881-1889, 1985.

30. Venart, J.E.S., Sousa, A. C. M., and Jung, D. S., *Nucleate and Film Boiling Heat Transfer in R-11; the Effects of Enhanced Surfaces and Inclination*, Proceedings 8th International Heat Transfer Conference,Vol. 4, pp. 2019-2024, 1986.

31. Wanniarachi, A.S., Marto, P. J and Rielly, J. T., *The effect of Oil Contamination on the Nucleate Pool Boiling Performance of R-114 from Porous-Coated Surface*, ASHRAE Transactions, Vol.92, pt. 2, 1986.

32. Wanniarachi, A.S., Marto, P. J and Sawyer,L.M., *Effect Of Oil on Pool Boiling Performance of R-114 from Enhanced Surfaces*, Proceedings 2nd ASME-JSME Thermal Engineering Joint Conference, Honolulu, Hawaii, Vol 1, pp. 531-537,1987.

33. Faw, R. E., Vanvleet, R. J., and Schmidt, D. L., *Pre-pressurization effects on initiation of subcooled pool boiling during pressure and power transients*,

International Journal Heat Mass Transfer, Vol.29, No. 9, pp. 1427-1437, 1986.

34. Normington, P. J. C., Mahalingam, M., and Lee, T.Y.T., *Thermal Management Control Without Overshoot Using Combinations of Boiling Points*, Proceedings, IEEE Third ITHERM Conference, pp. 49-58, 1992.

35. Bergles, A. E., and Roshenow, W. M., *The Determination of Forced-Convection Surface Boiling Heat Transfer*, Transaction, ASME Journal of Heat Transfer, Vol. 86, pp. 365-372,1964.

36. Eddington, R. I., and Kenning, D. B. R., *The Effect of Contact Angle on Bubble Nucleation*, International Journal of heat and Mass Transfer, Vol. 22, pp. 1231-1236, 1979.

37. Hooper, F. C., and Abdelmessih, A. H., *The Flashing of Liquids at Higher Superheats*, Proceedings 3rd International Heat Transfer Conference., Chicago, Vol. 4, pp.44-50, 1966.

38. Weisman J., Bussell G. and Hsieh T., *The Initiation of Boiling during Pressure Transients*, Journal Heat Transfer 96, pp. 535-555, 1974.

39. Lienhard, J. H., Alamgir, M. D. and Trela M., *Early Response of Hot Water to Sudden Release from High Pressure*, Journal of Heat Transfer, No. 100, pp. 473-479, 1978.

40. Stephan, K., *Influence of Oil on Heat Transfer of Boiling Freon 12 and Freon 22.* Proceedings of the XI International Congress on Refrigeration, Vol. 1, pp. 369-379, 1963.

41. Daugherty, R. L., and Sauer, H. J. Jr., *Nucleate Pool Boiling of Refrigerant-Oil Mixtures from Tubes*, ASHRAE Transaction, Vol. 80, pp. 175-193, 1975.

42. Sauer, H. J. Jr., Davidson, G. W., and Chongrungreong, S., *Nucleate Boiling of Refrigerant-Oil Mixtures from Finned Tubing*, ASME Paper, No. 80-HT-111, National HT Conf.,Orlando, FL., 1980.

43. Karasabun, M., *An Experimental Apparatus to Study Nucleate Pool Boiling of R-114 and Oil Mixtures*, M.S. Thesis, Naval Postgraduate School, Monterey, California, 1984.

44. Reilley, J. T., *The Influence of Oil Contamination on the Nucleate Pool-Boiling Behavior of R-114 from a Structured*

Surface, M.S. Thesis, Naval Postgraduate School, Monterey, California, 1985.

45. Sugiyama, D. C., *Nucleate Pool Boiling of R-114 and R-114/Oil Mixtures from Single Enhanced Tubes*, M.S. Thesis, Naval Postgraduate School, Monterey, CA, 1991.

46. Churchill, S.W. and Chu, F.H.S., *Correlating Relations from Laminar and Turbulent Free Convection from a Horizontal Cylinder*, International Journal Heat and Mass Transfer, Vol. 18, pp. 1049-1070, 1975.

47. Kline, S. J., and McClintock, F. A., *Describing Uncertainties in Single Sample Experiments*, Mechanical Engineering, p. 3, 1953.

INITIAL DISTRIBUTION LIST

		No. Copies
1.	Defense Technical Information Center Cameron Station Alexandria VA 22304-6145	2
2.	Library, Code 052 Naval Postgraduate School Monterey CA 93943-5002	2
3.	Professor Matthew D. Kelleher, Code ME/Kk Department of Mechanical Engineering Naval Postgratuate School Monterey, CA 93943-5002	1
4.	Professor Paul J. Marto, Code ME/Mx Department of Mechanical Engineering Naval Postgraduate School Monterey, CA 93943-5002	2
5.	Professor Stephen B. Memory Department of Mechanical Engineering McArthur Bldg. University of Miami Coral Gables, FL 33124-0624	1
6.	Mr. R. Helmick, Code 2722 Annapolis Detachment, C. D. Naval Surface Warfare Center Annapolis, MD. 21402-5067	2
7.	Mr. Bruce G. Unkel NAVSEA (CODE 56Y15) Department of the Navy Washington, D.C. 20362-5101	1
8.	Naval Engineering Curricular Officer, Code 34 Naval Postgraduate School Monterey, CA 93943-5002	1
9.	LT George D. Perry 13229 Ireland Lane San Diego, CA 92129	1